WIND INDUCED SEDIMENT RE-SUSPENSION IN A SHALLOW LAKE

Justin James Pringle

Submitted in fulfilment of the requirements for the degree of

Master of Science in Engineering

In the

Civil Engineering programme

University of KwaZulu-Natal

Durban

2011

Supervisor: Professor DD Stretch

ABSTRACT

Wind induced turbidity within shallow lakes can greatly affect the biological functioning of a system in either a positive or negative manner. This research aims to understand and model the physical processes that cause sediment re-suspension. Lake St Lucia on the east coast of South Africa, a UNESCO World heritage site was used as a case study. Lake St. Lucia is a shallow water system which commonly experiences high levels of turbidity. Coupled with the naturally shallow depth of the lake, it is currently drought stricken, resulting in abnormally low water levels. A simple model has been developed which accounts for sediment re-suspension due to wind-driven waves and their associated bed shear stresses. The wave heights within a shallow lake such as St Lucia are controlled either by the fetch (for a large water depth), or the water depth (for a large fetch). When the wind is strong enough, the wind-driven turbulent mixing causes the water column to become fully mixed. When the wave-driven boundary layer becomes turbulent, sediment, being entrained within the water column increases significantly. The model also accounts for the effects of temporal consolidation on the re-suspension of sediments by setting a time scale for the erosion processes. It was found that the median of the monthly turbidity levels over the past ten years exceeded the average turbidity levels over the past 92 years. In all cases it was shown that mouth linkage with the uMfolozi resulted in lower turbidity levels than without any linkage due to the higher average water levels.

The model was then developed to predict the spatial variation in turbidity within the Southern Lake. This was achieved through the use of existing bathymetric data for the Lake. This spatial model was then used to show how the turbidity varied for different wind and water depth conditions. Two conditions were considered, a NE and SW wind blowing at 8m/s for water levels of 0 EMSL and -0.5 EMSL. The spatial model showed that a decrease in water level increases the turbidity within the lake significantly. The wind directions appeared to yield similar results of sediment re-suspension. It was also shown that the high turbidity values were situated in the shallow depths even though the wave heights were small in comparison to those in deeper water.

PREFACE

I Justin James Pringle, declare that the whole of this dissertation is my own work and where use has been made of the work of others, it has been duly acknowledged in the text. This dissertation has not been submitted in partial or full to any other University. This research was carried out in the Centre for Research in Environmental, Coastal and Hydrological Engineering, School of Civil Engineering, Surveying and Construction, University of KwaZulu Natal, Durban, under the supervision of Professor D. D Stretch.

……. …….

J. J Pringle Date

As the candidates supervisor I have approved this dissertation for submission

……. …….

D. D Stretch Date

ACKNOWLEDGMENTS

I would like to express my acknowledgement of the following:

The Lord for blessing me with the desire and passion I required to complete this dissertation.

My family for their support and guidance.

Jade Clark for her never ending patience and heartfelt support.

All those who helped with the data collection, including helping to get a very stuck vehicle out of the mud a number of times – Christopher Maine and Katrin Tirok.

The Ezemvelo KZN wildlife authorities for allowing access to the park. Special gratitude is expressed to Ricky Taylor, Caroline Fox and Sbu for their guidance and trust.

SANPAD, education and research trust project 10/90, for funding this research, as well the NRF SEACHANGE Programme, Grant number 71051 (Society, Ecosystems & Change).

iSimangaliso wetland park authority (Andrew Zaloumis, Bronwyn James, Nerosha Govender).

The South African weather service for their provision of wind data.

TABLE OF CONTENTS

LIST OF FIGURES

LIST OF TABLES

LIST OF SYMBOLS

A = Maximum Semi-Orbital Excursion (m).

C = Concentration of sediment (g/L).

$\tilde{c}$, C_{bak} = Depth averaged, non-settling background concentration (g/L).

C_d = Drag Coefficient.

C_{er} = Concentration due to erosion (g/L).

C_g = Wave group celerity (m/s).

$C_{g,x}$ = Wave group celerity in the x direction (m/s).

$C_{g,y}$ = Wave group celerity in the y direction (m/s).

C_ζ, C_θ = Wave propagation velocities in the spectral space (ζ,θ).

d = Depth (m).

δ = Non-Dimensional Depth Number.

E = Wave energy (m^2) determined from the integral of the variance spectrum

ε = Non-Dimensional Energy Number.

E_r = Erosion Rate (kg/m^2s).

f_w = Wave Friction Factor.

g = Gravitational constant (m/s^2).

H_s = Significant wave height (m).

K = Model Parameter (g/L).

k = Wave Number.

L = Wave Length (m).

M = Erosion Rate Constant (kg/m^2s).

N	=	Wave action density.
v	=	Kinematic Viscosity of Water (m^2/s).
ν_f	=	Non-Dimensional Frequency Number.
ν_p	=	Frequency of Spectral Peak (Hz).
ω	=	Angular Frequency.
ρ	=	Density of Water (kg/m^3).
S	=	Source/Sink term in the wave action balance equation.
ζ	=	Intrinsic wave frequency (Hz).
τ_b	=	Bottom Shear Stress (Pa).
τ_c	=	Critical Shear Stress (Pa).
τ_{ref}	=	Reference shear stress (Pa).
τ_y	=	Plastic Yield Stress (Pa).
U_{10}	=	Wind Velocity at Reference Height 10m (m/s).
U_m	=	Maximum Horizontal Velocity (m/s).
w_s	=	Settling velocity (m/s).
x	=	Fetch Length (m).
χ	=	Non-Dimensional Fetch Number.
ζ	=	Sediment flux (kg/m^2s).

CHAPTER 1

INTRODUCTION

This chapter introduces the topic highlighting key aspects of the research. It includes the motivation behind the research and the associated aim and objectives; the dissertation outline concludes the chapter.

1. INTRODUCTION

St. Lucia is a lake and estuary system located along the north coast of Kwa-Zulu Natal. The focus area for the research is the lake situated to the north of the estuary, with particular interest to the south lake (refer to figure 1.3). It is a shallow system with average depths ranging from 0.96m to 2m (Carrasco *et al,* 2007). This shallow depth allows for turbid conditions to develop relatively quickly within the lake, the main cause of the turbidity would be due to the wind action on the lake coupled with the shallow depths of the lake.

The St. Lucia lake and estuary system has undergone many anthropogenic impacts that have affected the water level and sediment concentration within the estuary, one of the most significant impacts was the separation of the uMfolozi river in 1952 (Cyrus, *et al* 2010), which resulted in hypersaline conditions within the lake and estuary during drought. The uMfolozi was then diverted into the estuary, via a “back-channel,“ to prevent hypersaline conditions from occurring (Cyrus *et al,* 2010). The linkage could possibly increase the silt load on the lake and estuary if the sediment from the uMfolozi isn‟t successfully trapped. However, while this may have helped in increasing the water levels of the estuary and reducing the saline conditions, the uMfolozi has had no effect in increasing the water levels of the lake and reducing the saline conditions of the lake, since it is not linked directly to the lake in the north and the flows through the channel have been low.

Wind plays an important role in moving the water around the lake and it is through the interaction between the wind blowing over the water and the water surface that small waves are formed. These waves generate turbulence which causes the water particles to move in an orbital motion. The water particles exert a shear stress on the sediment

which results in the sediment being re-suspended, if the shear stress is greater than the critical shear stress (Jing & Ridd, 1996).

1.1 Background of St. Lucia

St Lucia has been labelled as a world heritage site (Cyrus et al, 2010). However over the past ten years the system has undergone a severe drought period, which has subsequently led to a decrease in the water levels. In 1952 the uMfolozi (which played an integral part in supplying the system with fresh water and recharging the water levels) was separated from the St Lucia mouth (Cyrus et al, 2010). During drought periods when the combined mouth would close, water levels in the lake would drop due to evaporation; as a result, water flowing from the uMfolozi would flow up the system recharging the water levels. In the lake basin the evaporation (MAE) is 1470mm while the rainfall (MAP) is 890mm (Lawrie & Stretch, 2011). Even though they represent present day figures, the MAE is significantly higher than the MAP, leading to a net water loss in the lake basin, when river inflow is low (typically during drought periods). This implies that if the mouths were combined during closure, water from the uMfolozi would flow up the St. Lucia system recharging the water levels. However due to severe siltation of the Narrows in 1951, the decision was made to separate the uMfolozi from the St Lucia system (Day et al, 1954). The siltation was a result of poor land use within the catchment and the intense farming activities which occurred along the flood plain of the uMfolozi. The farming increased the silt load of the uMfolozi because of two reasons. (1) Farming in the flood plain resulted in the removal of natural swamp land, hence the removal of a natural mechanism for sediment removal. (2) To protect the farm land from flooding, levies were built on either side of the uMfolozi and the river was canalised, increasing the flow and hence erosion (Whitfield & Taylor, 2009).

Figure 1.1: Aerial image of the uMfolozi and its associated flood plain which now comprises of sugar cane farms (Whitfield & Taylor, 2009).

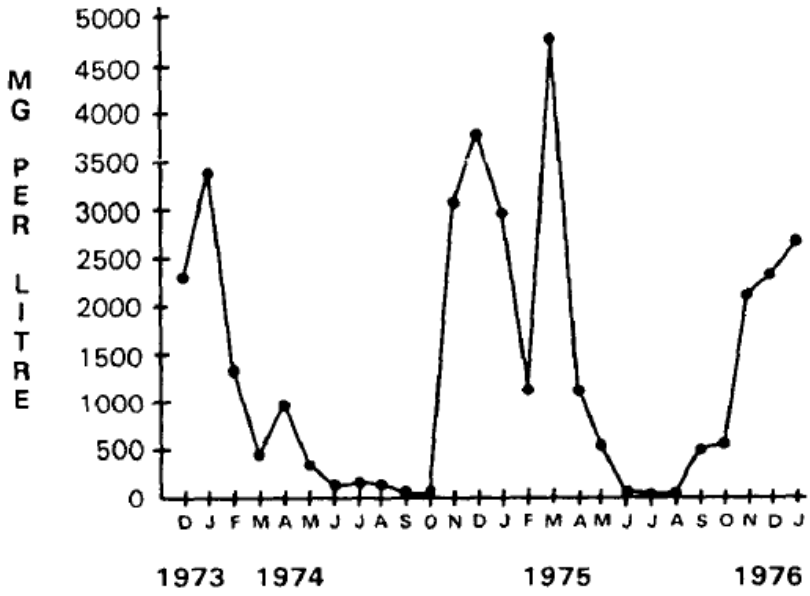

Figure 1.2: Average monthly sediment load of the uMfolozi during the period of November 1973 to January 1976 (Lund, 1976)

From figure 1.2 it is clear that during the summer months, when flows are high in the uMfolozi, the sediment load is high, reaching 5g/L. However the high flow rates would result in the opening of the combined mouth (assuming the uMfolozi and St. Lucia system were combined as they were in the past), therefore it is unlikely that these high sediment loads from the uMfolozi will be deposited within the St. Lucia estuary, as they would be transported out to sea.

Before the separation the combined mouth was so large that, in 1904 residents reported that ocean swells entered the bay and broke on the shore (Day et al, 1954), at times it was also possible for small ships to enter the bay (Whitfield & Taylor, 2009). This indicated that the size of the combined mouth was large, for; which would have played an important role in supporting a large variety of species because of its immense size. This implied that the role that the combined mouth played was not only physical but a biological one as well.

There have been a number of severe consequences that have arisen due to the separation of the mouths. It has become rare for the St. Lucia mouth to open naturally, thus in order to maintain interaction between the sea and the estuary, the mouth has had to be artificially opened (Lawrie & Stretch, 2011). St. Lucia has lost its main mechanism for flushing out any sediment build up within the narrows and estuary. Water supplied by the uMfolozi during mouth closure would result in stable water levels within the lake, thus during the wet season (when river inflow increased) the water levels within the lake would rise to a level that would overtop the beach berm. This beach berm normally formed to a height of 3 – 3.5m above MSL, and when breached resulted in flows of 1000m^3/s (Whitfield & Taylor, 2009), successfully flushing out any accumulated sediment. Thus it has required extensive dredging to remove this sediment build up (Cyrus & Blaber, 1988). For example after the mouth closed in 1950, it took 5 years to dredge the accumulated sediment to allow the mouth to open (Whitfield & Taylor, 2009).

A lot of focus has been paid to the area around the narrows and the mouth (refer to figure 1.3), since this area experiences the immediate effect of the mouth separation. However, as mentioned previously there is a net water loss from the lake basin with the mouth closed. This can cause situations of severe desiccation. Therefore from a managerial aspect, the controlling of the mouth state can have severe effects in the lake basin 22km upstream of the mouth. Desiccation leads to a number of unforeseen problems. For example high turbid conditions arise since wind can easily re-suspend sediment located on the lake floor and evaporation can lead to hypersaline conditions.

These two consequences which arise due to low water levels have shown to have severe negative effects on the biological functioning of a system (Cyrus et al, 2010; Whitfield & Taylor, 2009).

It is subsequently due to the low water levels that the research proposed by this report was undertaken. The low water levels allow for very turbid conditions to develop, affecting the biological functioning of the St. Lucia system.

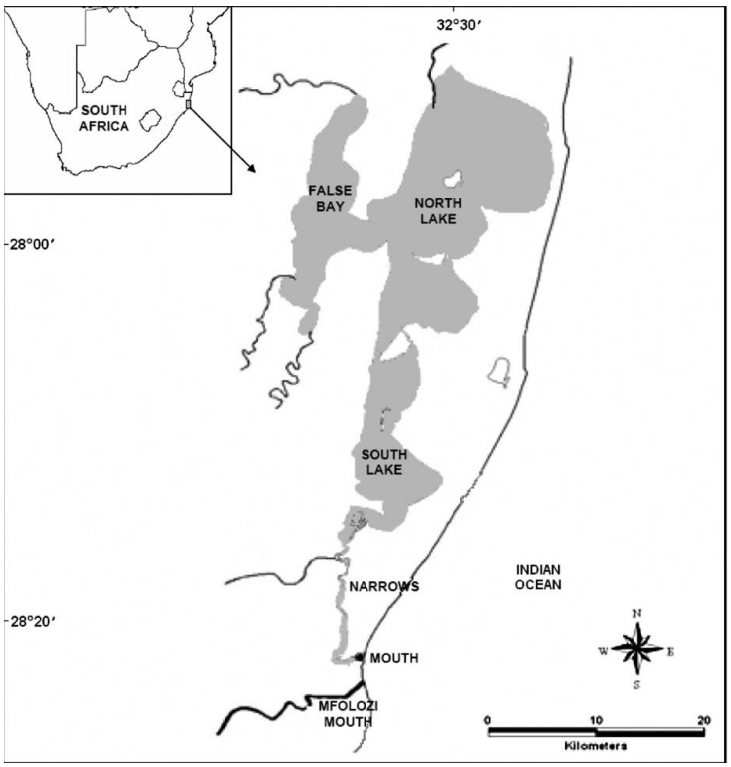

Figure 1.3: Map Showing the St Lucia Estuary and Lake System (Carrasco *et al*, 2007)

1.2 Motivation

Lake St Lucia is a naturally shallow system with an approximate maximum depth of 2m (Carrasco et al, 2007). The system has been drought stricken for the past ten years; this drought has subsequently lowered the water levels within the lakes to well below 2m. This results in large quantities of sediment re-suspension whenever the wind blows over the lake surface. The reason why this happens is because the wind-induced waves are able to easily interact with the lake floor (since the water depth is so shallow). Another reason why such large quantities of re-suspended sediment are

easily entrained within the water column is because the majority of the sediment found on the lake floor comprises mainly of clay with a D_{50} of 4µm (Chrystal & Stretch, unpublished). Thus a relatively low shear stress is required to re-suspend the sediment when compared to sand, which implies that at a relatively low wind speed (and subsequently small wave height) the clay sediment can easily be re-suspended.

When large quantities of sediment are entrained within the water column, the survivals of many biological species are severely affected. For example Carrasco et al (2007) found that at a sediment concentration of 2.58 g/L the survival of *Mesopodopsis Africana* (a mysid) is reduced significantly such that they are unable to be represented in numbers large enough to be consumed as a food source by species in a higher trophic level. Thus the negative effects of sediment re-suspension on the biological functioning of a system can be seen.

The model presented by this research could be used as an estimation tool in predicting the amount of sediment re-suspended. It will be linked with the existing water balance model developed by Lawrie & Stretch (2008), and will ultimately be used to form part of a bio-physical model which is currently still under development.

1.3 Advantages and Disadvantages of Turbidity

As mentioned above, Carrasco et al (2007) noted that increased levels of turbidity resulted in an increase in the mortality of zooplankton. However turbidity can have a number of beneficial consequences for zooplankton (Carrasco *et al,* 2007) such as:

1. Protection from larger predators due to decreased visibility.
2. Zooplankton may benefit nutritionally from the suspended particles, as dissolved organic matter could adsorb to surface charged particles.

These benefits correlate with those stated by Kessarkar *et al* (2009), where he stated that the turbid water acts like a nursery area for fish eggs. The turbidity behaves like a mask allowing the fish eggs to be protected from predators.

1.4 Research Question

What are the physical processes by which wind-driven sediment re-suspension occurs within Lake St. Lucia, given it is a naturally shallow system with cohesive sediment, and how can they be integrated into a predictive model?

Can a model be used to predict the lake average turbidity value as well as the spatial distribution of turbidity within the lake?

What are the biological effects of the associated turbidity levels, for example is the threshold concentration, proposed by Carrasco et al (2007) of 2.58g/L, exceeded?

1.5 Aim

To investigate and develop a model which predicts turbidity generation in the St. Lucia Lake as a result of wind for different cases of mouth linkage with the uMfolozi.

1.6 Objectives

Develop a model which:

1. Links wind with turbidity in the St. Lucia estuary.
2. Determines the orbital velocity at the lake bed due to water waves.
3. Determines the shear stress at the lake bed due to water waves.
4. Determines the turbidity in the water column around the vicinity of the lake bed.
5. Will be able to predict the turbidity within the water column for different wind and water depth data.
6. Can be applied to predict turbidity within the water column showing the spatial variation throughout the lake.
7. Determines the average turbidity for each month.
8. Determine whether the threshold proposed by Carrasco *et al* (2007) is exceeded.

1.7 Outline of Dissertation

The following chapters within this dissertation are outlined as follows:

Chapter 2 discusses the requirements for the development of a mathematical model, through a literature review. It discusses the development of wind-waves and the associated limits encountered by waves in finite depth water. Different types of models, such as empirical and that which is based on conservation equations are reviewed along with different techniques of wave measurement. The sediment re-suspension model is then derived by looking at boundary layers and the associated shear stresses resulting in sediment re-suspension.

Chapter 3 describes the field methods used to calibrate the model. This is done by describing the manner in which samples were taken, how results were then post processed and the manner in which the model was subsequently calibrated.

Chapter 4 discusses the manner in which the model was developed. This chapter describes the fundamental principles on which the model is based. The method by which the model determines the relevant physical parameters such as wave height, period, shear stress and erosion is then described.

Chapter 5 presents the results of the model, along with the associated discussions. The results of the model calibration are also presented.

Chapter 6 presents the conclusions drawn by this research as well as recommendations regarding further research.

CHAPTER 2

LITERATURE REVIEW

This chapter consists of a literature review. The review explains the process by which wind-induced waves are formed and the associated methods of modelling the waves. The different erosion modelling techniques are reviewed and a method is suggested. The associated parameters required for the model such as the wave boundary layer are discussed.

2.1 INTRODUCTION

Sediment re-suspension within shallow lakes is a predominately wind driven process. Currents caused from tributary inflows are generally too weak to re-suspend significant amounts of sediment. Thus any sediment re-suspension is due to the wind induced waves which propagate through the lake (Mehta & Jain, 2010). Currents induced on the surface of the lake due to the wind are only able to transport the re-suspended sediment throughout the lake; they too are not strong enough to re-suspend any sediment (Luettich et al, 1990).

What follows is an evaluation of the different parameters required to develop a mathematical model which predicts sediment re-suspension.

2.2 WIND INDUCED WAVES

When wind blows over the water surface it is easy to understand that the stress exerted by the wind on the water surface results in a change in the water level downwind (wind set-up), since the hydrostatic pressure should balance the stress exerted by the wind (refer to section 4.4.2). However it might not be so simple to understand the mechanism by which the wind waves are formed. Jeffreys (1925) suggests the formation of wind waves is due to the turbulence within the wind field, since when two fluids flow over each other, the slightest differences in velocities cause instabilities between the two fluids. Jeffreys (1925) used this theory to begin to

calculate the theoretical wind velocity at which capillary waves are formed; however the observed values seemed to differ significantly from the theoretical. Jeffreys (1925) found that the critical wind speed was around 640 cm/s; however this differed from the observed value of 110 cm/s, these calculations were based on irrotational motion. This represented the first attempt at wind wave prediction, and revealed the complexities involved when trying to determine wind induced waves.

While Jeffreys (1925) was unable to explain exclusively the initial formation of waves by wind, his description of how they grow seems to hold true, the explanation is as follows:

When wind blows over the water surface the air flow may not be able to follow the deformed shape of the water surface (due to the surface waves). Instead of flowing down the trough and up over the crest, the air flow separates at the wave crest. A zone of positive pressure exists where the air flow collides with the preceding wave. A zone of negative pressure forms in a region sheltered by the air flow, due to the presence of eddies on the face of the upwind wave. Thus the wave growth is due to the pressure differences which occur on the upwind and downwind faces, since the downwind wave face is pushed by the zone of positive pressure and the upwind wave face is pulled by the zone of negative pressure.

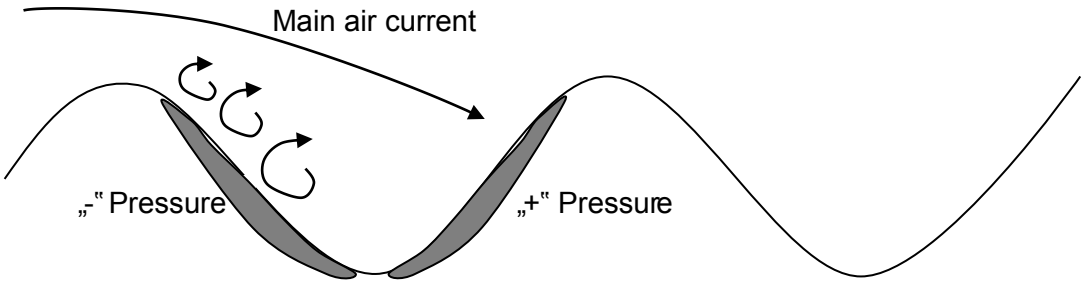

Figure 2.1: Illustration of Wave Growth According to Jeffreys, (Wright et al, 1999). The zones of „+" and „-„ pressure on the wave faces are illustrated by the shaded areas.

If no energy is lost from the system, then in theory the waves should continue to grow, to indefinite heights and lengths. However in practice this is never the case since there are continuous mechanisms by which energy is added to and removed from the system. Energy transfer to the waves is either by the push of the wind (if the waves are moving slower than the wind), frictional drag of the air on the sea surface and by pressure differences in the air above the waves (Kinsman, 1965). Factors which limit

the wave growth are turbulent dissipation; in the form of white capping and breaking waves, and the viscosity of the water. The degree that the viscosity limits the wave growth depends on the wave age since capillary waves are affected much more greatly by the viscosity than a fully aroused sea state, thus it can be said that in general, the dissipation due to turbulence is much greater than viscosity (Kinsman, 1965). The three ways in which waves grow according to Kinsman (1965) are as follows:

1. Frictional drag of the air on the sea surface. The transfer of energy can occur even if the waves are moving faster than the wind. The direction of the water motion at the crest of the wave is the same as that as the wind, thus the wind acts to speed the wave up. However the motion of the water in the trough is the opposite of the wind, thus the frictional drag acts to slow this motion down. This leads to the steepening of the wave profile.
2. Pressure differences in the air above the waves. This is the same process as mentioned by Jeffreys (1925), discussed previously.
3. The direct push of the wind on the waves. This process strongly depends on the shape of the wave, since a young steep chop would allow a better grip than a smooth swell.

While it is important to understand the processes in which waves are formed and grow, for the purpose of this research it would be beneficial to understand what limits wave growth. There are three main situations when considering wave propagation through water. The first is waves travelling through deep water, the second is waves travelling in transitional water and the third is waves travelling through shallow water. Each condition is defined by the ratio between the wave length (L) and the water depth (d), for the purpose of this discussion the situation whereby waves are travelling through transitional water will be ignored. This implies that waves are either travelling through deep water whereby $d/L > 0.5$, or shallow water whereby $d/L < 0.04$ (Reeve et al, 2004). The definition of wave propagation through either deep water or shallow water does not explicitly define how wave growth occurs in finite depth water, it would be better to classify the wave growth as either in fetch limited or depth limited conditions. For example when considering only the finite depth case; in the initial stage of wave growth the wave heights are only a few centimetres as well as the wave lengths, and even though the water depth, as an example, might be 0.5m by the definitions mentioned above, the waves would be propagating through deep water. In this situation the wave growth can be defined in the same manner as wave propagation in the ocean, where the wave growth is controlled mainly by the fetch. In the case where the wave grows to a point where it begins to “feel” the bottom, it is said that the wave is in depth limited

conditions (Holthuijsen, 2007). Therefore waves can also be defined as either being in a fetch limited situation or depth limited situation.

It is only due to the recent research conducted by Young & Verhagen (1996) that the physical processes of wind induced waves in finite depth water have begun to be fully understood. Essentially their research showed that at some critical depth the fetch no longer defines the wave growth but that it is rather defined by the water depth. This is a crucial factor in Lake St Lucia since it is a naturally shallow system, with depths ranging from 0.96m to 2m (Carrasco et al, 2007). The system has however been drought stricken for the past ten years which has subsequently led to a further drop in water levels, such that in September 2009 it was estimated that a precipitation of 1200mm was required to restore the lake levels back to their original state (Cyrus et el, 2010).

With reference to figure 1.3, the maximum fetch for the South Lake is approximately 6 Km North to South and 6 km West to East. This fetch, in combination with the naturally shallow water depth would result in depth limited conditions within the lake. Thus it can be assumed that the wind-induced waves are characterized by the water depth rather than the fetch length.

The waves propagate through the water surface in accordance with linear wave theory and they thus cause the water particles to oscillate in an orbital or elliptical motion (Reeve et al, 2004). Obviously when the oscillating water particles come into contact with the lake bed they exert a shear stress which re-suspends the sediment. Some researchers base the water depth at which the waves interact with the lake floor to be approximately half the wave length (Chao et al, 2008). This appears to be a very narrow minded approach since it has been shown by Young & Verhagen (1996) that the depth plays a very important role development of waves and that it almost appears too simple to just assume that at a water depth equal to half the wave length, sediment will be re-suspended. However it can be used as an indication as to the water depth at which sediment re-suspension would occur, or rather, since the water depth is known it would be better to use this fact as an indication of the wave length at which sediment re-suspension would occur.

2.3 WIND-WAVE MODELS

Wave modelling according to Holthuijsen (2007) is initially based on idealised conditions shown in figure 2.2, whereby parameters such as fetch (x), wind speed (U) and water depth (d) can be related with relative ease. Figure 2.2 shows wave

development for a constant wind speed, blowing perpendicular to the coastline and a water depth which is considered deep, i.e. greater than half the wave height (Reeve et al, 2004).

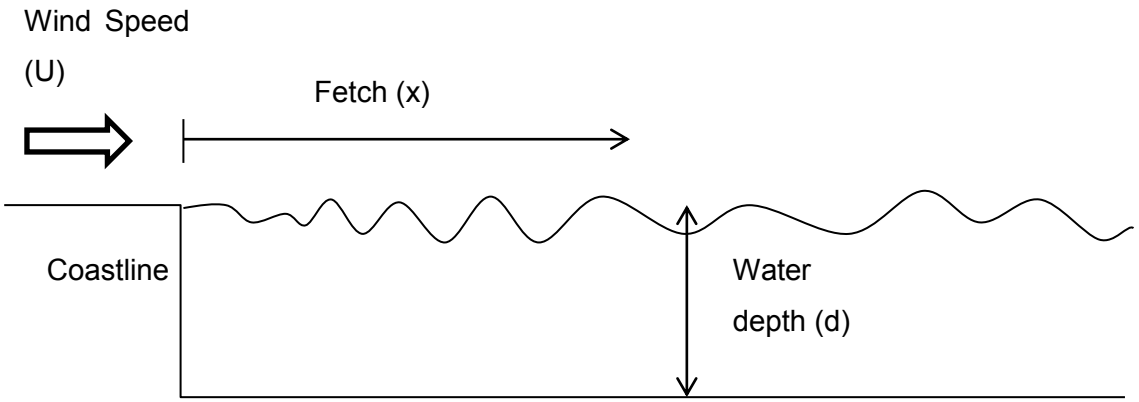

Figure 2.2: Idealised wave growth according to Holthuijsen (2007) defining important parameters such as wind speed (U), fetch (x) and water depth (d).

Carniello et al (2011) suggest that there are two methods by which wind induced waves can be modelled. These two methods are as follows:

1. Empirically derived relations which provide information regarding the wave characteristics.
2. A process based approach in which a set of appropriate conservation equations are solved.

Method one is relatively „user friendly" since all it requires is the input data for relevant empirical equations to estimate the desired wave characteristics. However it has a disadvantage in that can be inaccurate in very shallow and irregular shaped lakes because the estimation of fetch can be difficult (Carniello et al, 2011). The South Lake (the main focus area) is a fairly regular shaped basin (refer to fig 1.2) thus this shouldn't necessarily be a problem, however the water levels within the lake have been very low (as mentioned previously), which could potentially result in an inaccurate estimation of fetch due to the change in the shape of the lake.

Method two is where the wave energy equation is solved. Two approaches could be used to solve the equation, (1) A Lagrangian approach; whereby it is assumed that the wave energy is transported along rays. (2) Another way to solve the wave energy equation is by the Eulerian approach; whereby the wave energy equation is solved on a spatial grid (Carniello et al, 2011). The Lagrangian approach is not suited to in the

shallow water cases; because the waves no longer travel in straight rays- but rather they are curved due to refraction (Holthuijsen, 2007). The problem is not necessarily setting out a grid for the Southern Lake, however solving the conservation equations can be complicated and time consuming. What is required is a simple model which can predict the turbidity and the easiest way in which this can be done is through the use of empirically derived relations. The incorporation of basic physical concepts in the process based models can make the models very complicated and difficult to run. For example incorporating refraction in method two requires a fine mesh size is; this can require great computational effort. Whereas method one (the empirical method) is based on observed data, the foundation upon which the relations are formed, and is thus easier to use. The use of method two, while perhaps more strongly underpinned by theory, would require calibration, which would require a significant amount of observed data (such as wave heights, peak periods and bathymetry); this amount of observed data doesn't exist for Lake St. Lucia. In accordance with what was mentioned previously, the one objective of this model is to link it with an existing water balance model. The water balance model works out an average water depth for the South Lake by taking the total volume of water in the Lake and dividing it by the area, so it would be more important to produce a model that predicts lake average turbidity levels rather than on a spatial scale. This is not to say that it would not be useful to develop a spatial model.

2.3.1 Method 1 – empirical model

An example of the first method is the research conducted by Young & Verhagen (1996) in which they determined a set of empirical relations to describe the wave characteristics. According to Breugem & Holthuijson (2006) the research conducted by Young & Verhagen (1996) was the most comprehensive set of observations of wave growth in finite depth water. The wave characteristics are essentially defined by the following non-dimensional terms:

$$\varepsilon = \frac{g^2 E}{U^4} \tag{2-1}$$

$$\nu_f = \frac{v_p U}{g} \tag{2-2}$$

$$\chi = \frac{xg}{U^2} \quad (2\text{-}3)$$

$$\delta = \frac{dg}{U^2} \quad (2\text{-}4)$$

where: ε is the non-dimensional energy number, g is the gravitational constant (9.81m/s^2), E is the wave energy (m^2) derived from the integral of the variance spectrum (hence the different units for energy), U is the wind velocity (m/s) at reference height 10m, v_f is the non-dimensional frequency number, v_p is the peak frequency of the wave (1/s), χ is the non-dimensional fetch number, x is the fetch length (m), δ is the non-dimensional depth number and d is the depth (m).

CERC (1977) proposed limits to the non-dimensional energy and frequency terms, these limits are based on observations and represent the upper or lower bound (depending which parameter is considered) of the observed values shown in figures 2.4 and 2.6, they are as follows

$$\varepsilon = 1.4 \times 10^{-3}\delta^{1.5} \quad (2\text{-}5)$$

$$\nu = 0.16\delta^{-0.375} \quad (2\text{-}6)$$

Ijima & Tang (1966) combined the above equations (2-5 and 2-6) with available deep water fetch limited equations and developed a set of finite depth fetch limited wave growth terms for ε and v, whence:

$$\varepsilon = 5 \times 10^{-3}\left\{tanhA_1 . tanh\left({B_1}/{\tanh(A_1)}\right)\right\}^2 \quad (2\text{-}7)$$

where:

$$A_1 = 0.53\delta^{0.75} \quad (2\text{-}8)$$

$$B_1 = 5.65 \times 10^{-3}\chi^{0.5} \quad (2\text{-}9)$$

and

$$\nu = 0.133\left\{tanhA_2 . tanh\left({B_2}/{\tanh(A_2)}\right)\right\}^{-1} \quad (2\text{-}10)$$

where:

$$A_2 = 0.833\delta^{0.375} \quad (2\text{-}11)$$

$$B_2 = 3.79 \times 10^{-2}\chi^{0.33} \quad (2\text{-}12)$$

Equations (2-7) and (2-10) reduce to the limit defined by equations (2-5) and (2-6) for shallow depth and large fetch. Basing their work on the previously mentioned relations, Young & Verhagen (1996) were able to develop a set of relations that appeared to describe the results more accurately than equations (2-5) to (2-12). These relations are as follows:

$$\varepsilon = 3.64 \times 10^{-3}\left\{tanhA_1.tanh\left({B_1}/{\tanh(A_1)}\right)\right\}^{1.74} \quad (2\text{-}13)$$

where:

$$A_1 = 0.493\delta^{0.75} \quad (2\text{-}14)$$

$$B_1 = 3.13 \times 10^{-3}\chi^{0.57} \quad (2\text{-}15)$$

and

$$\nu = 0.133\left\{tanhA_2.tanh\left({B_2}/{\tanh(A_2)}\right)\right\}^{-0.37} \quad (2\text{-}16)$$

where:

$$A_2 = 0.331\delta^{1.01} \quad (2\text{-}17)$$

$$B_2 = 5.215 \times 10^{-4}\chi^{0.73} \quad (2\text{-}18)$$

The above expressions for ε and ν reduce to the following relations for shallow depth and large fetch; the following equations are the limits determined by Young & Verhagen (1996) based on field observations:

$$\varepsilon = 1.06 \times 10^{-3}\delta^{1.3} \quad (2\text{-}19)$$

$$\nu = 0.2\delta^{-0.375} \quad (2\text{-}20)$$

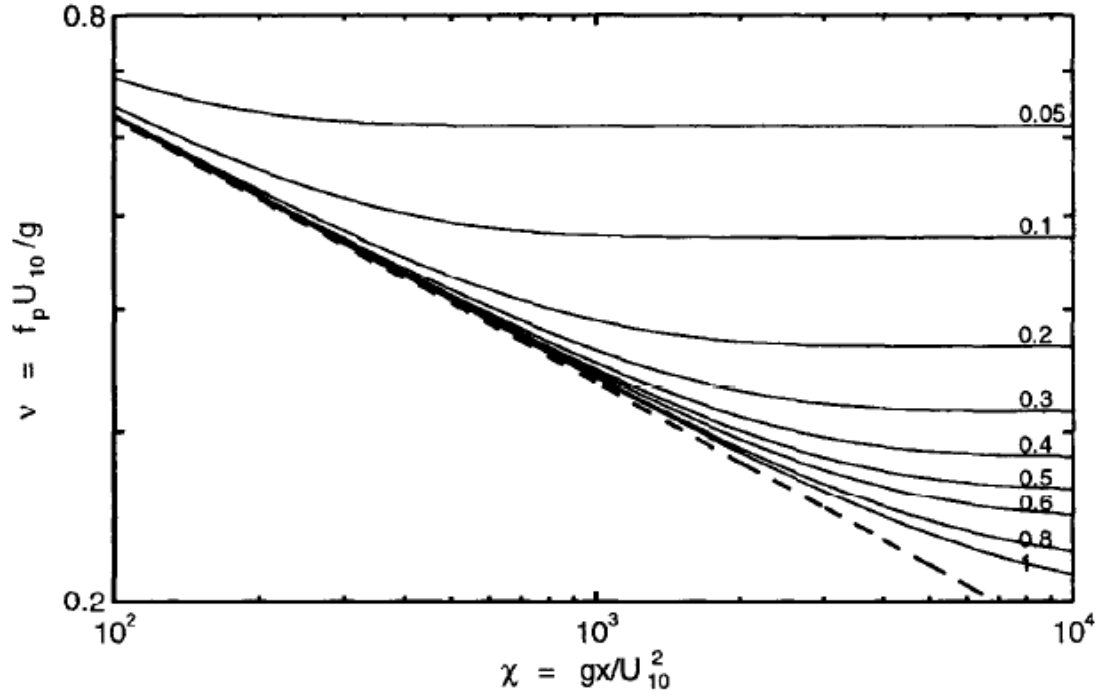

Figure 2.3: Graph of the non-dimensional frequency vs non-dimensional fetch (Young & Verhagen, 1996) showing the effect that depth has on the formation of the wave frequency. Each curve shows the effect of the depth limit (the value of the depth number, δ, for each curve is shown on the right), and are defined by equation (2-16), whereas the dashed line is the deep water form of equation (2-16).

Figure 2.3 shows the effect that the depth has on limiting the wave frequency for large fetch. The dashed line represents the deep water form of equation (2-16). Essentially it can be seen that at a small fetch the wave development is similar to that of deep water whereas at a large fetch the non-dimensional frequency, ν, appears to reach some asymptotic limit. This limit is attributed to the effect that the water depth has on wave development. Each solid line is a representation of the wave development for different depth numbers. This limit is shown in the figure 2.4.

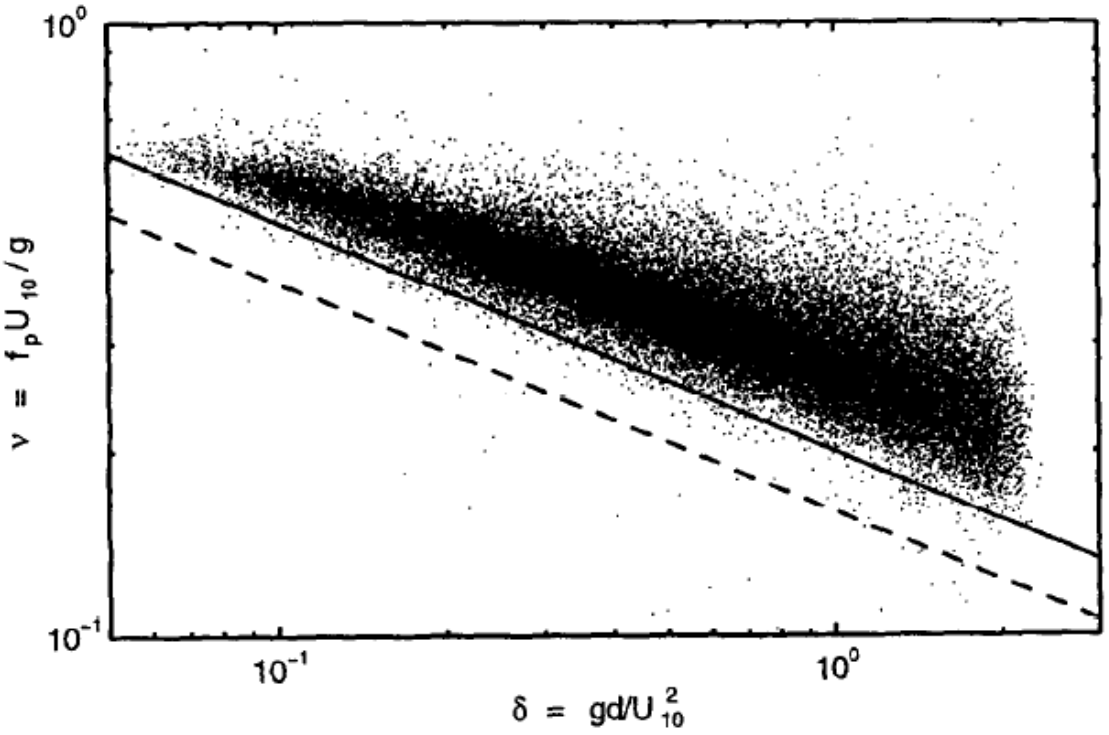

Figure 2.4: Graph of non-dimensional frequency vs non-dimensional depth (Young & Verhagen, 1996) the solid line is the depth limit suggested by equation (2-20) and the dashed line is equation (2-6).

Figure 2.4 shows the depth limit (the asymptotic limit, which the curves figure 2.3 appear to reach). The dashed line is the limit proposed by CERC (1977), equation (2-6), whereas the solid line is the limit proposed by Young & Verhagen (1996), equation (2-20). It is clear that equation (2-6) underestimates the wave frequency (and hence over estimates the wave period), the solid line however appears to fit the data set relatively well.

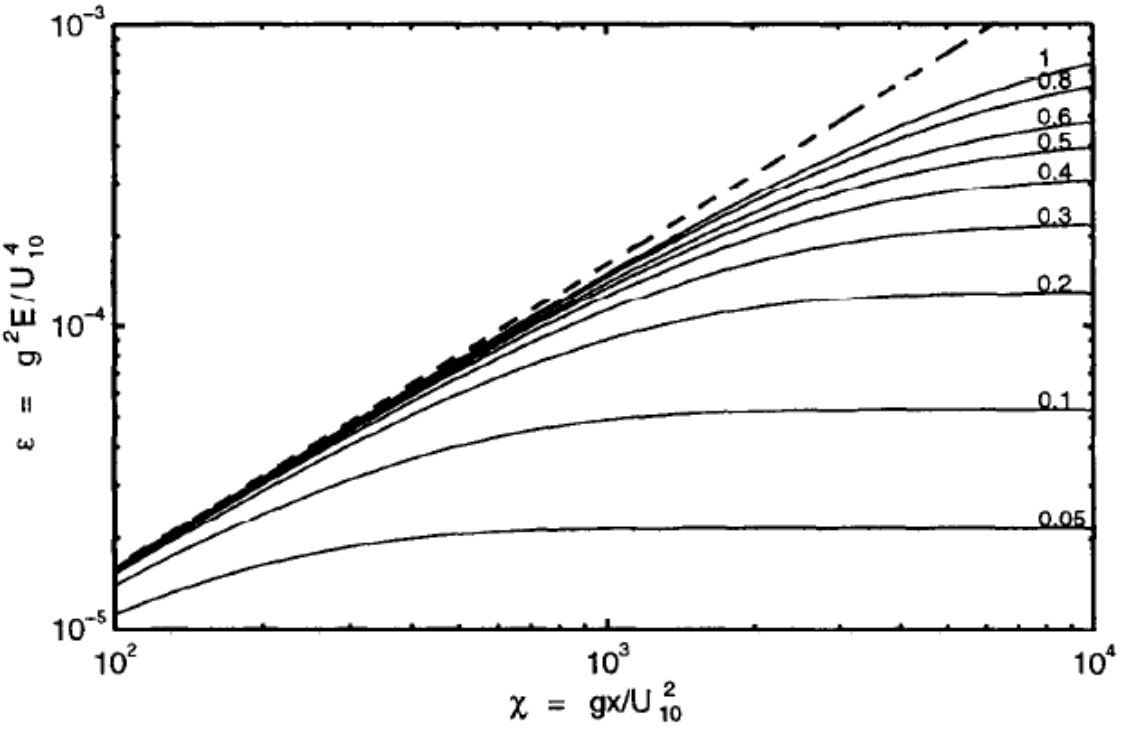

Figure 2.5: Graph showing relationship between non-dimensional energy and non-dimensional fetch (Young & Verhagen, 1996). Each curve shows the effect of the depth limit (the value of the depth number, δ, for each curve is shown on the right), and are defined by equation (2-13), whereas the solid line is the deep water form of equation (2-13).

Figure 2.5 shows how the wave growth is limited by the water depth for a large fetch. The dashed line represents the deep water form of equation (2-13). What the graph shows is at a large fetch the wave energy also appears to reach some asymptotic limit, Young & Verhagen (1996) attributed this to the effect that the water depth has on wave development, similar to what is shown by the figures 2.3-2.4. This depth limit is shown in figure 2.6.

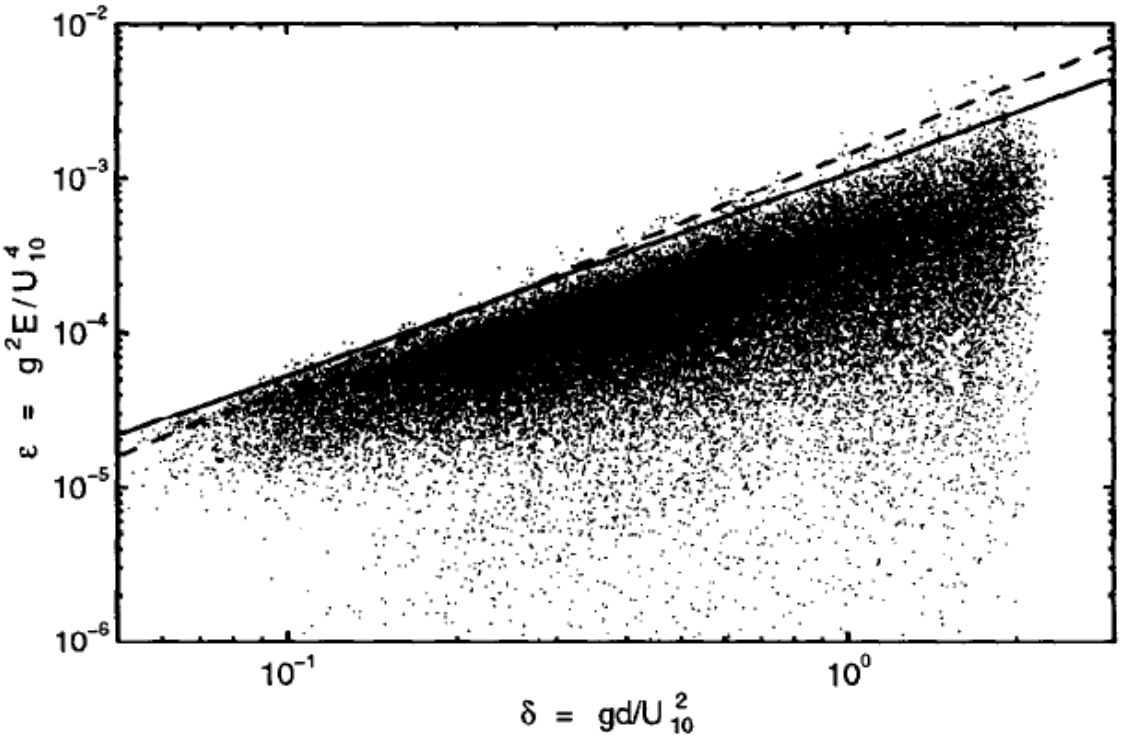

Figure 2.6: Graph showing the relationship between non-dimensional wave energy and non-dimensional depth (Young & Verhagen, 1996). The solid line is the limit defined by equation (2-20), whereas the dashed line is defined by equation (2-6).

Figure 2.6 shows the depth limit (the asymptotic limit, which the curves in figure 2.5 appear to reach). The solid line is represented by equation (2-19), while the dashed line is represented by equation (2-5). It is interesting to note how the limiting equation proposed by Young & Verhagen (1996) is very similar to that which was proposed by CERC (1977).

The depth limit was used to derive a depth-fetch domain. The reader is referred to section 3.4 for a full description of how this was done. Equation (2-13) reduces to the depth limit (equation (2-19)). It is at this depth (for a given wind speed and fetch) that the wave growth becomes depth limited. Therefore it is possible to delineate areas within the lake where the wave growth is depth limited.

The same concept of a depth limit also applies to the non-dimensional energy and hence wave growth. The wave energy can be related to the significant wave height through the following relation (Young & Verhagen, 1996):

$$H_s = 4\sqrt{E} \qquad (2\text{-}21)$$

To summarize, the research conducted by Young & Verhagen (1996) shows how the growth of waves in finite depth is defined by two factors. The first is the fetch and the second is the water depth. The way in which the two interact may be seen as follows: at the initial stage of wave growth, the waves are defined by deep water equations. What this implies is that when the fetch is small, the waves do not interact with the floor since the wave height is small and thus behave as they would if they were in deep water. However at a later stage in the wave growth (i.e. at a large fetch) the waves begin to interact with the floor and thus begin to be limited by the water depth, this is the asymptotic limit that is shown by Young & Verhagen (1996). This is applicable to the model in the sense that the wave energy and frequency would be calculated based on both the fetch and water depth, depending on which result yielded a greater value or lower value (as in accordance with what was mentioned previously) would define the wave growth.

2.3.2 Method 2 – process based approach

As mentioned previously this method involves solving the wave energy equation. This equation is given as follows (Carniello et al, 2011):

$$\frac{\partial N}{\partial t} + \frac{\partial}{\partial x} C_{gx} N + \frac{\partial}{\partial y} C_{gy} N + \frac{\partial}{\partial \sigma} C_{\sigma} + \frac{\partial}{\partial \theta} C_{\theta} = S \qquad (2\text{-}22)$$

where: N is the wave action density and is defined as the ratio of the wave energy E to the relative wave frequency (or intrinsic frequency) (ζ) , and is a function of space (x, y), time (t), frequency (ζ) and direction (θ), C_{gx} and C_{gy} are the x and y components of the wave group celerity. Carniello et al (2011) describes the terms within the equation as follows: the first term is the rate of change of the wave action density with time, the second and third terms propagate the wave action density in space. The fourth and fifth terms propagate the wave action density in the space of the wave frequency and direction. S describes the external factors which contribute to the wave growth. These external factors are for example, white capping and bottom friction.

The best manner in which the wave energy equation can be solved is by setting out a grid on the lake and solving it using finite element analysis. The SWAN (Simulating Waves Nearshore) model could be used to solve equation (2-22) (Holthuijsen, 2007). However this process is time consuming and possibly yields results which might be of

an irrelevant time scale. Since this model is essentially required to be used as an indicator tool for biologists. The time scales which are used by biologists (conducting research within Lake St. Lucia) are in the order of weeks and months (possibly days), thus if the model yields results on an hourly time scale it would contain a large amount of irrelevant data. The reason why the biologists require data on larger time scales is simply due to the reaction time of flora and fauna, since, flora and fauna take a certain periods of time to react to the change in environmental conditions. However the hourly data can be averaged or simply the time scale on the model can be changed. Therefore, the decision to not use a process based model was based on the lack of observed data for the South Lake.

The option could exist where the empirical relations mentioned previously could be used to determine the wave characteristics on a spatial grid. What this would require is a spatial grid with appropriate sizing of the elements. Appropriate sizing would imply square elements (cells) which are not large in comparison to the size of the lake (to improve the resolution). For example at zero EMSL (estuarine mean sea level) the area of the southern lake is 33km^2 (Hutchison, 1974) and if a spatial grid is used whereby each element has a length and breadth of 287.5m, the approximate area of each cell is 0.1km^2, which implies that the ratio between of the area of the lake to each cell is approximately 300, this also represents the number of cells within the grid. A larger number of cells within the grid results in an improvement of the resolution of the spatial model. The wave height and peak period could then be estimated in the same manner as proposed by Young & Verhagen (1996).

2.4 WAVE MEASUREMENT

There are many ways in which waves can be measured. Examples are accelerometers placed in wave buoys, pressure transducers, capacitance or resistive wave probes and Zwarts poles (Young & Verhagen, 1996; Tsai & Tsai, 2009; Smith & Lin, 1984). With regards to the research presented by this dissertation only one method can be used, however each method has its pros and cons. Another method is to record the water surface fluctuations using a video camera and a surveying staff, the footage could then be analysed to determine all the wave heights and determine the significant wave height (refer to figure 3.5 for setup).

2.4.1 Accelerometers

Accelerometers are used in the wave rider buoys (Niclasen & Simonsen, 2008), the advantage of using accelerometers to measure the wave height is that they measure the actual surface change rather than inferring the wave height from theoretical calculations (such as with pressure transducers). However inaccuracies in measurement can occur due to the way in which the buoy is moored (Niclasen & Simonsen, 2008). If the buoy is moored too loosely the wave rider might be steered around the peak of the wave which would cause an underestimate of the wave size. The accelerometer appears to be a good solution to determine the wave height however it only yields accurate results for longer period waves, and the waves which will be formed in the lake are short period waves with a period of around 1s - 2s, as mentioned by Massel (1996), the wave rider buoy does not follow waves with a period of less than 1.8s.

2.4.2 Zwarts Pole

A successful use of the Zwarts pole was by Young & Verhagen (1996) in their research mentioned previously in this paper, their description of the pole follows: Essentially the pole consists of two concentric aluminum poles which form a co-axial transmission line. The outer pole has a number of holes drilled into it to allow water to flow through. An electromagnetic wave is sent down the poles and then reflected once it reaches the water surface, the time it takes to travel from the source to the water surface and back is recorded and the water surface elevation is measured. This appears to be an elegant solution to measuring the wave height however it can be time consuming to build and would still need to be calibrated.

2.4.3 Pressure Transducers

Pressure transducers measure the pressure fluctuations which occur due to the wave which propagate through the water surface. Massel (1996) suggests that the use of pressure transducers to measure waves can be complicated and that the results can

be inaccurate due to pressure fluctuations caused by trapped air bubbles, as well as the fact that the wave heights are inferred from theoretical calculations.

2.4.4 Capacitance & Resistive Wave Gauges

Capacitance and resistive wave gauges measure the wave heights in very similar manners. Capacitance gauges according to Massel (1996) use the principle of linear variation of capacitance with sea level change to measure the change in surface elevation using the sea water as a ground. Resistive wave gauges consist of two parallel wires with a fixed distance between them. The conductance is measured and is proportional to the distance of the wires below the sea water, thus when the water level changes so does the conductance, and hence the wave height can be measured. According to Massel (1996) the use of these wave gauges are better suited for laboratory set ups, however they have been adapted to be used in the field (Sadjadi, 2011). While this might be seen as a very good way in measuring the wave heights in the field, it comes with its problems. These are the fact that the power source and the system used to log the data would need to be made water proof. Another concern would be the space on the boat, since the boat which will be used in the field trips undertaken for this research will be a semi-rigid which is only 4.8m long.

Thus in order to obtain an easy yet accurate method of determining the significant wave heights, it was decided that a video camera and a surveying staff could be used (a diagram of the setup is shown in figure 3.5). The waves formed in a shallow lake have a narrow-band spectrum (Holthuijsen, 2007), i.e. the wave heights are approximately equal to each other (Massel, 1996). This would imply that a long sampling period of 20 minutes would not be required. A representative sample size could be obtained within a matter of minutes. The significant wave height is defined as the average of the highest one-third of the wave heights (Reeve et al, 2004). From this method it is not possible to measure the peak period very easily, however it can be assumed that if the wave heights measured correlate with what is predicted by Young & Verhagen (1996) then the peak period should correlate with what they predict.

2.5 WAVE BOUNDARY LAYER

The wave boundary layer is crucial when determining the shear stress exerted on the lake bed. Essentially the shear stress exerted by the waves on the lake bed is as follows (Reeve et al, 2004):

$$\tau_b = 0.5\rho f_w {U_m}^2 \quad (2\text{-}23)$$

Where: τ_b is the shear stress at the bed (Pa), f_w is the wave friction factor, U_m is the maximum horizontal velocity at the bed (m/s), ρ is the density of the fluid (kg/m^3).

Since the re-suspended sediment comprises of fine silt and clay (refer to section 2.6), the boundary layer which develops is assumed be that for a smooth surface.

Essentially the boundary layer depends on the semi-orbital excursion, the period of the wave and the kinematic viscosity of water (Liu, 2001), i.e. the Reynolds number. This is what is expected since the oscillating water particles are essentially responsible for the development of this boundary layer, thus the length over which they oscillate would need to be known (it is over this length that the boundary layer is formed), and the time at which the particles take to travel this distance (this is obviously the period). If the particles travel the distance in a relatively fast time, it is very likely that the associated boundary layer would be turbulent and vice versa; for if the particles travel this distance in a longer time the associated boundary layer would be laminar. Once it has been ascertained whether the wave boundary layer is either laminar or turbulent, the friction factor according to Liu (2001) can be estimated as follows:

For a laminar boundary layer on a smooth bed, $A^2\omega/v < 3\times10^5$

$$f_w = 2(v/A^2\omega)^{0.5} \quad (2\text{-}24)$$

For a turbulent boundary layer on a smooth bed, $10^6 < A^2\omega/v < 10^8$

$$f_w = 0.024(v/A^2\omega)^{-0.123} \quad (2\text{-}25)$$

where: v is the kinematic viscosity of water (1×10^{-6} m^2/s), A is the semi-orbital excursion (amplitude of a water particle on the bottom), ω is the wave angular frequency (2π/T), T is the wave period (s).

2.6 EROSION AND DEPOSITION

The erosion and deposition of cohesive sediment depends largely on the physical, electro-chemical and biological characteristics of the sediment (Bureau of Reclamation, 2006). The sediment that exists in Lake St Lucia (due to the fluvial deposits of the feeder tributaries) comprises of mainly fine silt and clay particles with a D_{50} of 4μm (Chrystal & Stretch, unpublished), thus erosion and deposition cannot be defined by non-cohesive sediment relations. The shear stress exerted by the waves on the lake bed is continuously varying in both magnitude and direction. It is highly unlikely that the erosion which results would be mass erosion, since the wave boundary layer is small; Guang & Yi-gang (2007) suggest that the wave boundary layer for laminar flow is in the order of 2mm and for turbulent flow is 10mm. While it seems arbitrary to state the size of a boundary layer without stating the size or length of the waves, water depth and even the bed surface characteristics, the estimation of the size of the boundary layer, according to Guang & Yi-gang (2007), can be used as an indication that the boundary layer for waves is much smaller than that for currents. The associated boundary layer for currents is equal to the water depth (Bailey & Hamilton, 1996). Partheniades (1962) suggested the following formula to predict the surface erosion rate:

$$E_r = \begin{cases} \mathrm{M}(\tau/\tau_c - 1), & \text{if } \tau > \tau\mathrm{c} \\ 0, & \text{if } \tau \leq \tau\mathrm{c} \end{cases} \qquad (2\text{-}26)$$

where: E_r is the surface erosion rate (kg/m^2/s), τ is the shear stress exerted by the waves on the bed (Pa), τ_c is the critical shear stress (pa), M is the erosion rate constant (kg/m^2/s).

The above formula is based on experiments done in a long rectangular flume. The flow characteristics in a rectangular flume are very different from those which occur due to wind induced waves in a lake. These differences are namely the boundary layer (as mentioned previously); the flow in a flume is all in one direction, whereas the flow associated with waves is oscillatory and the shear stress exerted by the flow in the flume is constant for that specific flow, the shear stress exerted by waves vary due to the spectral range of the waves.

The previously mentioned formula (2-26) should still nonetheless be sufficient in defining the erosion characteristics of the wind induced waves, since it makes sense that once the shear stress exerted is greater than some critical shear stress erosion

should occur. The problem which arises from this formula is that if the critical shear stress is zero there holds no solution for the equation.

An important factor to consider which would influence the erosion would be the degree of consolidation of the sediment. This is important since the sediment being re-suspended is cohesive in nature. As each layer of sediment is removed from the bed because of erosion, a new layer of sediment is exposed. This new layer is acted upon by the same shear force (due to the waves) as the previous layer. However the new layer has a higher degree of packing (due to consolidation) and thus has a higher resistance to the shear force, implying less of it is re-suspended (Krone, 1962). In order to incorporate this effect of consolidation, equation (2-26) can be multiplied by some time scale. This notion implies that it will take a certain period of time for the waves to erode the bed to a point where the critical shear stress is equal to the wave exerted bed shear stress. In order to obtain a total suspended solids (TSS) value in g/L, the amount of eroded material per square metre (estimated by equation (2-26) once multiplied by the time scale) can be multiplied by the area and divided by the volume. Since the volume is quite simply the depth multiplied by the area, equation (2-26) can be divided by the depth because the areas cancel. The following formula results:

$$C_{er} = \begin{cases} \frac{T\mathrm{M}(\tau/\tau_c - 1)}{d}, & \tau > \tau\mathrm{c} \\ 0, & \tau \leq \tau\mathrm{c} \end{cases} \qquad \text{(2-26a)}$$

where: C_{er} is the concentration of sediment due to erosion (g/L).

Formula (2-26) was adapted by Luettich et al (1990) to read as follows:

$$C_{er} = \begin{cases} 0, & \tau \leq \tau\mathrm{c} \\ \mathrm{K}\left(\frac{\tau - \tau_c}{\tau_{ref}}\right)^{\mathrm{n}}, & \tau > \tau\mathrm{c} \end{cases} \qquad \text{(2-27)}$$

where: C_{er} is the concentration of sediment due to erosion (g/L). K is a model parameter with units of g/L, τ is the shear stress exerted by the waves (Pa), τ_c is the critical shear stress (Pa), τ_{ref} is a reference shear stress (Pa) required to make the term in brackets dimensionless and n is some exponent.

Luettich et al (1990) argued that the critical shear stress in equation (2-27) should be set to zero. This was based on work by Lavelle and Baker (1984) and Lavelle & Mofjeld (1987) who argued that the critical shear stress for incipient motion should be set to zero. Lavelle and Baker (1984) and Lavelle & Mofjeld (1987) clearly distinguished between the critical shear stress for incipient motion and the critical shear stress at

which the single particles are eroded. Setting τ_c to zero does not take into account the effect that consolidation has on sediment re-suspension, but it has been seen (from the field work undertaken for this research) that a layer of fluid mud appears to develop in the vicinity of the lake bed. For arguments sake this fluid mud has no critical shear stress because it is a fluid. One could argue however that this mud has already been re-suspended. Formula (2-27) takes into account the fact that the critical shear stress could be zero. The fluid mud layer or „fluff" layer has been observed in a number of situations involving sediment re-suspension in shallow lakes (Luettich et al, 1990; Mehta & Jain, 2010). The argument proposed by Mehta & Jain (2010) was that there were three different manners in which the fluid mud layer was formed which are as follows:

1. $\tau \leq \tau_c \leq \tau_y$. The shear stress exerted by the waves is too small to erode the bed; however there is a buildup of pore pressure due to penetration of the wave orbits. The effective normal stress vanishes, mud rigidity decreases and the lake bottom is said to be in a "fluid mud like transitory state." τ_y is the plastic yield shear stress.
2. $\tau_c \leq \tau \leq \tau_y$. The shear stress exerted by the waves is strong enough to erode the surface of the lake bed. This causes the water to become turbid. Once the wave action stops, the fluid mud returns to its bed like state.
3. $\tau_c \leq \tau_y \leq \tau$. The bed erodes rapidly causing the water to become significantly turbid. There is no change to the density below the eroding surface. Once the wave action ceases, where there is hindered settlement, fluid mud layers form, over time the bed reverts back to its original state.

For the purpose of this research the critical shear stress will be taken into account to accommodate for the effects of consolidation.

An evaluation of the two methods of sediment re-suspension, equations (2-26a) and (2-27) is required in order to determine which would be the best suited for modelling in the case presented by this research. This can be done by comparing the results obtained by the two methods. The evaluation of (2-26a) is as follows:

- By multiplying (2-26) by a time scale it allows the erosion to be limited, incorporating the effect that the critical shear stress has on limiting the amount of sediment that is re-suspended. It cannot be seen as representative of when the water column reaches a steady state, i.e. when the vertical sediment flux is

zero (Hamilton & Mitchell, 1996), since this method does not incorporate deposition.

- The problem arises if the critical shear is zero.
- This method is sensitive to depth since it is directly related to the water depth.

Evaluation of (2-27) is as follows:

- It allows for when the critical shear stress is equal to zero.
- The problem arises when determining K. According to (Hamilton & Mitchell, 1996) if $E = M|\tau|^n$ then at the steady state condition (when erosion equals the deposition), $C_e = \frac{E}{w_s}$, where C_e is the equilibrium concentration and w_s is the settling velocity, $K = \frac{M}{w_s}$. However this implies that in order to check the calibrated K value against the expected values the equilibrium concentration must be known, which is difficult to measure.
- This method incorporates the sediment flux through the model parameter K, which is the erosion rate constant divided by the settling velocity therefore including the effects of deposition.
- The method is indirectly related to the depth, through the wave height and shear stress prediction, thus it is less sensitive to the method mentioned above.
- The exponent, n, was assumed to have a value of one. This is in accordance with what the Bureau of Reclamation (2006) which states that through a number of investigations the erosion rate appears to be linear.

The use of equation (2-27) would be more accurate representation of the physical process of re-suspension unlike equation (2-26a). While both methods limit the amount of sediment re-suspension, the manner in which this is described by equation (2-27) is accurate for the reasons given previously. The physics upon which equation (2-27) is based is as follows (Luettich et al, 1990):

At any given time the vertical sediment flux is given as follows:

$$\zeta = E_r - w_s C \qquad \text{(2-27a)}$$

where: ζ is the sediment flux (kg/m^{2}s), E_r is the erosion rate (kg/m^{2}s) , $w_s C$ is the deposition flux (kg/m^{2}s) .

Dividing equation (2-27a) by the settling velocity (w_s) yields the concentration of sediment within the water column. The model parameter K, as mentioned previously, is

the erosion rate constant divided by the settling velocity. Thus it can be seen that the method proposed by Luettich et al (1990) is based on basic physics.

A method of reconciling (2-26a) and (2-27) is possible as follows: once the timescale is established through calibration, the depth could be divided by this value, hence yielding a settling velocity. M could then be divided by this number to yield the model parameter K. This implies that M and T would remain constant while K and w_s would change accordingly.

The Bureau of Reclamation (2006) suggest that M lies between the values $1x10^{-5}$ - $5x10^{-4}$ kg/m^2/s, this correlates with what was suggested by Chao et al (2008) where it is suggested that the values of M lie between $1x10^{-5}$ - $4x10^{-4}$ kg/m^2/s. Mehta & Jain (2010) suggest that the range of the critical shear stress is between 0.1 to 0.3 Pa.

In order to incorporate the effects of deposition Luettich et al (1990) solved the three-dimensional mass transport equation, it was assumed that the water column was well mixed, which is the same assumption that this research paper makes. Therefore the only terms considered in the three-dimensional mass equation were those in the z direction i.e. the molecular diffusion terms have been dropped, such that:

$$\frac{\partial \bar{c}}{\partial t} + \frac{\partial[(\bar{w} - w_s)c)}{\partial z} = -\frac{\partial[\overline{w'c'}]}{\partial z} \tag{2-28}$$

Assuming there is little stratification throughout the water column, equation (2-28) becomes:

$$h\frac{d\tilde{c}}{dt} = -w_s\bar{c}|_{-h} + \overline{w'c'}\big|_{-h} \tag{2-29}$$

Where: $\tilde{c}$ is the depth averaged concentration (g/L), w_s is the settling velocity (m/s), w is the velocity in the z direction (m/s), h is the water depth (m).

$$\beta = -\frac{w_s\bar{c}|_{-h}}{\tilde{c}} \tag{2-30}$$

$$\mathrm{E} = \overline{w'c'}\big|_{-h} \tag{2-31}$$

β can be defined as being the settling velocity multiplied by a factor which depends on the vertical stratification of the sediment (Luettich et al, 1990), since for this model it is assumed that the water column is well mixed, β is the settling velocity. E is the erosion as mentioned earlier, calculated by either equation (2-26a) or (2-27). By solving equation (2-29) a simple analytical solution can be derived, which can be used to estimate how the sediment concentration varies with time, such that:

$$\tilde{c} = C_e + C_{bak} + \left(\tilde{c}_i - C_e - C_{bak}\right)\exp\left[\frac{-\beta}{h}(t - t_i)\right] \quad (2\text{-}32)$$

where: C_e is the concentration of sediment due to erosion (g/L); C_{bak} is the background concentration which exists in the lake, possibly due to biology. The initial solution is obviously such that $\tilde{c} = \tilde{c}_i$ at $t = t_i$.

As mentioned previously when working out the total erosion, the erosion rate can be multiplied by a specific time scale that limits the amount of erosion in order to represent the effects of consolidation. It can be used in equation (2-32) if the time scale is less than the time step used for the unsteady case. For the present application, the smallest time step of interest is 1 hour. From visual accounts (when undertaking the field trips required for this research) it appears that the concentration of sediment reaches a constant equilibrium value in a couple of hours when wind conditions are approximately steady. The use of equation (2-32) would not be useful when looking at a time step of days or months, as the model calculates turbidity independently for each day and month. However deposition can be incorporated through the time limit proposed in equation (2-26a) which can be used to limit the sediment re-suspension based on the sediment flux equilibrium.

In order to determine the settling velocity the flocculation processes need to be accounted for. Flocculation depends on a number of factors - Burban et al (1990) suggested that the median floc diameter could be estimated from:

$$d_m = \left(\frac{\alpha_0}{CG}\right)^{0.5} \quad (2\text{-}33)$$

where: d_m is the median floc diameter; α_0 is equal to 1×10^{-8} $g^2/cm^2/s^2$ for cohesive sediment in freshwater (this however would need to be changed since the South Lake is hardly ever fresh water according to Lawrie & Stretch (2008)). C is the concentration of sediment (g/cm^3), G is the fluid shear stress ($dyne/cm^2$).

The settling velocity can then be calculated as follows (Burban et al, 1990):

$$w_s = a d_m^{\,b} \quad (2\text{-}34)$$

where: $a = 9.64 \times 10^{-4}(CG)^{0.85}$ and $b = -[0.8 + 0.5\log(CG - 7.5 \times 10^{-6})]$.

Equations (2-33 – 2-34) are based on empirical relations determined from laboratory data. It is advised by the Bureau of Reclamation (2006) that the settling velocity due to flocculation must be determined experimentally, since it is sight specific.

Krone (1962) suggests the following formula based on flume experiments:

$$w_s = aC_s^{4/3} \quad (2\text{-}35)$$

where: w_s is the settling velocity (m/s), C_s is the concentration of sediment (g/L) and a is an empirically derived constant dependent on the type of sediment (Bureau of Reclamation (2006) suggest 0.001).

This method was based on flume studies; the process of sediment re-suspension is completely different to what is experienced in a shallow lake. This is because the flow is in one direction, whereas water waves cause oscillations of the water particles in the vicinity of the lake bed.

It would therefore be advised to base the settling velocity on appropriate relations derived by observing the behaviour of the Southern Lake sediment. This however falls out of the scope of this research, thus a settling velocity must be assumed when using equation (2-32).

2.7 LIGHT ATTENUATION THROUGH WATER

Limiting the amount of light penetrating a body of water greatly affects the biological functioning of the system. Reduced visibility can reduce predation, shifting the balance of the ecosystem to allow for larger numbers of certain species to exist within lower trophic levels. Limited light penetration also decreases primary production due to the decrease in available energy (Cloern, 1987).

The process by which light travels through water and the factors affecting it are defined by Sadar (1998):

Even when light travels through pure water some of the water particles scatter light to a certain degree. Where suspended sediment is present in samples, the manner in which the light is scattered depends on the size, shape and composition of the sediment as well as the wavelength of the transmitted light. Essentially when a very small (minute) particle interacts with an incident light beam, it behaves as a point source by absorbing the light energy and then re-radiating it in all directions. The spatial distribution of the light emitted from the particle depends on the ratio of the particle size to the wavelength of the light source. Particle sizes which are much smaller than the wavelength of the light source emit the light in a uniformly scattered distribution around

the particle. However as the ratio of the particle size to the light wavelength increases a number of inference points are created (due to light being emitted from different points on the particles), this leads to a forward scattering of the light, and this is shown by the figure 2.7 below.

Another important factor in light scattering is the colour of the suspended solids. Since each colour absorbs light energy in different bands of the visible spectrum of light, thus changing its properties. A particle"s shape and refractive index also affect how the light is scattered, for example spherical particles (sand) exhibit a more forward-to-back scatter ratio than coiled or rod shaped particles.

The concentration of the sediment also affects the light scattering. Essentially as the concentration increases, more scattered light strikes the particles, more scattering occurs and absorption increases. Therefore an upper limit of measurable turbidity exists.

This is very important when understanding how nephelometers work in the field; it also helps explain differences and errors experienced during sampling. It is highly unlikely that the upper limit of measurable turbidity will be reached in the South Lake; however the limit of the YSI 6920 (instrument used in field) will need to be evaluated. This limit to measurable turbidity poses the threat of inaccurate readings out in the field, however this can be avoided by diluting the sample and multiplying the reading by the factor of dilution to obtain the actual turbidity.

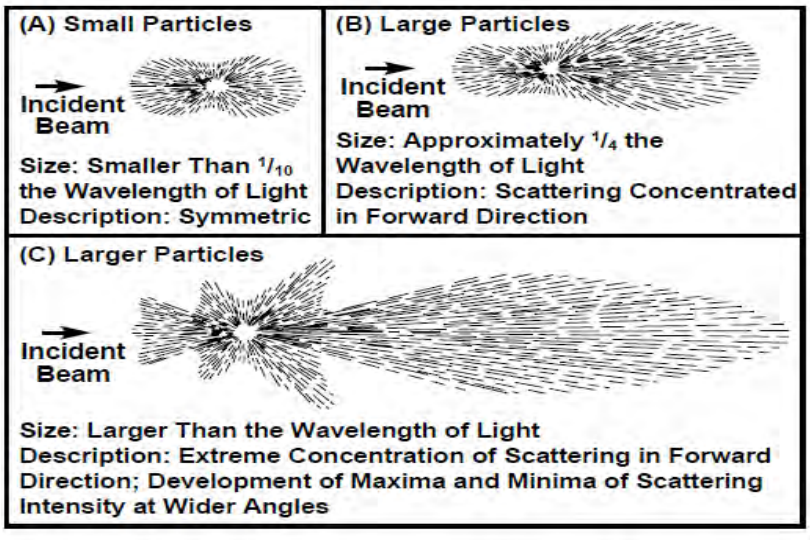

Figure 2.7: Light scattering by particles (Sadar, 1998).

The attenuation of light through water is caused by absorption and scattering (Davies-Colley & Smith, 2001). In the process of absorption, the energy of the light is simply transformed into heat energy, whereas the attenuation of light due scattering is as a result of the sediments that are suspended within the water (Davies-Colley & Smith, 2001). It is because of this scattering that the water appears to be „murky" or turbid. The more turbid the water is the less clear it appears to be however Davies-Colley & Smith (2001) suggest that the concept of water clarity is distinctly different to turbidity but they are related via an inverse relationship. Water clarity can be measured using a secchi disk (Tyler, 1968).

Turbidity can be determined by emitting a light (usually of wavelength 830nm to 890nm) and then recording the light which is scattered by the suspended sediment, the angle between the emitted light and the detected light is 90° (YSI Environmental monitoring systems manual). Both Grayson et al (1996) and Davies-Colley & Smith (2001) state that the readings between two different turbidity metres are not consistent for the same water sample. This arises due to the different optical designs between nephelometers, for example, differences in the spectral emission of the light source, the spectral intensity of the detector and the angular range of the detector. Thus, when recording turbidity measurements it is vital to be consistent with the nephelometer used and to not switch between two or more different devices. Therefore it is important to state the nephelometer used to avoid any potential discrepancies in results between different researches. For the purpose of this research the nephelometer used is an YSI 6920.

Cyrus and Blaber (1988) suggest classifications of turbidity with which one can gauge how turbid a system is. The classifications are as follows:

- Less than 10 NTU, clear.
- Turbidity ranging from 10 to 50 NTU is a semi-turbid system.
- Turbidity ranging from 51 to 80 NTU is a predominately turbid system.
- Greater than 81 NTU is a very turbid system.

These classifications can be used to gauge whether the level of turbidity within St. Lucia is high or low.

2.8 SUMMARY

This literature review highlights the different parameters required to develop a mathematical model which predicts the sediment re-suspension within the Southern Lake. It is important to be able to measure parameters such as wave height and sediment re-suspension so that the model can be calibrated, resulting in the development of an accurate model. The use of a camera and graduated staff to measure the wave height was seen as adequate, however this methods limits one in the ability of measuring the peak frequency. The use of a nephelometer to measure the sediment concentration within the water column was seen as adequate. However the nephelometer would need to be calibrated to give measurements of TSS, allowing an instantaneous measurement of the sediment concentration within the lake.

Equations (2-27) and (2-26a) can be used to determine the concentration of sediment within the water column. These two equations can be compared and the method which is judged to be better by certain criteria can then be used to predict the concentration.

The proceeding chapter outlines the methods used to obtain and analyse the data.

CHAPTER 3

EXPERIMENTAL METHODS

This chapter discusses the procedures used in obtaining field measurements of the parameters required for this research. These parameters were turbidity readings, wave height measurements and TSS values. The procedure used to calibrate the model is also discussed.

3.1 Field Study

A field study was conducted within the Southern Lake. The reason why field measurements were used instead of already existing measurements was due to the unreliability of the few readings that were taken. Turbidity readings were recordered by Cyrus & Blaber (1987) during the period from 1980 to 1983. The turbidity readings were taken 3m and 10m from the shore by Cyrus & Blaber (1987) who saw this as a reasonable indication of the turbidity within the lake, however this is certainly not the case as will be shown in this dissertation. Field measurements were taken on the following dates: 21st – 25th March 2011, 18th – 21st April 2011 and 13th – 15th June 2011.

The aim of the field trip was to obtain a good data set of turbidity readings. This implied that sampling would need to occur at a number of points on the lake; this would show the spatial variability of the sediment re-suspension throughout the lake for a specific wind. In order to achieve a good calibration of the model it would be ideal to get a large number of data points, which varied in value. To achieve this one approach is to start measuring the turbidity values early in the morning until late in the afternoon. This approach relies on the diurnal pattern of the wind, which is generally light in the morning gradually increasing around midday followed by a decrease in the afternoon. This diurnal pattern in wind speed would imply that the turbidity readings should follow a similar trend to that of the wind speed, except when there is a decrease in wind speed, since the deposition of the re-suspended sediment is not instantaneous. To determine how the parameters varied in relation to one another, ideally the measurements would be taken as follows:

1. Measure the depths along a line of constant fetch. In theory if the wind speed stays the same then these measurements would show how the non-dimensional depth number varies in relation to the energy number along a line of constant fetch.
2. The next step would be to carry out the above method along a line of different fetch. This would show how the non-dimensional fetch number varies in relation to the energy number along lines of constant depth.

3.1.1 Data Collection

The parameters that were measured in the field were: Turbidity (NTU), wind speed (m/s), wind direction (degrees), water depth (m), the GPS coordinate, significant wave height (m) and a water sample at each point was taken.

The following apparatus was used:

- A nephelometer, used to measure the turbidity (NTU). This was a YSI 6920.
- A graduated survey staff, used to measure the water depth, as well as in determining the wave height.
- A Kestrel 4500 wind anemometer, used to measure the wind speed and direction (refer to appendix E).
- A motorized boat, used as a mobile platform to take samples from and move throughout the lake.
- A „pop" bottle, used to take the water samples.
- 1 litre bottles, used to store the water samples.
- A video camera to record the wave pattern so as to determine the significant wave height.

Due to the very low water levels it was difficult to obtain a large data set with good variation in turbidity measurements. This was due to the fact that there was only one channel which was deep enough to navigate the boat through (refer to figures 3.1-3.4). Thus while there was potential to take a large number of readings, the variability of these readings was low, thus only a selected number were chosen. The measurements which were chosen had a good variability. The second issue which arose from the low water depths was that it was impossible to take a number of readings along a line of

constant fetch, and then vary the fetch to see how the non-dimensional wave numbers related to each other.

Figure 3.1: Sampling points in the South Lake on 22nd March 2011, (Google Earth, 2011).

Figure 3.2: Sampling points in the South Lake on 24th March 2011, (Google Earth, 2011).

Figure 3.3: Sampling points in the South Lake on 19th April 2011, (Google Earth, 2011).

Figure 3.4: Sampling points in the South Lake on 20th April 2011, (Google Earth, 2011).

The sampling procedure for each point in figures 3.1-3.4 may be summarized as follows:

1. The boat was stopped and anchored in place.
2. The wind speed was recorded. This was done by holding the Anemometer at an approximate height of 1.9m. The wind speed was averaged for a time period of 2-3 minutes.
3. Using the YSI the turbidity measurement was recorded. In order to determine whether the water column was well mixed, the turbidity value was checked at three different levels: (1) just below the water surface, (2) at a depth of half the water depth, (3) near the bottom of the lake. Since the lake bed is not well defined, due to the „fluff" layer which forms near the bottom of the water column, accurate turbidity readings at or near the lake bed were difficult to achieve, thus this depth ended up being very similar to that of (2). Once it was determined that the water column was well mixed the YSI was held in position for 2-3 minutes, this averaged reading was then recorded. The depth and position of the YSI was the same as that of the water sample, which varied for each sample point.
4. While the turbidity reading was being taken, a water sample was taken. This was done by lowering a „pop" bottle to the same position where the turbidity sample was being taken and then the water sample was taken. The way in which the „pop" bottle works is such that it prevents a water sample, taken at any depth, from being contaminated when lowering the sample into the water. Two strings are attached to the bottle, one to the bottle and the other to a cork which is placed in the bottle neck preventing water from entering. Once the bottle is at the desired depth a sharp jerk is applied to the string, releasing the cork and allowing the water to enter the bottle.
5. From the water sample the TSS was calculated, which was related to the turbidity. This will be discussed in the proceeding chapter 3.1.2.
6. The wave height was then determined, this too will be discussed in more detail in the following sub-chapter.

3.1.2 TSS and Turbidity Relationship

From the water samples taken out in the field the TSS values for each sample was then measured. This was then related to the turbidity reading at each sample point.

The relationship between the TSS and turbidity could then be used in the model when calculating the turbidity from the predicted TSS. In order to check whether the turbidity recorded for that particular sample was the actual turbidity, the sample was mixed and then the turbidity of that sample was measured. This was then compared to what was measured in the field and if the difference was not significant, say 5% more or less, then the original reading was used.

The apparatus comprised the following:

- Vacuum pump.
- Whatman GF/F 0.7µm filters.
- Filtration apparatus.
- 20ml pipette.
- 100ml measuring cylinder.

The measurement procedure used standard methods for the examination of water & wastewater (2005) as follows:

- The filters were dried in an oven at 110°C overnight. Each filter was then weighed; this was the dry weight of the filter.
- The water was shaken until it was considered well mixed. A 100ml sample was then prepared using the pipette and the cylinder.
- The dry filter was placed over the filtration apparatus which was connected to the vacuum pump.
- The 100ml water sample was then filtered.
- Each filter was then placed in an oven at 110°C overnight and weighed; this was then the combined weight of the filter paper and the sediment.
  The TSS was calculated as follows: TSS = $10x(W_{(f+s)}-W_{(f)})$, where: $W_{(f+s)}$ is the combined dry weight (g) of the sediment and the filter and $W_{(f)}$ (g) is the dry weight of the filter.
- A graph of the turbidity vs TSS was then plotted and the relationship was found (refer to Chapter 5 for the plot).

3.1.3 Wave Height

The significant wave height was determined for each sample point, from the data observed in the field. What follows is a description of the procedure used in determining the significant wave height.

- A rope was attached to the surveying staff, which was then placed in the water away from the boat.
- If the waves were strong enough to push the staff over then the staff was held in place as far away from the boat as possible and as vertical as possible.
- The staff was filmed using the video camera for approximately 5 minutes, resulting in a sample size of around 100 – 200 wave heights.
- The film was then replayed using Adobe Premier Pro.; this recording was slowed down making it easier to determine the wave heights.
- The height of each wave was then recorded. The wave height was taken as the height reading of the crest minus the proceeding height of the trough.
- The significant wave height was then calculated as the average of the highest one third of the wave heights.

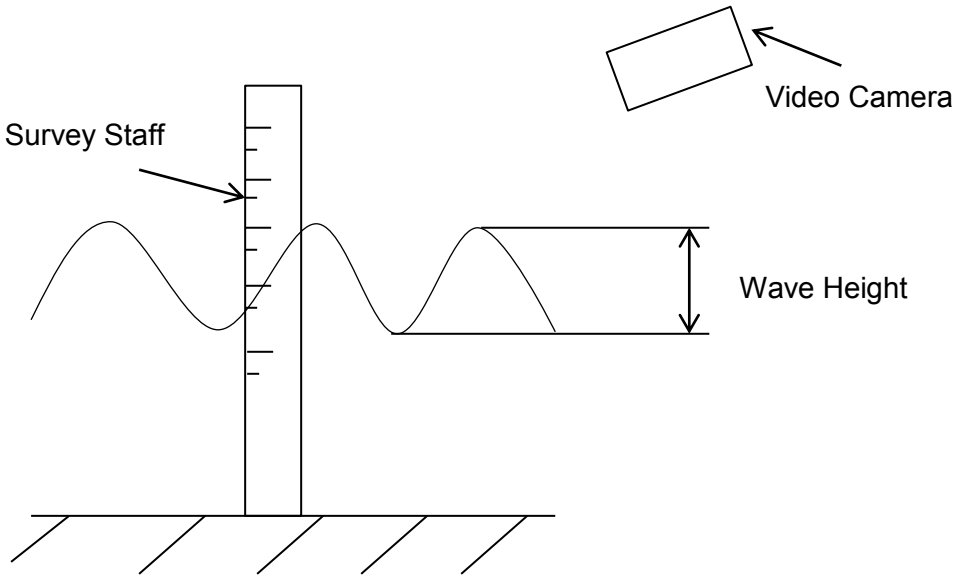

Figure 3.5: Set up for the wave height measurement.

3.1.4 Turbidity Build Up

In order to determine how the sediment re-suspension responds to the daily wind pattern, turbidity was measured at one sample point from the morning until early afternoon. The apparatus used was a YSI 6920, anemometer and a motorized boat. What follows is a description of the procedure used to measure the turbidity build up.

- The boat was anchored in position.
- The procedure of measuring the turbidity was the same as what was mentioned in 3.1.1.
- Turbidity readings and wind velocities were taken approximately every 30 minutes.
- Measuring the wind speed was also the same as mentioned in 3.1.1.

3.2 Model Calibration

The model was then calibrated using the data sampled from the field trip. The difference between the observed turbidity values and predicted values was squared (in accordance with the least squares optimisation). Using the *solver* tool on Excel the sum of the squared differences was set to a minimum. For equation (2-26a) the parameters adjusted by the *solver* tool were: the critical shear stress, τ_c, erosion rate constant, M, and the time scale.

For equation (2-27) the parameters adjusted by the *solver* tool were: the critical shear stress, τ_c, the model parameter, K and the reference shear stress, τ_{ref}.

Constraints were placed on the above parameters to ensure that they were within the expected values. The erosion rate constant was constrained to a maximum value of $5x10^{-4}$ kg/m^2/s (this is the upper limit suggested by the Bureau of Reclamation (2006)), the critical shear stress was constrained to maximum of 0.3 Pa (the upper limit proposed by Mehta & Jain (2010)) and from observations the time scale was constrained to 9000s. The other parameters (such as, K) were not limited since no significant research on the proposed limits was found.

The depths used in the calibration were the depths at each sample point. Ideally the average depths over the fetch should be used since it is more representative of the

depth over which the fetch generating the waves has travelled. However this was not possible since the only available bathymetric map was drawn in 1970, and was considered to be out-dated.

Half the data set was used to calibrate each model. The remaining half of the data set was then used to validate the model. The sample points were independent of each other. This was because at each sample point the water depth, location, fetch, time and hence wave heights were different and because the turbidity measurement depended on these parameters, each turbidity reading recorded at each sample point was independent of the rest.

3.3 Sensitivity Analysis

A sensitivity analysis was conducted for the model (refer to section 5.1.5 for results). This was done to determine the response of the model to any change on parameters. The parameters investigated were the wind speed and the water depth. The critical shear stress and erosion rate constant were excluded from the sensitivity analysis. From the manner in which the equation (2-27) is formulated it is clear that these relationships are linear. The main parameters which drive the sediment re-suspension within Lake St Lucia are the wind speed and the water depth. Therefore gauging the sensitivity of the model towards these parameters would be more important. The percentage change in turbidity was determined by subtracting the old value (no change in the parameter of interest) from the new value (estimated after increasing the parameter of interest) and dividing by the old value.

3.4 Depth–Fetch Domain

In order to delineate locations in the lake where wave growth is in depth limited conditions or fetch limited conditions, a depth-fetch domain was estimated using the model. This was done as follows:

- The wind speed was kept constant.
- The fetch was then incrementally increased for each constant wind speed, the increments were: 250, 500, 1000, 1500, 2000, 3000, 3500, 4000, 4500m.
- For each of the fetch increments the depth was adjusted until the energy in equation (2-19) equalled that of equation (2-13).

- This depth was the depth below which the lake was considered in depth limited conditions.
- The process was then repeated for wind speeds of 4, 6, 8, 10 m/s.

CHAPTER 4

MODEL DEVELOPMENT

This chapter discusses the development of the mathematical model. The theory upon which the wind-wave model is based is discussed and then linked to the mathematical model. A step by step procedure is given explaining how each parameter is estimated in the model.

4.1 Model Structure Overview

A brief description of the model structure is given in the following paragraph. It describes the manner in which each parameter is estimated from the initial input parameters (the water depth and wind velocity). Refer to appendix C for the model flow diagram. These parameters are described in more detail in section (4-4).

Input parameters were the water depth and wind velocity. The depth no. (2-4) and fetch no. (2-3) were then estimated. The energy no. (2-13) and depth limited energy (2-19) were then estimated using the depth no. and fetch no., from these values the significant wave height was predicted using equation (2-21). The depth no. and fetch no. were then used to estimate the peak frequency no. (2-16) and depth limited peak frequency (2-20). The wave period (2-21) was then estimated from the latter. The friction factor was predicted using either equation (2-24) or (2-25). The wave exerted bed shear stress was then estimated using equation (2-21). The erosion was then predicted using equation (2-27), using this in combination with the assumed settling velocity, the suspended sediment concentration was then estimated using equation (2-32). The turbidity was then estimated using equation (4-9).

4.2 Wind-Wave Growth

The process of wind-wave growth has been described in chapter 2.2 and will not be discussed further here, except for the fact that the understanding of this process is important for the development of an accurate model.

4.3 Formulation

Consider the figure 4.1, an arbitrary area of water which has a uniform depth d, and a fetch length x. The parameter, U_{10}, is the wind speed at 10m above the water level, for the purpose of discussion U is equal to U_{10}. Consider a point within the area called A1, which has a fetch length x_1.

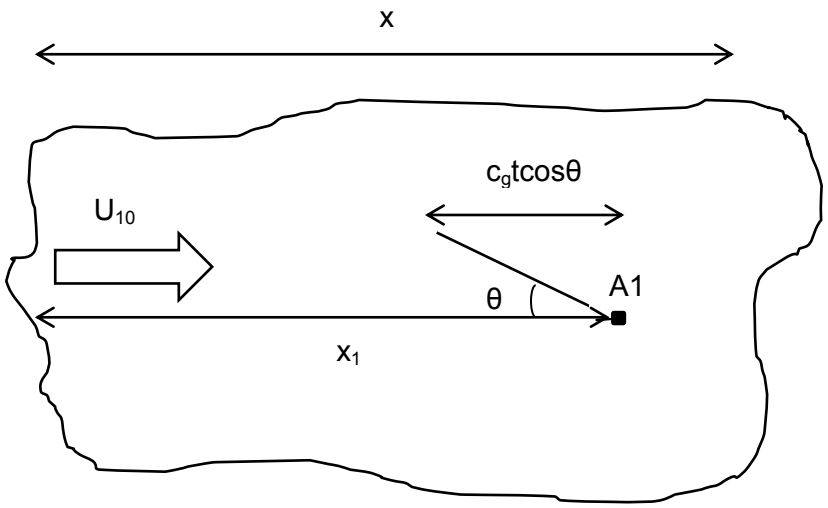

Figure 4.1: Wave growth for an arbitrary volume of water.

The wave growth is a function of the fetch (x), wind speed (U), the water depth and duration. The duration that the wind blows is an important parameter with regards to wave growth, but this is incorporated through the fetch and wind speed (known as equivalent fetch, x_{eq}), in the following way after Holthuijsen (2007):

An arbitrary wave component, travelling at an angle θ to a line perpendicular to the coast, which has arrived at A1 at some time t has effectively travelled a distance of $c_g t\cos\theta$, where c_g is the group velocity (m/s). It is assumed that this distance ($c_g t\cos\theta$) is the distance from A1 where this wave component has developed. If this individual component developed independently of the spectrum then the wind blowing perpendicular to the coast line would have travelled a distance of $c_g t\cos\theta$, assuming that it travelled with the wave. This distance is known as the equivalent fetch and is representative of the time in which the wind transfers energy to the wave. This equivalence exists for each wave component, but because each component of the spectrum has a different frequency and direction, considering the spectrum as a whole, no relationship between fetch and duration can exist. This can be applied to the spectrum peak, which is justified by the fact that the energy of a developing sea is concentrated around a peak i.e. it is assumed that the spectrum peak carries the

energy from the wind. The direction of the peak component is equal to the wind and therefore constant, however the frequency and hence the group velocity is not, therefore the group velocity must be integrated over the duration to obtain the equivalent fetch. Therefore if the actual fetch is longer than the equivalent fetch then it is said that the waves are in fetch limited conditions.

This implies that waves which form in finite depth conditions are either in fetch limited or depth limited situations.

For illustrative purposes, suppose the depth is approximately constant over the defined area and the ratio between the depth and the fetch is approximately zero. Initially the waves which are formed are defined by deep water relations, since the wave height in comparison to the water depth is small, and the ratio of the wave length to the water depth is large. As the waves propagate through the water they grow, assuming that there is still energy transfer from the wind to the water. This growth continues until the wave heights are limited by the water depth, since a wave height which is equal to the water depth would have broken. It is at this point when the wave growth is said to be depth limited. It will be shown that the majority of the South Lake is depth limited. However it is not as simple as stating that the wave formation is in depth limited conditions by only considering the water depth alone, since wave growth depends on three factors; the water depth, wind speed and fetch. The wave height in finite depth water is said to be either depth limited or fetch limited (limited by the fetch in not necessarily the same manner as mentioned previously, but rather controlled by the fetch, this will be shown in the preceding text) according to Young & Verhagen (1996).

The parameters which are important in wave growth are as follows:

The wind speed, U (m/s), the fetch length, x (m), the water depth, d (m), the acceleration due to gravity, g (m/s^2), the energy of the wave spectrum derived from the integral of the variance spectrum, E (m^2), the significant wave height, H_s (m), and the peak wave frequency, ν_p(Hz).

The above parameters can be combined using dimensional analysis to form dimensionless terms which can be used to empirically model the finite depth wave characteristics. Considering the dimensions Length L, mass M, time T the above parameters have the following dimensions:

[U] – L/T

[X] – L

[g] – L/T^2

[E] – L^2

[v_p] – 1/T

[d] – L

H_s can be related to the energy of the wave spectrum, therefore it is not included in the dimensional analysis.

These dimensionless groups are: the non-dimensional energy, $\varepsilon = \frac{g^2 E}{U^4}$, the non-dimensional frequency, $\nu_f = \frac{v_p u}{g}$, the non-dimensional fetch, $\chi = \frac{xg}{U^2}$, and the non-dimensional depth, $\delta = \frac{dg}{U^2}$.

The non-dimensional groups are used to estimate the wave characteristics. However as Young & Verhagen (1996) found, it is not as simple in finite depth conditions to simply use these equations as they stand. The effects that finite depth has on limiting the wave growth must also be considered. These non-dimensional groups can make it easier to understand this depth limit, shown by equations (2-19) and (2-20).

In order to explain the transition of waves from deep water to shallow water the following equations were proposed by Young & Verhagen (1996), they are based on existing equations describing wave growth in limited-depth water (Holthuijsen, 2007):

$$\varepsilon = \varepsilon_\infty \left\{ tanh(k_1 \delta^{m_1}) . tanh\left({k_2 \chi^{m_2}} \Big/ {\tanh(k_1 \delta^{m_1})} \right) \right\}^p \quad (4\text{-}1)$$

$$\nu = \nu_\infty \left\{ tanh(k_3 \delta^{m_3}) . tanh\left({k_4 \chi^{m_4}} \Big/ {\tanh(k_3 \delta^{m_3})} \right) \right\}^q \quad (4\text{-}2)$$

Where: ε_∞ and ν_∞ are the deep water limits to spectral energy and peak frequency respectively. k_1 - k_4, m_1 - m_4, p and q are coefficients determined by observations. δ and χ are the non-dimensional depth and fetch number respectively.

Young and Verhagen (1996) found the following values for the coefficients:

Table 4.1: Values for the relevant dimensionless coefficients determined by Young & Verhagen (1996).

Coefficient	value	Coefficient	value
k_1	0.493	m_1	0.75
k_2	3.13×10^{-3}	m_2	0.57
k_3	0.331	m_3	1.01
k_4	5.215×10^{-5}	m_4	0.73
p	1.74	q	-0.37

As mentioned earlier ε_∞ represents the deep water depth limit and ν_∞ represents the deep water frequency limit. It seems logical to simply replace these two terms with some shallow water depth limit, however this scaling would apply to all values for all fetch conditions, hence at short fetch values the wave heights and frequencies would be underestimated (Holthuijsen, 2007). Thus in order to correctly predict the right wave characteristics, the inclusion of the fetch resulted in equations (4-1 – 4-2) (Holthuijsen, 2007).

Since tanh(x) = x, when $x \ll 1$, equation (4-1) reduces to: $\varepsilon = \varepsilon_\infty \, k_2 \chi^{m_2}$, for very small fetch, and the same applies to equation (4-2). This is what would be expected since, at very small fetch the wave characteristics are defined by the fetch rather than the water depth. At large fetch the depth obviously starts to play a significant role in limiting the wave height and period. Equation (4-1) reduces to: $\varepsilon = \varepsilon_\infty tanh(k_1 \delta^{m_1})$, since tanh(x) $\rightarrow 1$ as $x \rightarrow \infty$, the same applies to equation (4-2). Equations (4-1, 4-2) reach what is called a “plateau” value at large fetch (Young & Verhagen, 1996). This value is defined by the limits represented by equations (2-19, 2-20).

4.4 Mathematical Model

This section provides an explanation of the method to estimate the wave characteristics and ultimately the sediment re-suspension.

The input parameters required for the model are: wind Speed, U (m/s), wind Direction (degrees), and water Depth, d (m).

4.4.1 Wind Speed

The wind speed was obtained from the South African weather service. This wind speed was the hourly average wind speed, coupled with the corresponding direction. The period within which the wind speed was obtained was from January 2000 to September 2011. To investigate the diurnal pattern of the wind speeds an E.M.D (empirical mode decomposition) was used. This is important when estimating the wind speed responsible for causing the sediment re-suspension, a more detailed discussion is given in section 5.2.5, and it is based on the fact that the average wind for a day might lead to an underestimation of the average turbidity. Thus a percentage of the maximum wind speed (determined by the E.M.D) could be used. The method used for the EMD is as follows (Huang et al, 1996):

- The average hourly wind data for each month during the period of 2000-2011 was used.
- All maximum and minimum values were identified; a cubic spline was used to set up an envelope of maximum values and minimum values.
- The mean of this envelope value was determined, for purpose of discussion let it be called a(t).
- At each data point the difference between the data point and a(t) was determined, let this function be called b(t).
- b(t) then became the new data, this was subjected to the same method as mentioned above, whereby the mean is found and the difference between the mean and the data becomes the new data set.
- This was continued until some approximately constant value was established.
- From the separated signals the diurnal pattern was determined, by simply removing the noise (wind gusts) and summing the rest of the signals.
- The 95th percentile of this new maximum value was used as the wind speed contributing to sediment re-suspension.

The average direction was estimated by taking the average of the X and Y components of the wind velocity, this was necessary for the spatial model. The average direction was calculated as follows:

$$\bar{\theta} = \arctan\left(\frac{\bar{X}}{\bar{Y}}\right) \quad (4\text{-}3)$$

Where: $\bar{X}$ is the average X component of the wind velocity and $\bar{Y}$ is the average of the Y components of the wind velocity. The reason why X is divided by Y is because the directions are in the metrological coordinate system, where north is 0°.

Determining the average direction was not necessary when estimating the lake average turbidity values because an average fetch was used. The method of determining this fetch is discussed in chapter 4.4.4. The average direction was required for the spatial model.

4.4.2 Wind Setup

In order to determine whether the wind induced surface currents were strong enough to re-suspend any sediment, it would be important to estimate these wind induced currents. This was important when considering the model since the sediment re-suspension was based on vertical re-suspension by waves only.

Since this was a simple measurement to determine the expected wind induced currents a number of assumptions were made, such as: the shape of the lake was assumed to be rectangular, the lake bed was flat and the average wind speed acted along the length of the lake with a constant magnitude.

Hutchison (1976) calculated the wind setup that occurred within the Southern Lake for wind speeds of 5, 10 and 15m/s blowing either from the north or the south direction. The water depth upon which the wind setup was estimated was one metre. It was estimated by Hutchison (1976) that at low wind speeds (5m/s) it would take approximately one day and for higher wind speeds (10-15m/s) it would take approximately 2.5 days for an equilibrium set-up level to be reached. The set-up equilibrium occurs when the hydrostatic force on the downwind side of the lake and the force due to the wind balance the opposing hydrostatic force on the upwind side of the lake (Socolofsky & Jirka, 2004); refer to figure 4.2. The currents due to the wind setup is based on the model proposed by Socolofsky & Jirka (2004) refer to figure 4.2, where: F_r is the hydrostatic force per unit width on the downwind side (N/m), F_l is the hydrostatic force per unit width on the upwind side (N/m), and τ_w is the associated shear stress caused by the wind (Pa), *a* is the wind setup (m) and $\bar{d}$ is the average water depth.

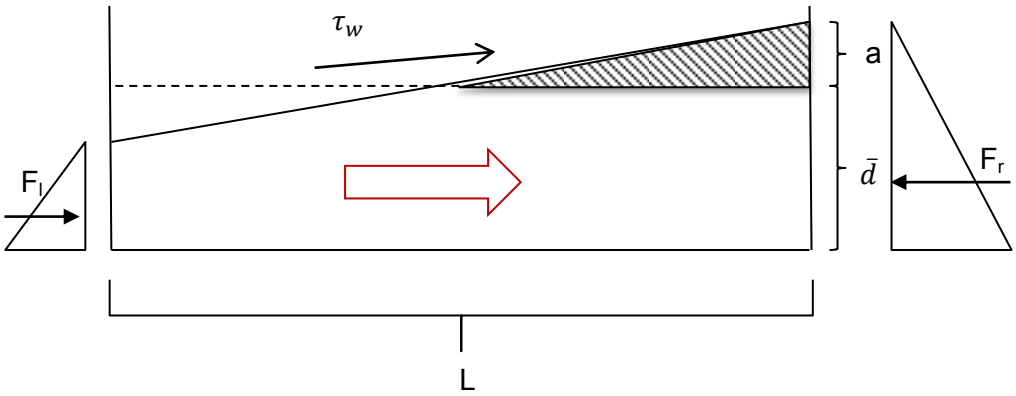

Figure 4.2: Figure depicting the setup caused by wind stress as well as the associated hydrostatic pressure distribution (Socolofsky & Jirka,2004). The red arrow indicates the direction of the current.

Table 4.2 shows the wind setup for the Southern Lake, the time in which equilibrium is reached, the associated flow rate and velocity. The lake average orbital velocity is also given, this is based on a water depth of 1m, wind speed of 5, 10 or 15m/s and an average fetch of 3000m (based on the calculation explained in section 4.4.4). The fetch used for the wind setup (i.e. L, according to figure 4.2) was the length of the Southern Lake. According to *Google Earth* this length was 7000m, this implied that the width of the lake was 4714m. The width was based on the assumption that the shape of the lake was rectangular and that the area of the lake was that at 0 EMSL, i.e. 33km^2 (Hutchison, 1974). The flow rate was calculated by determining the area of the shaded region in figure 4.2 (the length of the shaded region was assumed as half the total length, L), multiplying by the width (4714m) mentioned previously and dividing by the equilibrium time (that established by Hutchison (1976)). The use of the equilibrium time to estimate the current represents the time averaged current. This time averaged current is used in comparison to the wave induced orbital velocity. The velocity was then calculated by dividing this flow rate by the water depth and width of the lake (4714m).

Table 4.2: Wind setup and the associated currents for northerly and southerly wind directions after Hutchison (1976), in comparison to the lake average orbital velocities due to surface waves.

Wind Direction	Wind setup, a, (m)	Wind speed (m/s)	Time (hr)	Flow rate (m^3/s)	Velocity (m/s)	Average orbital velocity (m/s)
North	0.07	5	24	6.68	$1.4x10^{-3}$	$8x10^{-2}$
	0.28	10	60	10.7	$2.3x10^{-3}$	$2.3x10^{-1}$
	0.54	15	70	17.7	$3.8x10^{-3}$	$3.7x10^{-1}$
South	0.09	5	27	7.6	$1.6x10^{-3}$	$8x10^{-2}$
	0.38	10	65	13.4	$2.8x10^{-3}$	$2.3x10^{-1}$
	0.8	15	70	26.2	$5.6x10^{-3}$	$3.7x10^{-1}$

From table 4.2 it is clear that the wind induced currents are significantly smaller than the lake average orbital velocities caused by the wind induced waves. Since the shear stress is directly related to the square of the velocity (refer to equation (2-23)) it is evident that the shear stresses exerted by the wind induced currents are significantly smaller than the shear stresses caused by the wind induced waves. Therefore the assumption made by this dissertation, vertical mixing is by wind induced waves only, is valid.

4.4.3 Water Depth

Water depth data was obtained from the existing water balance model developed by Lawrie & Stretch (2008). This model predicted the average lake water levels for three situations which follow:

- The system as it exists at present, with separate inlets for the uMfolozi and St. Lucia systems.
- The system with a combined inlet, i.e. restoring the combined mouth of the St Lucia and uMfolozi systems. This represented what the water levels would have been like if the uMfolozi wasn't separated in 1952.

The water balance yields water levels on a monthly time step, where daily water levels are required a simple linear interpolation was used.

4.4.4 Wave Height Prediction

From the wind speed and water depth the non-dimensional depth number is calculated using equation (2-4).

From the wind direction the non-dimensional fetch number is calculated using equation (2-3). As mentioned previously the model was used to calculate the turbidity on either a lake average scale or on a spatial grid. The fetch calculation required for the lake average value was done as follows:

- The shape of the lake was assumed to be circular.
- The area (obtained from Hutchison (1974)) was then used to calculate an equivalent diameter.
- The radius was used as the average fetch.

In order to calculate the significant wave height the energy of the spectrum was required. Young & Verhagen (1996) suggested that there were two different energy numbers required to determine the significant wave height in finite depth situations. These two numbers were required because the waves were travelling in either fetch limited conditions or depth limited conditions. The procedure for wave height calculation was as follows:

1. Estimate the energy for fetch limited conditions, using equation (2-13).
2. Estimate the energy for depth limited conditions, using equation (2-19).
3. If the energy in (1) was greater than (2), the energy for (2) was used, as the waves were in depth limited conditions.
4. If the energy in (1) was less than (2), the energy from (1) was used, as the waves were in fetch limited conditions.
5. The significant wave height was calculated using equation (2-21).

4.4.4 Wave Period Prediction

The wave period prediction follows a similar pattern to the wave height prediction; however it is the peak frequency which is calculated. Again there are two types of non-dimensional frequency numbers which need to be calculated. The first is that governed by the equation (2-16) this is for the when the wave growth is characterized by deep water relations. The second is governed by equation (2-20) whereby at some fetch the peak frequency is limited by the water depth. The following procedure was used to determine the peak period:

1. Estimate the peak frequency for fetch limited conditions, using equation (2-16).
2. Estimate the peak frequency for depth limited conditions, using equation (2-20).
3. If the frequency in (1) is greater than (2), the frequency from (1) was used.
4. If the frequency in (1) is less than (2), the frequency from (2) was used.
5. The period was then calculated by equation (2-2).

4.4.5 Orbital Velocity

The wave orbital velocities at depth, d, and wave height, H, are given by (Reeve et al, 2004):

$$U_m = \frac{H.\pi}{T.\sinh(k.d)} \qquad (4\text{-}4)$$

where k is the wave number and defined as $k = \frac{2\pi}{L}$.

In order to estimate the wave length it must first be established whether the wave is propagating through deep, transitional or shallow water. However, in order to determine whether the wave is propagating through deep, transitional or shallow water the ratio between the water depth and wave length is required. Therefore either the water depth (relative to the wave propagation) must be assumed or the wave length must be assumed. For purposes of the present investigation it was assumed that the wave was either propagating through deep or transitional water which can be justified because of the naturally shallow water depths. Out of these two conditions it was more likely that the wave was travelling through transitional water. This assumption was based on the fact that the water levels within the lake have been low over the past 10 years, ranging

anywhere from -1.73 to -0.03 EMSL (Lawrie & Stretch, 2011), accompanied by the fact the waves generated by the wind have a limited area in which they can develop, limiting the wave height and wave length. The maximum fetch across the South Lake is approximately 6km (refer to figure 1.3); therefore waves are limited in their growth.

The ratio between depth and wave length in transitional water is given as follows (Reeve et al, 2004):

$0.04 < \frac{d}{L} < 0.5$

The wave celerity is calculated as follows (Reeve et al, 2004):

$$c = \frac{g.T.\tanh(k.d)}{2\pi} \quad (4\text{-}5)$$

The wave length was calculated from the definition of wave celerity:

$$c = L/T \quad (4\text{-}6)$$

However a trial and error approach would be required since the wave length, L, due to the inclusion of k in the right hand term of equation (4-11), k is defined as; $k = \frac{2\pi}{L}$. Using numerical methods proposed by Reeve et al (2004) the wave length can be estimated as follows:

$$\frac{c^2}{g.d} = [y + (1 + 0.6522y + 0.4622y^2 + 0.0864y^4 + 0.0675y^5)^{-1}]^{-1} \quad (4\text{-}7)$$

Where: $y = k_0 d$, $k_0 = \frac{2\pi}{L_o}$, $L_0 = \frac{g.T^2}{2\pi}$, L_o is the deep water wave length.

Therefore by substituting (4-12) into (4-13) to derive equation (4-14), the wave length was calculated as follows:

$$L = T\sqrt{gd[y + (1 + 0.6522y + 0.4622y^2 + 0.0864y^4 + 0.0675y^5)^{-1}]^{-1}} \quad (4\text{-}8)$$

4.4.6 Bed Shear Stress

In order to determine the bed shear stress the orbital excursion would first need to be calculated using the following formula (Reeve et al, 2004):

$$A = \frac{T.U_m}{2.\pi} \quad (4\text{-}9)$$

The shear stress exerted and its associated boundary layer was then classified into either a laminar boundary layer or turbulent.

If $\frac{A^2\omega}{\nu} < 3x10^5$ then the boundary layer which develops is laminar, therefore the wave friction coefficient is given by equation (2-24)

If $10^6 < \frac{A^2\omega}{\nu} < 10^8$, then the associated boundary layer is turbulent and the friction coefficient is given by equation (2-25):

It must be noted that the wave friction coefficient mentioned above is based on an assumption of a smooth surface. This is based on the fact that the sediment which makes up the lake bed is of a cohesive nature with a D_{50} of 4µm (Chrystal & Stretch, unpublished). The shear stress is then calculated as using equation (2-23).

4.4.7 Erosion

The concentration of sediment due to erosion was calculated in two ways, in accordance with what was mentioned in chapter 2.6. Equations (2-26a) and (2-27) were used to calculate the erosion and hence turbidity. The relationship between TSS and turbidity was found to be as follows:

$$TSS = 1372.1(Turbidity) - 138.98 \quad (4\text{-}10)$$

The manner in which equation (4-10) is interpreted is explained in more detail in section 5.1.1. If the estimated TSS concentration fell between 0-0.1 g/L then the associated turbidity would be 12.7 NTU, for TSS concentrations above this range the turbidity could be calculated using equation (4-10).

When a time step of days, months or years is required, equations (2-26a, 2-27) are good enough to suffice without including the effects of deposition. At some point during the day the maximum suspended sediment concentration will be reached. This is due to either one of two things, firstly the shear stress exerted on the lake bed has reached the critical shear stress of the sediment and no more sediment can be re-suspended. This would be due to consolidation, as a layer of sediment is removed, a new layer is exposed with a higher degree of packing and hence higher critical shear stress, this continues until the bed shear stress equals the critical shear stress. Secondly, equilibrium is reached between the erosion and deposition flux, it is at this point when erosion and deposition are the same. As the erosion continues there is a continual increase in suspended sediment concentration. Deposition flux is directly proportional to the suspended sediment concentration (refer to the deposition flux term in equation (2-27a)). Therefore at some point the deposition flux will equal the erosion flux, since the two processes are equal there is no net gain or loss in suspended sediment concentration.

4.4.8 Deposition

Deposition was included in the model when considering an average time step which was smaller than a day (i.e. considering a time step of 3 hours). The reason why the model didn't include the deposition for time steps larger than a day was because the monthly turbidity was calculated independently, i.e. the turbidity for the previous month was not used to determine the turbidity for the current month. Equation (2-32) requires the turbidity from the previous time step to determine the turbidity for the current time step. Once the settling velocity has been ascertained then the concentration of sediment can be calculated based on equation (2-32). This equation was based on the assumption that water column is well mixed. The settling velocity was calculated according to equations (2-33 & 2-34).

4.5 Spatial Model

A spatially explicit model was developed in order to determine the spatial variation of turbidity within the Southern Lake. Figure 4.3 was used to set out the depths of the Southern Lake on a spatial grid. It is noted however that figure 4.3 is an out dated

bathymetric map, but it is the only one that exists for the location and was therefore used for illustrative purposes.

It was decided that a square cell with a length of 287.5m would be used. This seemed sufficient because the ratio between the area of the lake (at 0 EMSL) and that of each cell is about 400.

The spatial model was designed for N, NE, E, SE, S, SW, W, NW wind directions, it was also set up to allow for a change in EMSL and hence bathymetry.

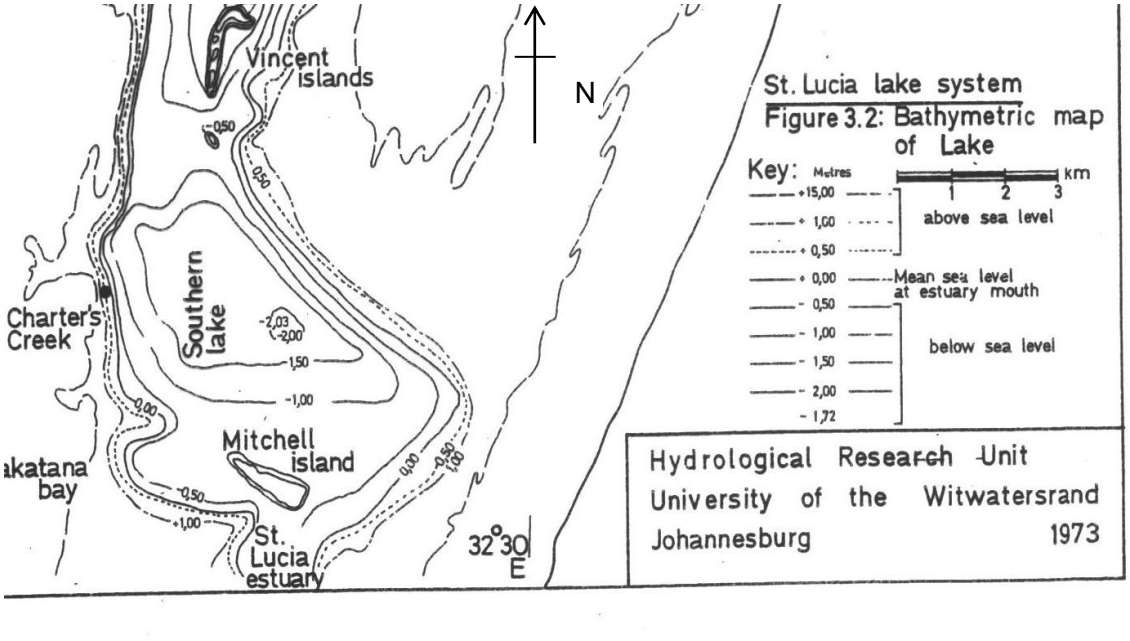

Figure 4.3: Bathymetric map of the Southern Lake (Hutchison, 1974), the levels represented here are relative to 0 EMSL.

The effective depths for each cell were estimated as follows:

- The depth of each cell that was located on the contours was kept at the relevant contour value.
- All the depths in between the contours were then interpolated using the method stated below. The average of the 8 cells around the given cell for which the depth was required was done. This is shown through the illustration as follows:

A1	A2	A3
B1	B2	B3
C1	C2	C3

The average depth of cell B2 is equal to the following equation:

$$B2 = \frac{[A1+A2+A3+B1+B3+C1+C2+C3]}{8} \quad (4\text{-}11)$$

An important aspect of the average depth along a line of fetch is what happens when the average depth is greater than the actual depth. This is important since the waves will begin to either break or due to frictional resistance from the lake bed, they will decrease in height. A simple method was used to reflect this change in height. It was achieved by specifying a rule in the model so that if the actual water depth was less than the fetch averaged water depth, then the water depth to be used would be the actual water depth. While this is a rather simplistic approach which doesn't include the effects of friction and bottom percolation, for the developing and testing a basic spatial model it was judged to be adequate. However in order to improve the results of the spatial model, the effects described above will need to be included in future developments.

The wind-wave model as discussed in the preceding chapters was used to determine the wind induced waves. The sediment re-suspension was then calculated in accordance with what was mentioned in chapters 4.4.5 – 4.4.7.

Since the effects on sediment re-suspension by breaking waves and the associated turbulence were not accounted for, an upper limit was specified on how much re-suspension could occur. This was necessary because in very shallow water the turbidity values were predicted to be unrealistically large. This limit was specified as 2000 NTU.

CHAPTER 5

RESULTS & DISCUSSION

Chapter 5 presents the results for the field work sampling during the period from March 2011 – June 2011. The model calibration is presented and the appropriate method of sediment re-suspension is chosen. Results for the sensitivity analysis are shown as well as turbidity predictions for the three different management strategies suggested in chapter 4.4.3. The spatial model is also presented in this chapter.

5 PRESENTATION OF RESULTS

For ease of reading the results have been separated into two sections. The first deals with the model calibration and field results. The second section presents the outputs of the model simulations, i.e. the spatial model as well as the turbidity values for the different scenarios.

5.1 Model Calibration

5.1.1 TSS & Turbidity calibration

Figure 5.1 shows the relationship that exists between TSS and turbidity. This was derived from the samples taken during the field analysis. Each sample was filtered through a 0.7µm filter, this seemed adequate since it was expected that the sediment would comprise mainly of clay with a D_{50} of 4µm (Chrystal & Stretch, unpublished manuscript). It is evident from figure 5.1 that there is a strong relationship between TSS and turbidity ($r^2 = 0.93$).

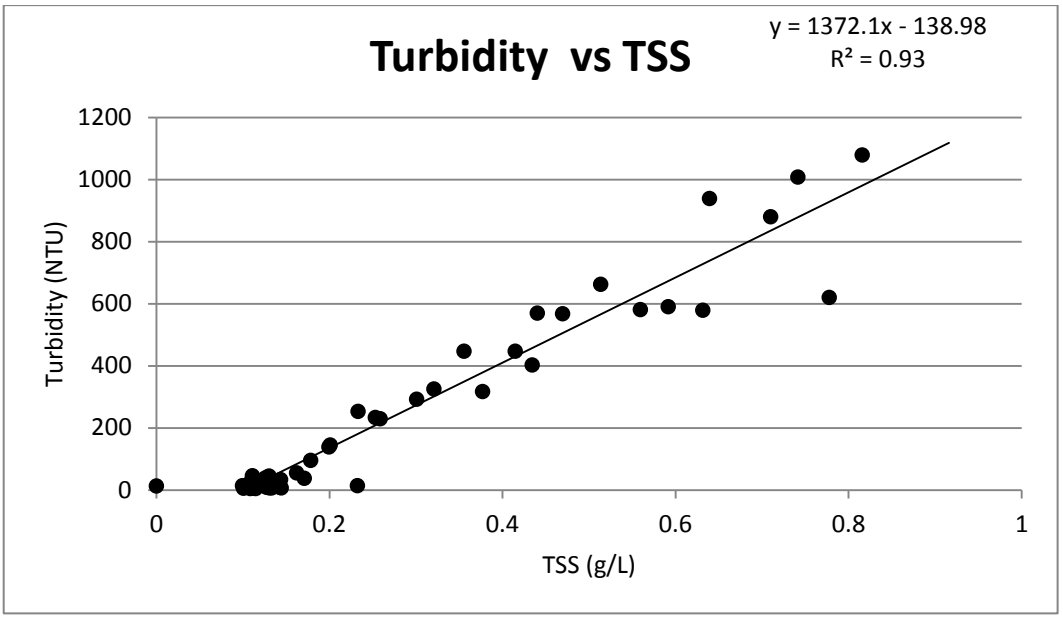

Figure 5.1: Relationship between TSS (g/L) and Turbidity (NTU).

The relationship between TSS and turbidity can be described by:

$$Turbidity = 1372.1(TSS) - 138.98 \quad (4\text{-}10)$$

Since it is unrealistic to have a negative turbidity reading, the way in which this relationship was interpreted was that between concentrations of 0 – 0.1 g/L the turbidity was 12.7 NTU (this was the estimated background light scatter, due to biology), for concentrations above 0.1 g/L the TSS was estimated from the previously mentioned relationship. The concentration at which the trend line crosses the x-axis is approximately 0.1 g/L.

The turbidity is measured in nephelometric units (NTU) and the TSS is measured in g/L.

Figures 5.2 – 5.3 show results obtained by others. Note how the relationship obtained by Cyrus & Blaber (1988) is very similar to that obtained in the present study. The TSS-turbidity correlation reported by Carrasco et al (2007) is significantly different. Both the relationships obtained by Cyrus & Blaber (1988) and Carrasco et al (2007) show a trend line which passes through the origin. This was not found by the observations presented by this research.

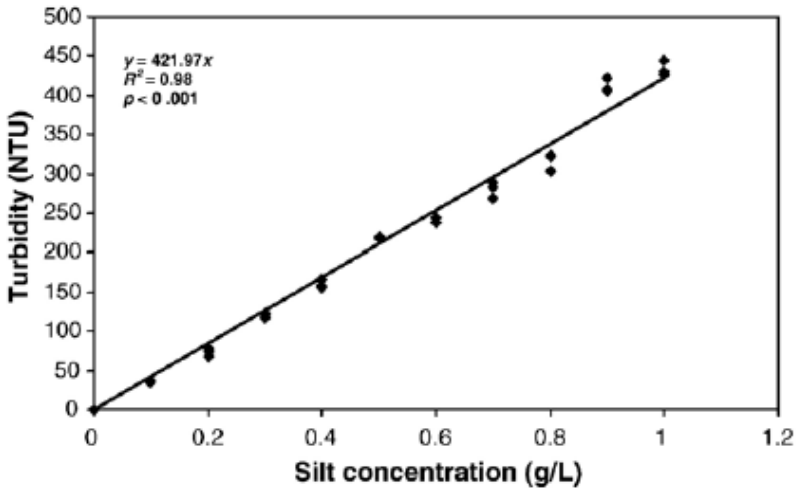

Figure 5.2: TSS (g/L) and Turbidity (NTU) relationship measured by Carrasco et al (2007)

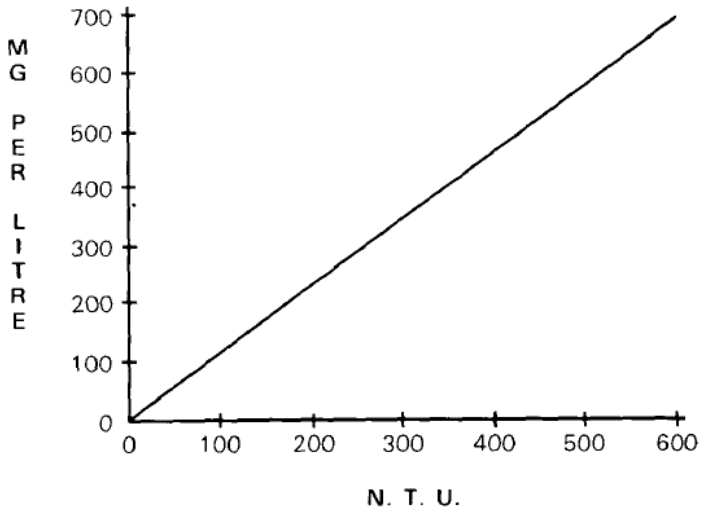

Figure 5.3: Relationship between TSS (mg/L) and Turbidity (NTU) measured by Cyrus & Blaber (1988)

From the figures 5-1 – 5-3 it can be seen that the relationship obtained by this research corresponds closely with what was reported by Cyrus & Blaber (1988).

The gradient obtained from Cyrus & Blaber (1988) appears to be approximately 1000. The gradient obtained by Carrasco et al (2007) appears to be approximately 400. The latter gradient is significantly different from what was obtained in the present work. This is because the sieve size used by Carrasco et al (2007) was 63µm, whereas the sieve

size used in this research was 0.7µm. This is an important difference since the smaller sieve size would retain the clay and fine sediment which is the sediment which is being re-suspended since the critical shear stress is almost zero. The location where the turbidity readings are taken is also important. This is because different particle shapes have different optical properties, mentioned in chapter 2.7, depending where the sample is taken in the estuary system, the types of sediment found in specific areas change. For example, in the Lakes up to the north, it is likely that the sediment would comprise mainly of clay, whereas closer to the mouth the predominant sediment is sand. Thus clay, which has a flat plate type shape, would have completely different optical properties to sand which is elliptical. This is relevant since the readings taken by Carrasco et al (2007) were done near the St. Lucia estuary mouth, hence the different results.

In order to fit the trend line it was assumed that when there is no sediment re-suspension occurring within the water column the turbidity reading is 12.7 NTU. This is the value measured in the field when the wind speed was zero and the water was clear. This indicates the background light refraction due to organisms present, which was suggested by Luettich et al (1990). From the trend line it is clear that the expected turbidity values between concentrations of 0 – 0.1 g/L would be negative. This is not possible as light attenuation through water cannot be negative. Therefore turbidity readings between 0 - 0.1 g/L would be assumed to be 12.7NTU. This observed pattern would need to be investigated further, as there is a possibility that there was a potential error in the instrument when taking readings.

5.1.2 Wave Height Prediction

Figure 5.4 shows the observed wave heights, those predicted by the model and how they compare to each other. Note that the wave heights predicted by the model are very similar to those observed (average absolute error of 0.01m). Figure 5.5 shows the ratio between the water depth and wave length at each sample point.

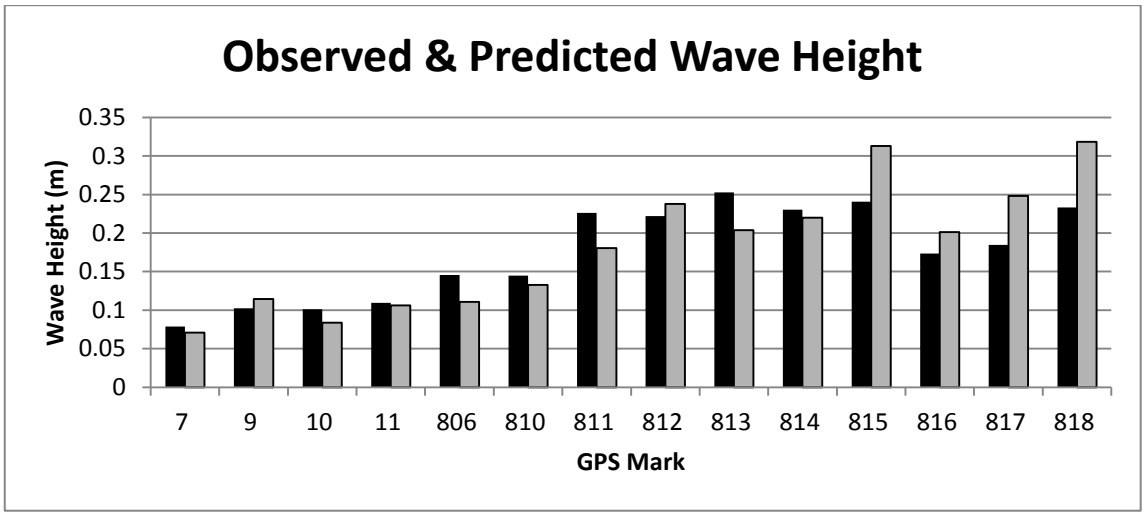

Figure 5.4: Graph showing the observed wave height (grey bar) compared to the predicted wave height (black bar). The GPS label refers to the location of the sample point – see plates 3.1-3.4.

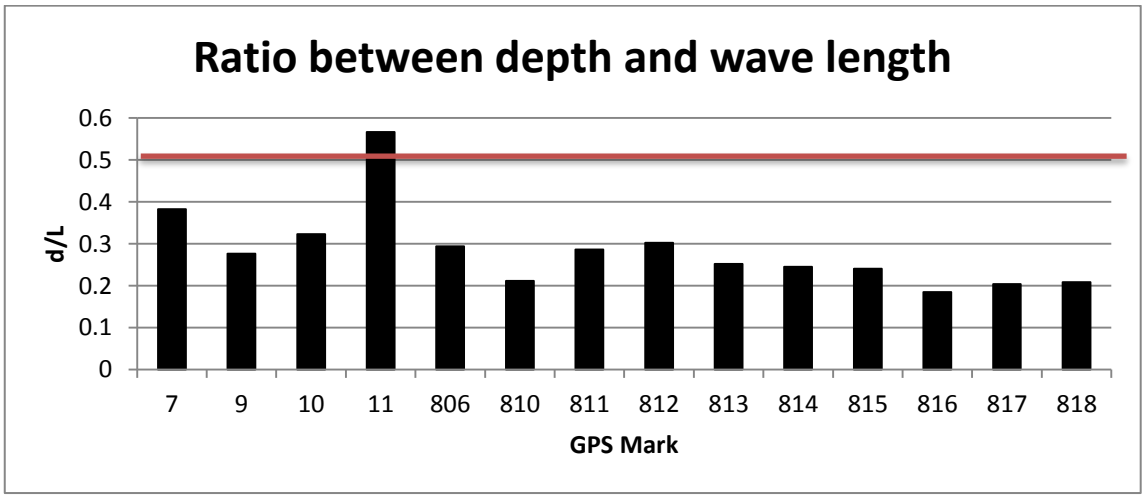

Figure 5.5: Graph showing the ratio between water depth and wave length for each sample point, if the ratio is greater than 0.5 (shown by the horizontal line) then the waves are said to be in depth limited conditions. The GPS label refers to the location of the sample point – see plates 3.1-3.4.

The water depth used to determine the wave height was that taken at the sampling spot. The depth used by Young & Verhagen (1996) to determine the depth number was the average depth along the fetch. The lack of bathymetric data resulted in the inability to estimate the fetch-averaged depth, and yet the model produced reasonable results. Possible reasons for this could be that the fetch-averaged depth required for the wave height prediction could be very similar to the depth measured at the sampling spot, or the wave heights could already have been limited by the water depth before the sampling point and perhaps were reduced due to bottom friction by the time the wave group reached the sampling points.

There appears to be no obvious relation between where the model overestimates or underestimates the wave height in comparison to whether the waves are propagating through deep water or transitional water. However as mentioned previously the water depths used in figure 5.5 are the depths at the sampling locations and are not the average depths along the fetch. It must be noted however that the assumption that the waves are travelling through either deep water or transitional water appears to be correct since, since at every sample point other than GPS mark 11 the waves are travelling in transitional water. However at point 11 there is significant disagreement. The deep water wave length estimated for point 11, given by $\mathrm{L}_0 = \frac{g.T^2}{2\pi}$ was 0.12 m, whereas the wave length estimated by equation (4-8) was 0.11 m. this showed that while the assumption that the waves were in transitional water was wrong, there is only a small disagreement in the wave length.

5.1.3 Turbidity Build up

Figure 5.6 shows the observed build-up of turbidity due to sediment re-suspension that was recorded in the Southern Lake over a 4-hr period. Note the relationship between the wind speed and associated reaction time of the sediment re-suspension. There appears to be a delay in the aforementioned. This may be attributed to the height above the lake bed at which the turbidity measurement was taken. This height was approximately 0.5m above the lake bed.

Wind speed and turbidity values were only recorded from 09:27 in the morning. Thus in order to gauge how long it took for the equilibrium concentration to be reached, hourly wind speeds from 06:00 – 09:00 were obtained from the weather station located at Charters Creek. It is difficult to estimate the time in which the equilibrium is reached by looking at the wind speeds only, because from 06:00, the wind speed does not consistently increase to the maximum value which occurring at 09:27, at 08:00 the wind speed decreases and then proceeds to increase again. Another contributing factor would be the fact that the turbidity would not be zero at 06:00, since the wind speed would be significant enough to re-suspend sediment. However from 08:00 to 09:27 there is a rapid increase in wind speed, the time limit based on this would be 1.5 hours. This time limit differs significantly to that obtained through calibration, refer to section 5.1.4.

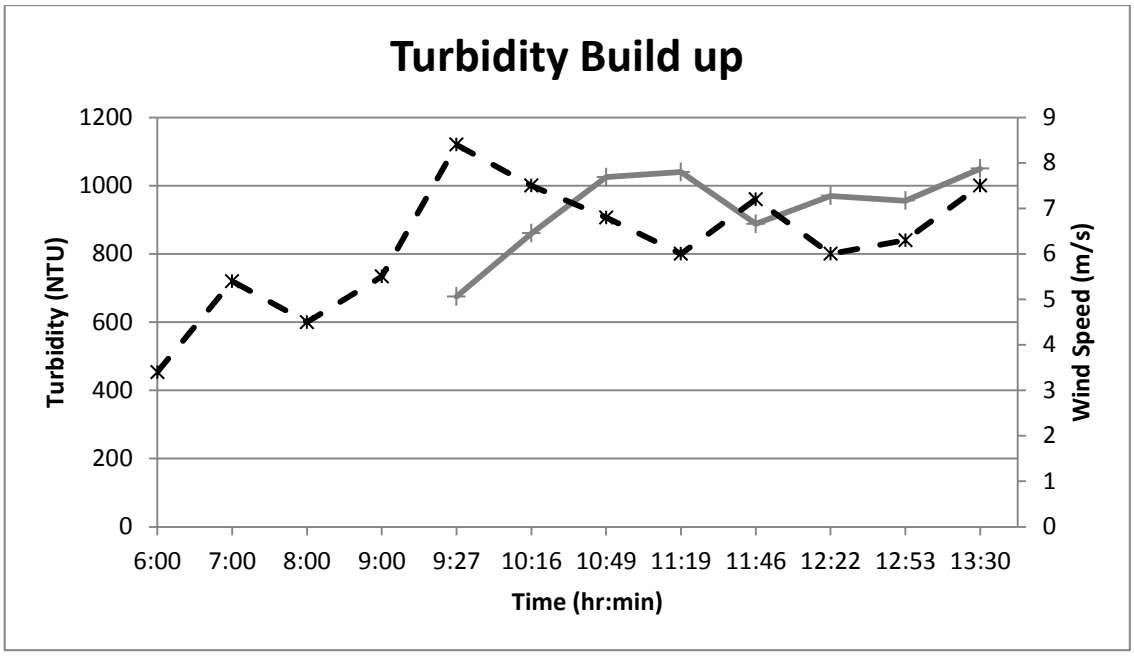

Figure 5.6: Graph showing the build of turbidity within the Southern Lake. The solid grey line is that for the turbidity, the dashed black line is that which represents the wind speed.

Figure 5.7: Sampling point of the data collection for the turbidity build up. The red line represents the associated fetch for the sampling point, approximately 2600m

Figure 5.6 shows the evidence that the sediment re-suspension reaches some equilibrium value as mentioned by (Hamilton & Mitchell, 1996). It is possible from this figure to determine a rough estimate of the equilibrium concentration. This value can

then be used to determine the settling velocity and hence the K value proposed by Luettich el at (1990). The equilibrium concentration was estimated to be 0.82 g/L, which can be used to find the K value and the erosion rate constant, if they are not known (refer to section 2.6). At the equilibrium concentration, the net sediment flux at the surface is zero, hence dividing the erosion rate by the settling velocity, and knowing the shear stress and settling velocity, the erosion rate constant and K can easily be calculated. According to the calibrated model (chapter 5.1.4), if this concentration was to be matched, assuming a settling velocity of $9x10^{-5}$ m/s (Maine, 2011) a K value of 5.44 g/L is calculated. This is based on the fetch estimated for the sampling point to be 2600m (refer to plate 5.1), the water depth measured was 0.7m, and the average wind speed during the sampling period was 6.9m/s from which a shear stress of 0.328 Pa was calculated.

Since this value has not been experimentally derived for the Southern Lake in more than one location, it would need to be estimated using the mathematical model. In order to determine if the value is realistic it would need to be compared to existing values which other research has determined. Other K values reported in the literature are:

- $8.6 \text{ X } 10^{-7}$ g/L – 0.125 g/L (Luettich et al, 1990).
- 0.008 g/L – 0.158 g/L (Hawley & Lesht, 1992).

The K value estimated from the present data doesn't fall within the range suggested by previous research. This could be attributed to the fact that because it incorporates the settling velocity, which depends largely on the sediment characteristics, it is not as simple to state that from the above mentioned method, of determining model parameter K, that this is the correct value. This is because the settling velocity, and hence K, is site specific and cannot be generalised to other situations.

5.1.4 Model Calibration and Validation

The figures 5.8 – 5.13, which follow, show the comparison of three different methods of erosion prediction. The first method is that proposed by the Bureau of Reclamation (2006) and then modified by equation (2-26a). The second method is that proposed by Luettich et al (1990) and uses equation (2-27) to predict the erosion. The third method is the combination of the two above methods (refer to section 2.6).

Figures 5.8 - 5.10 show the calibration of the model in accordance with the three methods mentioned in the preceding paragraph. Half the observed data was used to calibrate the models. The sample points were independent from each other in the following manner: at each sample point there is a different water depth, a different fetch, a different wind speed and the samples were taken at different times at different locations. Therefore the wave characteristics, and hence the concentrations of sediment, were different for each point and did not rely on the other sample points.

Figure 5.11 – 5.13 show the model validation for the three different methods. The remaining half of the data (once the models had been calibrated) was then used to validate the models. All methods of estimating the turbidity yield similar values to the observed data, however method one and method three (figures 5.11 and 5.13) significantly overestimate the turbidity at points 808 and 810.

Table 5.1 shows the comparison between the different model parameters estimated by each method and that established by Luettich et al (1990).

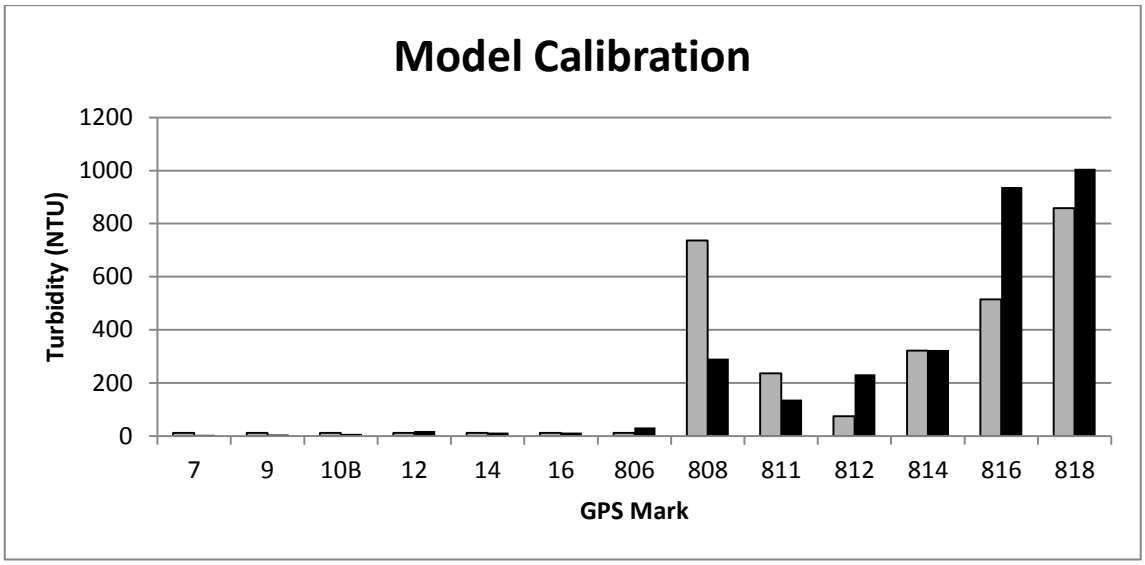

Figure 5.8: Model calibration for method 1. The solid black bar represents the observed turbidity values while the grey bar represents the predicted values. The GPS label refers to the location of the sample point – see plates 3.1-3.4.

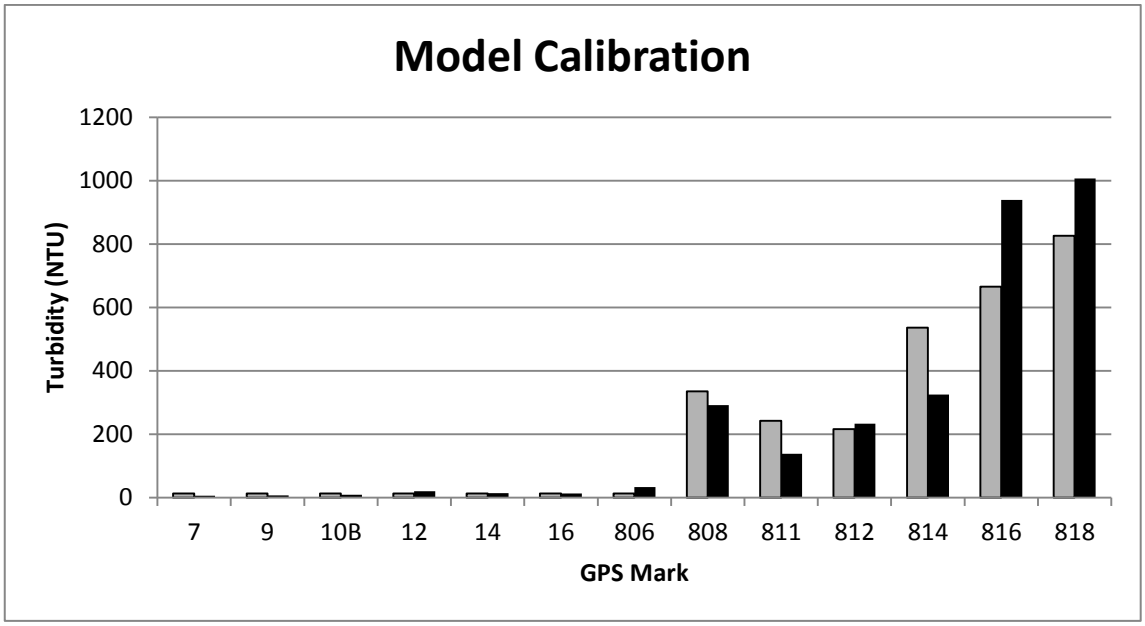

Figure 5.9: Model calibration for method 2. The solid black bar represents the observed turbidity values while the grey bar represents the predicted values. The GPS label refers to the location of the sample point – see plates 3.1-3.4.

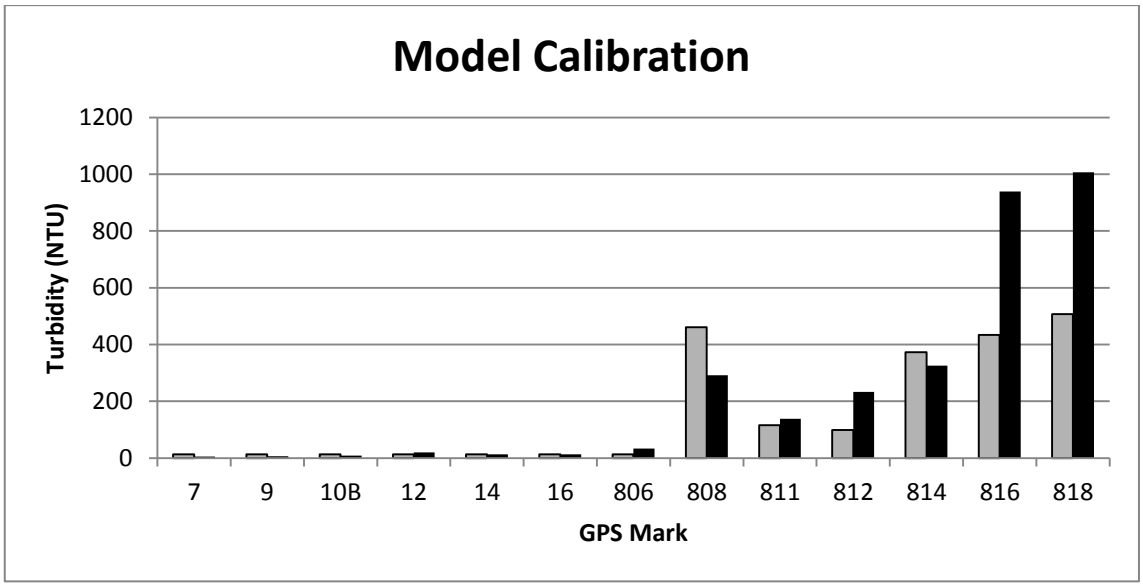

Figure 5.10: Model calibration for method 3. The solid black bar represents the observed turbidity values while the grey bar represents the predicted values. The GPS label refers to the location of the sample point – see plates 3.1-3.4.

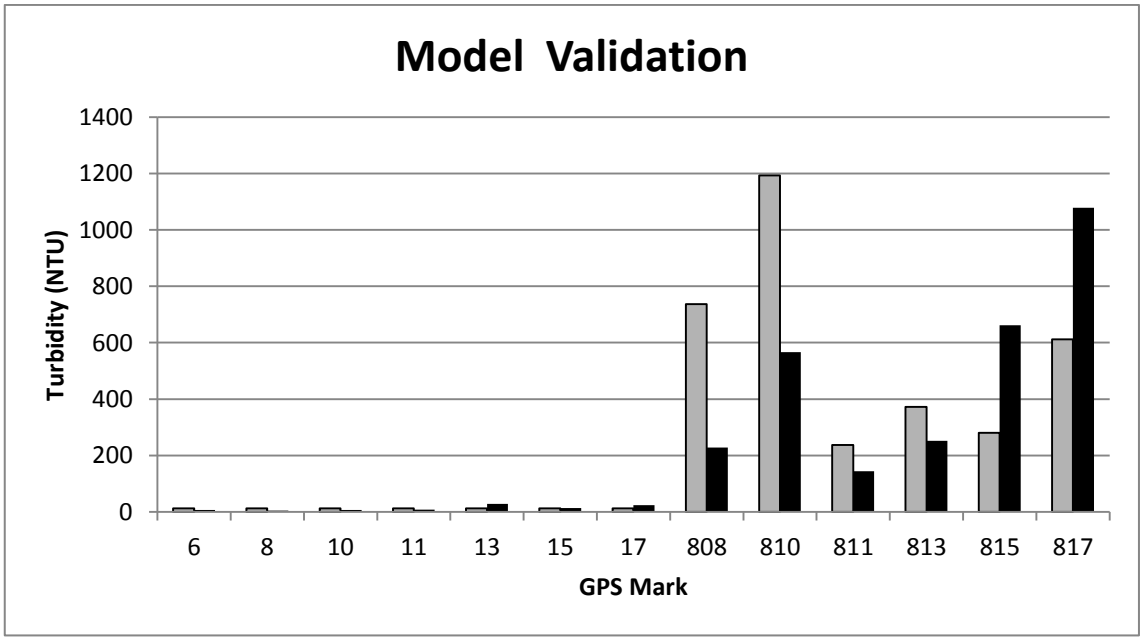

Figure 5.11: Model validation for method 1. The solid black bar represents the observed turbidity values while the grey bar represents the predicted values. The GPS label refers to the location of the sample point – see plates 3.1-3.4.

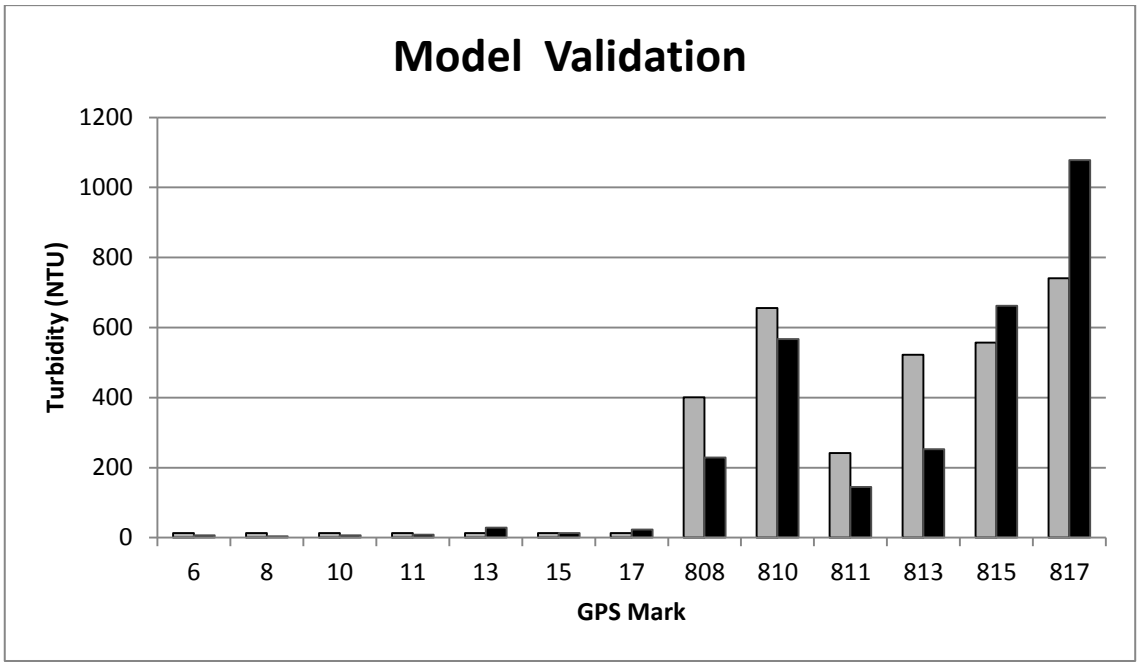

Figure 5.12: Model validation for method 2. The solid black bar represents the observed turbidity values while the grey bar represents the predicted values. The GPS label refers to the location of the sample point – see plates 3.1-3.4.

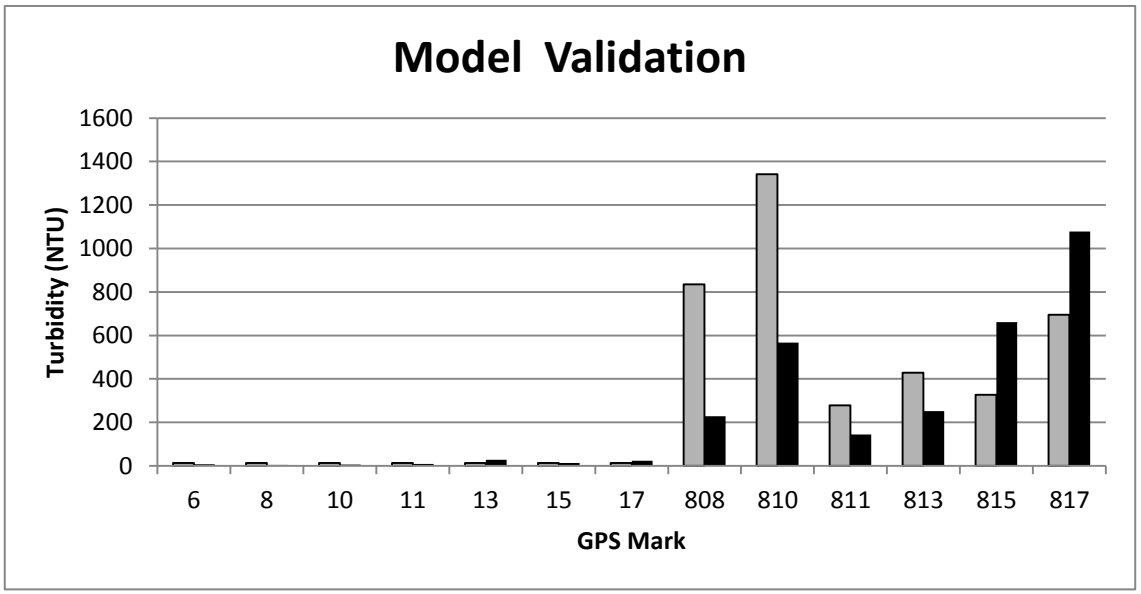

Figure 5.13: Model validation for method 3. The solid black bar represents the observed turbidity values while the grey bar represents the predicted values. The GPS label refers to the location of the sample point – see plates 3.1-3.4.

Table 5.1: Comparison of the model parameters for the different methods.

	Method 1	Method 2	Method 3	Luettich et al (1990)
K (g/L)	$3.72x10^{-1}$-1.22	$4.08x10^{-1}$	$2.03x10^{-1}$-$5.18x10^{-1}$	$1.5x10^{-5}$
M (kg/m^2s)	$5.84x10^{-5}$	$3.67x10^{-5}$	$2.6x10^{-5}$	$3.3x10^{-9}$
τ_c(Pa)	0.3	0.3	0.3	0
τ_{ref}(Pa)	na	0.119	0.12	$7.2x10^{-3}$
T(s)	8974	na	8974	na
w_s(m/s)	$3.9x10^{-5}$-$1.28x10^{-4}$	9×10^{-5}	$5.01x10^{-5}$-$1.28x10^{-4}$	$2.2x10^{-4}$

For the purpose of this discussion method one will be used to describe calculation of turbidity values using equation (2-26a), the modified equation suggested by the Bureau of Reclamation (2006). Method two is that proposed by Luettich et al (1990) which makes use of equation (2-27). Method three is the combination of both equation (2-26a) and (2-27).

The least squares value (NTU^2) obtained for each method is as follows (refer to section 3.2 for explanation of the least squares value):

Method 1 – 435 932

Method 2 – 165 438

Method 3 – 555 897

It can be seen, from figure 5.9 and the least squares value, that method two appears to fit the data set significantly better in comparison to the other two methods. Each method has the same number of adjustable parameters required to predict the concentration of sediment due to erosion. Method one and three require the erosion rate constant, M, the critical shear stress, τ_c, and the time scale, T. Method two requires the model parameter, K, the critical shear stress, τ_c, and the reference shear stress, τ_{ref}. Therefore the comparison of the least squares value calculated for each model can be used to gauge the degree to which each model fits the observed data. If one model had more adjustable parameters, then it would be expected that the least squares value would be less than the other models‟ values. It must be noted however

that method three is very similar to method one- it differs only in the that instead of dividing by the critical shear stress, the excess shear stress is divided by some reference stress, making the term dimensionless refer to equation (2-27). To avoid confusion method three differs from method two in that the model parameter K is not constant.

From figures 5.8, 5.10, 5.11 and 5.13 it can be seen that the results obtained by method one and method three are very similar. Except for the time scale and the critical shear stress, the other model parameters differ. This could imply that the model is very sensitive to these two parameters and since they are the same for both methods, the results obtained from both methods were very similar.

It is important when comparing the different models to see whether the parameters used in each method (for example, the critical shear stress and erosion rate constant) are similar to those found in previous research. In the case of method one and method three the erosion rate constant (5.84×10^{-5} & 2.6×10^{-5} kg/m^{2}s respectively) appears to fall within the range of expected values according to what was reported by the Bureau of Reclamation (2006) and Chao et al (2008), namely $1 \times 10^{-5} – 5 \times 10^{-4}$ kg/m^{2}s. The critical shear stress for all methods, 0.3 Pa (for methods 1 – 3 respectively) appears to be at the upper limit of the range suggested by Mehta & Jain (2010) which was 0.1 – 0.3 Pa. The K value using equation (2-27) (method two) was found to be 4.08×10^{-1}g/L, this differs significantly to the values determined by Luettich et al (1990), which ranged from 8.6×10^{-7} – 0.125 g/L. Note that the K value is approximately half of the equilibrium concentration discussed in section 5.1.3. The K value incorporates the settling velocity, since in order to determine the K value the erosion rate constant, M, is divided by the settling velocity following Hamilton & Mtichell (1996). The settling velocity depends largely on the sediment type as well as the flocculation of the sediment, thus the K value calculated from the present case study may be expected to be different to that found by Luettich el al (1990). However even though the values are different, it would be expected that the estimated model parameters would only differ to those established by Luettich et al (1990) by some relation. This is because the only difference between of the model presented by this research and that that proposed by Luettich et al (1990) is the sediment. There doesn't appear to be a relation between the two models and the associated model parameters. The erosion rate constant estimated by Luettich et al (1990) was 3.3×10^{-9} kg/m^2/s which falls out of the range suggested by the Bureau of Reclamation (2006). One main difference between the two models is that Luettich et al (1990) estimated that the critical shear stress was zero, this was not the case presented by this research, and is a matter of the sediment characteristics. Thus

in order to establish the accuracy of the model proposed by this research, an investigation into the sediment characteristics is required, however this falls out of the scope of this research.

Since method two is based on the sediment flux given by equation (2-27a), effectively limiting the concentration of sediment within the water column, it would be a more accurate representation of what is physically occurring when the sediment is being re-suspended. Method one and method three have a time limit to erosion incorporating the critical shear stress and essentially limiting the concentration of the sediment within the water column by considering erosion only. However the question must be raised whether the velocity estimated by equation (2-27) is representative of the actual settling velocity. Factors that affect the settling velocity include electrochemical properties, biological properties and the turbulence (Bureau of Reclamation, 2006), The assumption of the settling velocity value, $9x10^{-5}$m/s, in method two, is potentially flawed since it doesn't take into consideration the previously mentioned sediment properties. Given the aforementioned factors method two, (equation (2-27)), was selected for predicting the sediment concentration within the water column.

Data collection within the Southern Lake was time consuming and significantly difficult due to a number of reasons. The most efficient boat to use within the lake would have been a flat bottomed boat due to the very shallow water. This was not possible and the only available boat was a semi-rigid with a deep hull. This resulted in the boat having to be pushed a distance of approximately 900m before it was in deep enough water to use the engines. Pushing the boat through the shallow water was very dangerous because of the crocodiles which inhabited the area. This resulted in the use of a number of poles to push the boat through the water, which proved to be time consuming and difficult in windy conditions. All these obstacles acting in combination resulted in the relatively small data set obtained by this research.

5.1.5 Sensitivity Analysis

Figure 5-14 – 5.16 shows the sensitivity of the model to a percentage change in the model parameters. The model parameters changed were the wind speed (figure 5.14) and the water depth (figure 5.15) and each parameter was changed by 20%. The fetch was kept constant and had a value of 3000m.

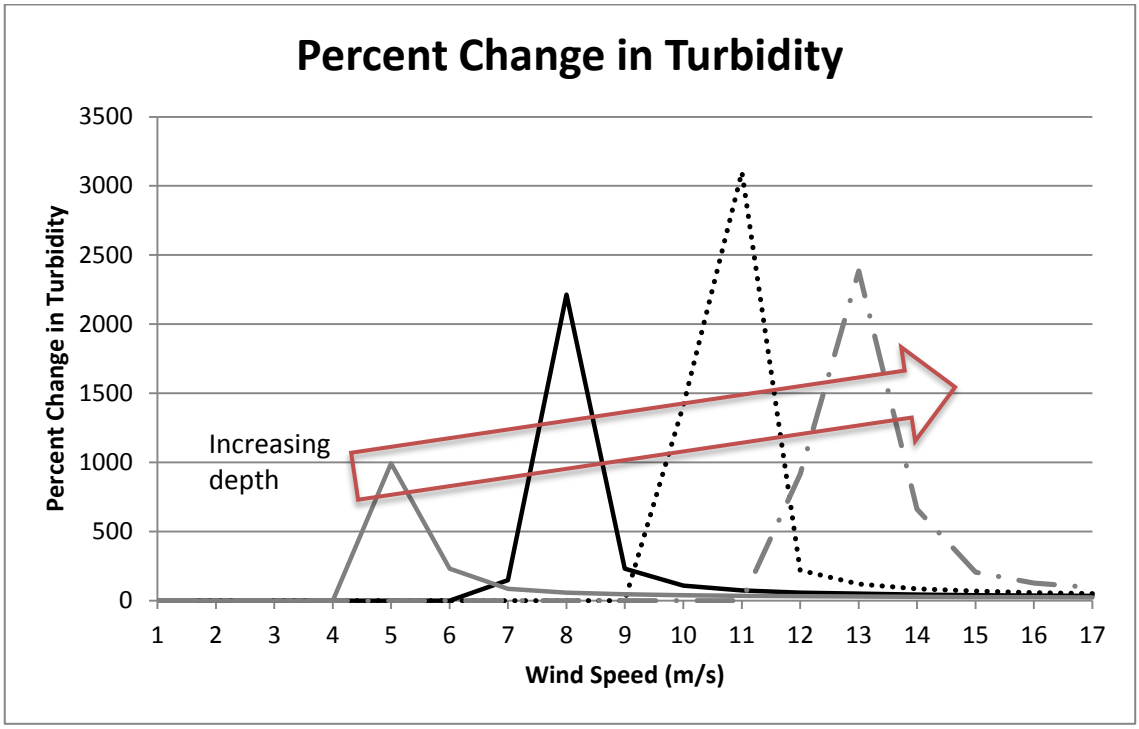

Figure 5.14: The percentage change in in turbidity for a 20% change in the wind speed for varied depths. The solid grey line is for a 0.5m depth. The solid black line is for a 1m depth, the dotted black line is for a 1.5m depth, dashed grey line is for a water depth of 2m. The arrow points in the direction of increasing water depth.

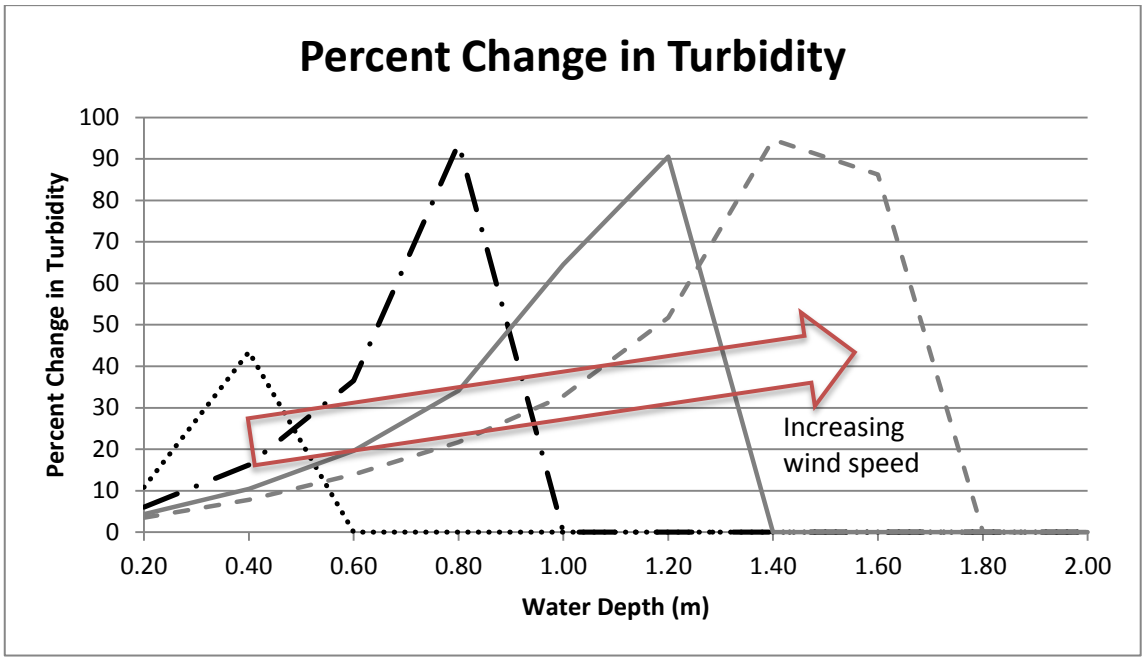

Figure 5.15: Percentage change in turbidity for a 20% increase on water depth. The dotted black line is for a wind speed of 6m/s, the dashed black line – 8m/s, the grey line – 10m/s, the dashed grey line – 12m/s. The arrow points in the direction of increasing wind speed.

Both figures 5.14 and 5.15 show there appears to be a nonlinear relationship between the associated parameters (wind speed and water depth) and the turbidity. The reason why figure 5.14 shows changes of more than 100% is because the 20% change in wind speed was an increase in wind speed and hence an increase in turbidity. Whereas figure 5.15 shows a percentage change of less than 100%, the reason why this occurred was because the 20% change in water depth was an increase in depth, hence a decrease in turbidity.

Both figure 5.14 and 5.15 show an increase to a point after which the change drops to zero (figure 5.15) or the change approaches some constant value (figure 5.14). This can be explained as follows:

For a certain wind speed and water depth, initially the wave heights are determined mainly by the wind speed and fetch. This occurs up to a point when the depth limit comes into effect at a large wind speed, since the fetch was kept constant. Thus the wave heights are now said to be determined by the depth limit and since the water depth is kept constant (refer to figure 5.14) the change in wave height becomes proportional to the square of the change in wind speed (refer to equation (2-4)). This change in wind speed is constant (20%) thus the change in wave height approaches a

constant value. Since turbidity is related to the wave height the observed trend is similar to what was observed with the wave heights.

As mentioned previously in figure 5.15 the general trend for the percentage change is an increase until a maximum value is reached after which the change drops to zero. This is because initially the wave heights are determined by the water depth (since the wind and fetch are constant). As the water depth increases the wave height increases to a point where the depth no longer controls the wave height but it is rather controlled by the wind speed and fetch, and since these two parameters were kept constant the change in wave height became zero. The turbidity largely depends on the wave height hence the relative change in turbidity corresponds to the above mentioned trend.

The sensitivity analysis was not only conducted for one constant water depth (in the case of figure 5.14) or one constant wind speed (in the case of figure 5.15), but it was carried out for a number of different water depth and wind speed conditions. For figure 5.14 what this change in depth showed was that the percentage change in turbidity increased with an increasing water depth, however from the peaks of the graphs it can be seen that the maximum change in turbidity was reached fairly rapidly above a water depth of half a metre. It also reveals that the wind speed at which this maximum value occurs increases with increasing depth. This is expected since a larger depth implies a greater wind speed would be required before depth limited conditions arose. Figure 5.15 shows that the percentage change in turbidity increases with increasing wind speeds. What is also revealed is that the maximum change in turbidity increases with increasing wind speed and it appears to be tending towards a constant value.

The reason why the readings were truncated at 17 m/s and 2m water depth was because the water depth in the lake is seldom greater than 2m and wind speed greater than 17 m/s is significantly higher than the average, i.e. it is representative of an extreme event. For argument"s sake, a sensitivity analysis can be carried out for a number of different conditions, and it is important to limit these conditions to represent realistic conditions.

5.1.6 Depth-Fetch Domain

Figure 5-16 shows the results for the depth-fetch domain limits for the Southern Lake. Each line represents a different wind speed and delineates the domain where the wave growth changes from being fetch limited to depth limited.

Note how each line appears to be described by a power-law relationship.

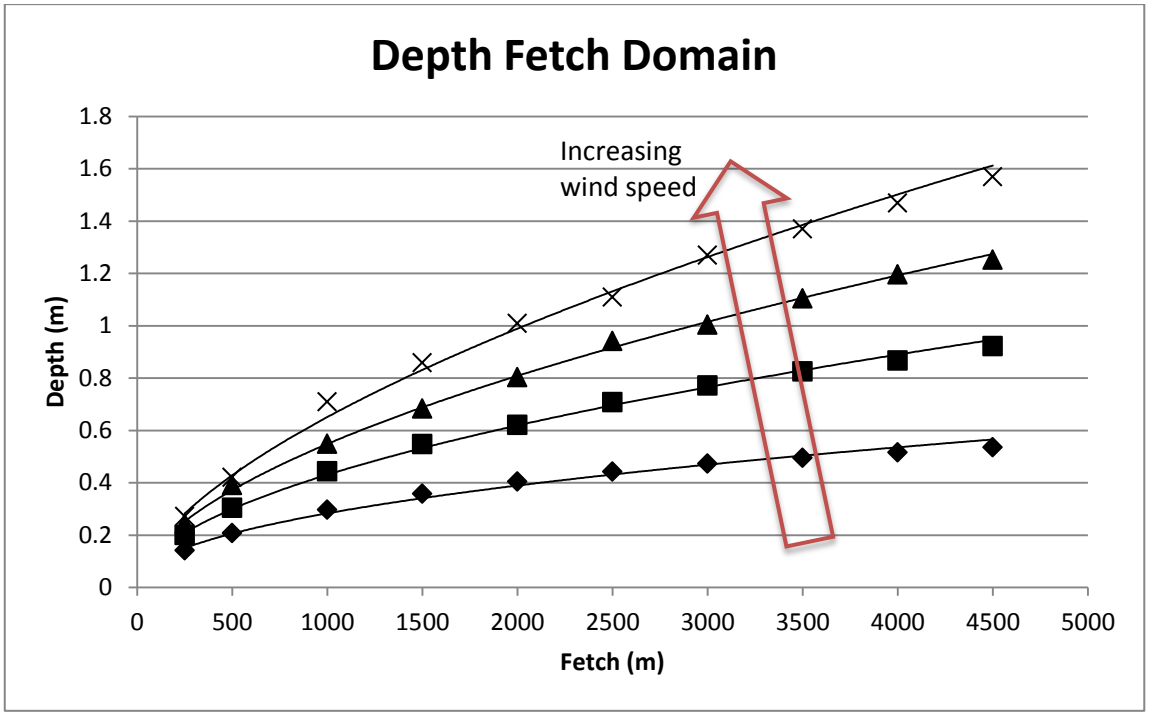

Figure 5.16: Depth-fetch domain for the Southern Lake. Each line represents the point at which the wave generation changes from being in fetch limited conditions to depth limited, for different wind speeds. The line joining the diamonds is for a wind speed of 4m/s, the squares are for a wind speed of 6m/s, the triangles are for a wind speed of 8m/s and the crosses are for a wind speed of 10m/s. The arrow points in the direction of increasing wind speed.

Power equations which define the line for each different wind speed are as follows:

$y = 0.0118x^{0.4599}$, for a wind speed of 4m/s. (5-1)

$y = 0.0116x^{0.5236}$, for a wind speed of 6m/s. (5-2)

$y = 0.0114x^{0.4607}$, for a wind speed of 8m/s. (5-3)

$y = 0.0101x^{0.6029}$, for a wind speed of 10m/s. (5-4)

where: y is the water depth (m) and x is the fetch (m).

As mentioned previously, there appears to be a power relation which delineates the depth-fetch domain into depth or fetch limited regions. This is what would be expected since at very small fetch (and hence the wave height is controlled by the fetch) equation (4-1) converges to $\varepsilon = \varepsilon_\infty\, k_2 \chi^{m_2}$, hence the energy is controlled by the fetch raised to some power. While at large fetch the energy is controlled by equation (2-19), the depth limit, i.e. the energy is controlled by the depth raised to some power.

The relationships ascertained from the depth-fetch domain were used in the spatial model to determine how much of the Southern Lake is in depth limited conditions.

5.2 Model Simulation Results

5.2.1 Monthly Average Turbidity Values

Figure 5.17 shows the monthly averaged turbidity readings for the two management scenarios defined in section 4.4.3. The two scenarios are (1) the current situation, a separated mouth system with an inefficient link channel, and (2) a combined uMfolozi and St. Lucia mouth.

Note that over the past ten years from 2000-2009 there appears to be an increase in turbidity values for the current situation. Whereas mouth linkage with the uMfolozi shows that the turbidity levels would stay relatively uniform. Mouth linkage with the uMfolozi results in significantly lower turbidity values in comparison to the current situation. This can be attributed to thee more stable water levels (and depths).

Note also the seasonal change in turbidity values. During the summer months the turbidity values are much higher than in the winter due to the seasonal wind patterns.

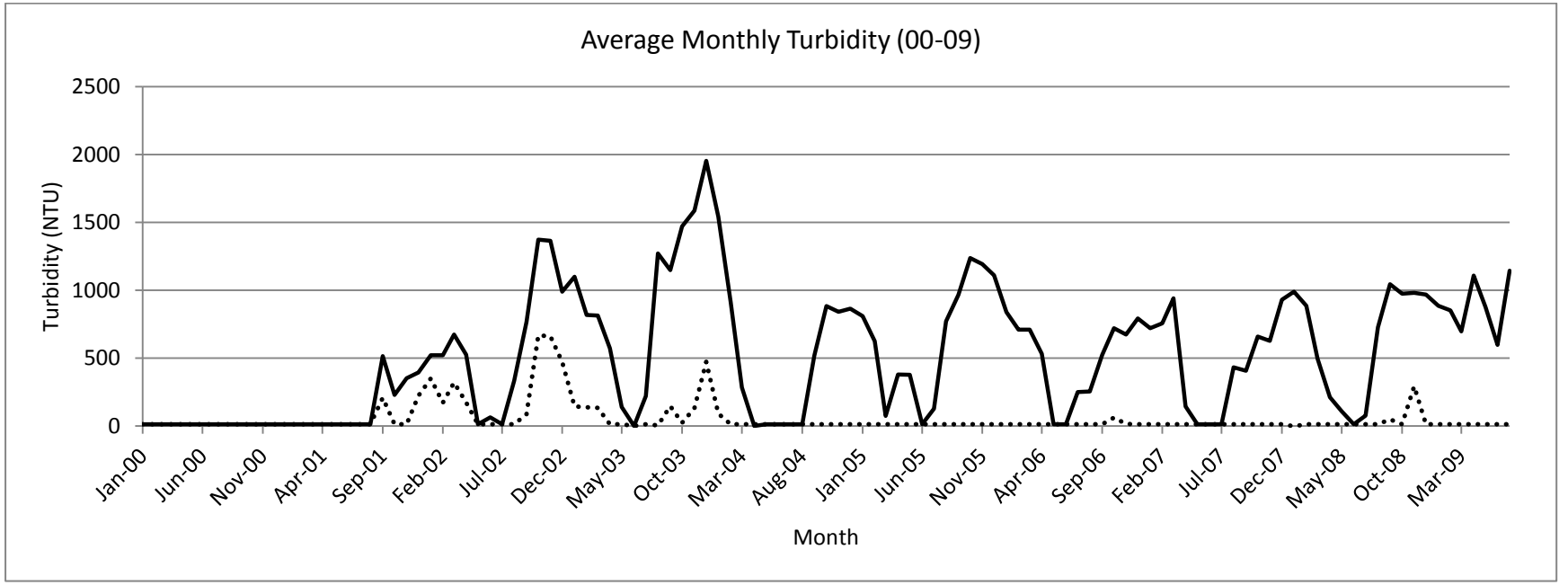

Figure 5.17: Monthly average turbidity trends for the two management scenarios. The solid black line is for scenario 1 (the current situation), and the dotted black line is for scenario 2 (combined mouth).

It can be seen that the turbidity values for the current situation are much greater than those for a combined mouth scenario.

Over the last ten years, under the current situation (separated uMfolozi and St. Lucia systems), the turbidity values have been increasing. This can be attributed to the low water levels, which have been caused by the drought and separation of the system from the uMfolozi (Cyrus et al, 2010). Therefore this trend is what is expected. What is clear from figure 5.17 is that if the mouths had been combined, not only would the turbidity values be significantly reduced from current day values, but the turbidity values would have stayed relatively uniform. This shows how important the uMfolozi is as a drought protection tool. The way in which the uMfolozi acted as a drought protection tool historically is as follows according to Cyrus et al (2010):

During drought the mouth shared by both the systems would close. This was due to sediment accumulation in and around the mouth, since flows through the combined systems would be small. Once this mouth would close, water levels within the St. Lucia system would drop due to the high evaporation rates, levels would drop below the system"s mean water level. This implies that water from the uMfolozi would then flow up the St. Lucia system recharging the lake water levels.

There is a significant period where the turbidity for the combined system is 12.7 NTU. This is not to say that there wasn"t any sediment re-suspension during this period. Due to the TSS-turbidity calibration there is a possibility that the concentration of sediment could have fallen within the range of 0 – 0.1g/L. However the combined system represents a hypothetical situation since this has not occurred since 1952. The water depths determined by the water balance model are the estimated values and since no measured depths exist for the combined system it is difficult to gauge the accuracy of these readings. However, regardless of the values of the estimated water depths, figure 5.17 shows the importance of uMfolozi in stabilizing the water levels within the St. Lucia system as mentioned previously.

Figure 5.17 also shows the seasonal variation in turbidity. What can be seen is that during the summer months the turbidity readings are high and during the winter months the turbidity levels are significantly less. This corresponds to the wind speed pattern, high wind speeds during the summer months (October – February) and low wind speeds during the

winter months (May – July). This is shown in figure 5.18, the typical seasonal pattern of wind speeds for the period of 2000.

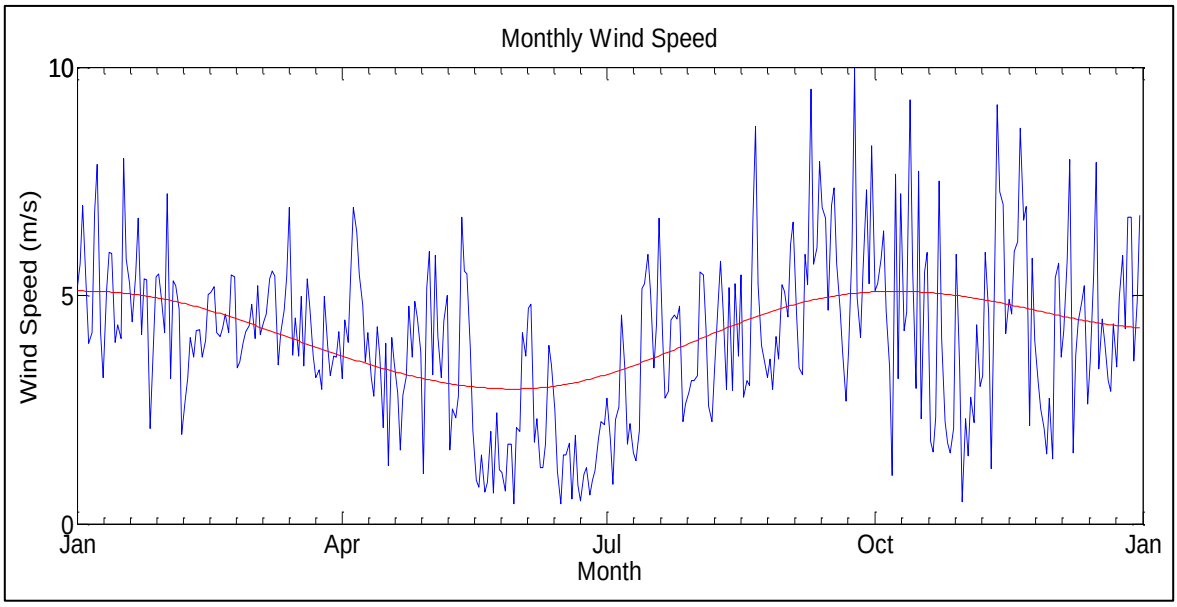

Figure 5.18: monthly wind speeds for the year 2000. The red line represents the general monthly trend for the year 2000.

This natural seasonal change in turbidity corresponds with the biological functioning of an estuary system. For example fish located on the seaward side of the estuary breed during winter, and during the spring to summer months the juvenile fish enter the open mouth, if the mouth is open (Perissinotto el al, 2010a). The higher levels of turbidity act as a mask for the juvenile fish. Protecting them from predation and allowing them to grow in a relatively safe environment. The resident estuarine species tend to breed during the winter months, when the mouth is closed (Perissinotto et al, 2010a). This allows them to feed on the more visible zooplankton. The reason for the large numbers of zooplankton is because the turbidity is low; this correlates with the findings of Carrasco et al (2007), which states that the mortality of zooplankton increases with an increase in turbidity.

5.2.2 92 Year Average Depth

Figure 5.19 shows the general trend in turbidity for the period of one year. The wind speed used to determine the turbidity was the average of the 95% percentile (mentioned in chapter 4.3.1) over the past ten years. The water depth used was that of the median for each month over the last 92 years, this was obtained from the existing water balance model (Lawrie & Stretch, 2008). The predicted turbidity levels are similar to those measured by Cyrus & Blaber (1988), refer to figure 5.21. The observed trend by Cyrus & Blaber (1988) is the same as that estimated by the model (figure 5.19), high during the summer months and low during the winter months.

The two situations considered were a combined system with the uMfolozi and the current situation.

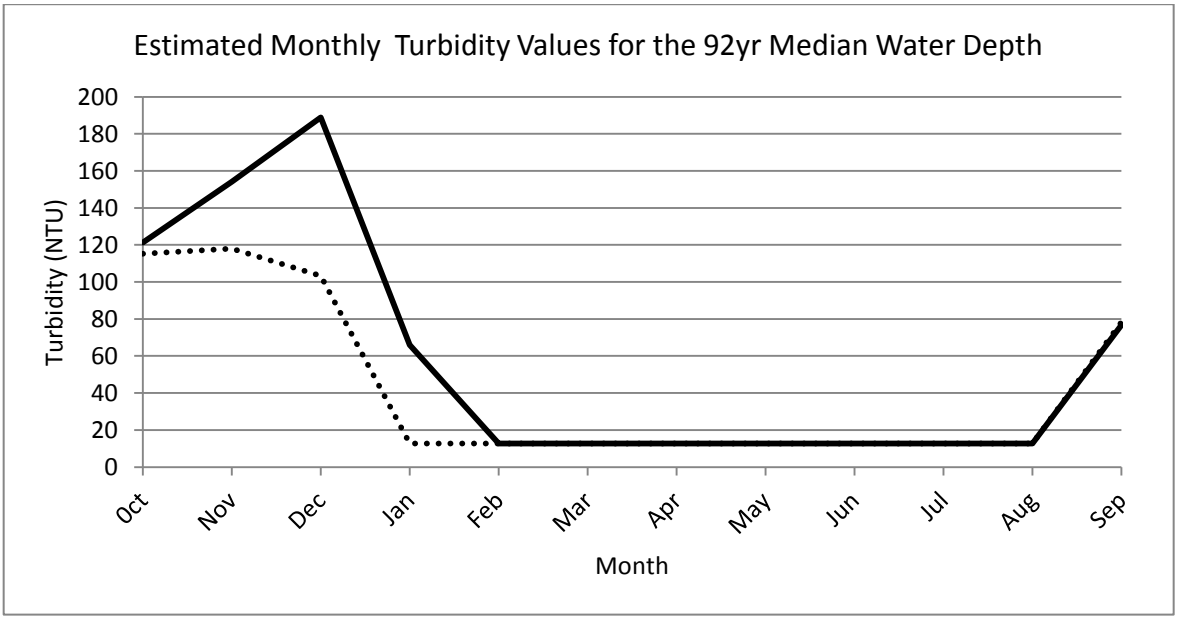

Figure 5.19: Model predicted turbidity values for each month for the 92 year average depth. The solid black line is turbidity values for the current situation. The dashed black line is turbidity values considering a combined system. The dotted black line is measured values by Cyrus & Blaber (1988).

It is clear from figure 5.19 that the trend in turbidity values is the same as that mentioned in chapter 5.2.1, i.e. high during the summer months and low during the winter months. The

reason for this is the same as mentioned previously, high wind speeds during summer and low during winter.

It is also clear that if the St. Lucia system was combined with the uMfolozi the turbidity values would be significantly lower than the current situation during the summer months. This is because the water levels would be higher and more stable thus preventing episodes of high turbidity values. This is shown in figure 5.20. The effect of the uMfolozi in recharging the water levels during winter can also be seen in figure 5.20; this effect is explained in section 1.1. The trend in estimated water depths observed for the current situation is not what is expected. During the summer months the water levels are lower than in the winter months. This could possibly be explained by the fact that during the summer mouths, when the mouth is open the water levels are approximately 0 MSL (1.08 average water depth (Lawrie & Stretch, 2008)). Once the mouth closes the water levels would gradually build to a level that would eventually breach the beach berm and hence reduce back to 0 MSL.

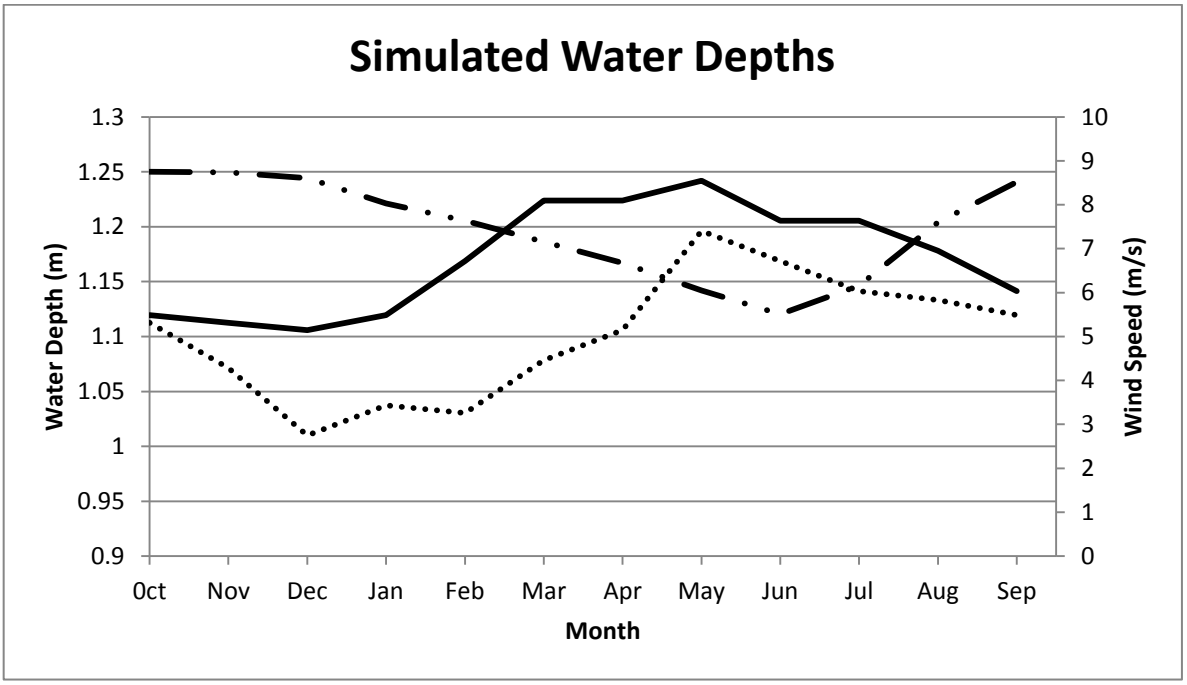

Figure 5.20: The 92 year median of the simulated water depths. The solid black line is the median of the simulated depths for a combined system. The dotted line is the median of the simulated depths for the current scenario, i.e. no mouth linkage with the uMfolozi. The dashed line shows the variation in wind speed.

The values predicted by the model don't appear to be similar to that measured by Cyrus & Blaber (1988). The reason for this is because measurements done by Cyrus & Blaber (1988) where done within the St. Lucia estuary near the mouth, which is approximately 22km downstream of the Lake (refer to figure 1.3). Therefore the measurements by Cyrus & Blaber (1988) are expected to differ because the St. Lucia estuary has a completely different fetch and average water depth. The estuary would also be affected by the tides, thus sediment re-suspension would be due to the tidal currents acting in combination with the shear stress exerted by the wind induced waves. Therefore the two measurements of turbidity cannot be directly compared, but what is clear is that the trend is the same. The measured values of Cyrus & Blaber (1988) support the notion of high turbidity during the summer months and low readings during the winter months.

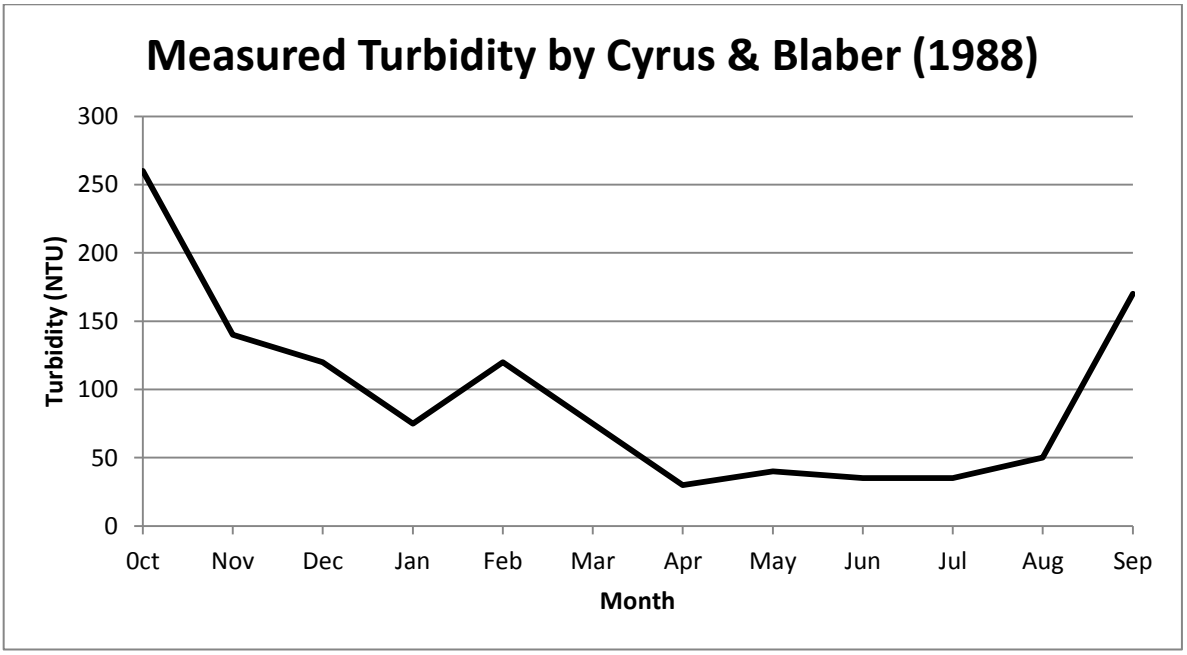

Figure5.21: Measured turbidity values by Cyrus & Blaber (1988).

Both the effects of wind speed and water depth must be considered when considering sediment re-suspension, since the two parameters act in conjunction. The turbidity in the combined system reduces to almost zero in January, unlike the current situation, where the turbidity decreases to the same value only in February. Since the wind speeds are the same it must be attributed to the water depth (refer to figure 5.20). The water depths are higher and more stable for the combined system due to the effect the uMfolozi has on

recharging water levels within the lake (Whitfield & Taylor, 2009). Thus the decrease in January would be explained by the decrease in wind speed in combination with the increase in water depth (this is shown in figure 5.20). This shows the non-linear relationship between turbidity and water depth established in section 5.1.5. A slight increase in water depth and a slight decrease in wind speed can significantly reduce the estimated turbidity value. It takes much longer for the current situation to drop to the same value since the water depth is so low that even low wind speeds are capable of re-suspending sediment. The water depth increases after February and this fact coupled with the decrease in wind speed would result in the decrease in turbidity after the month of February for the current situation.

5.2.3 Turbidity for the Past Ten Years

Figure 5.22 shows the median of the monthly turbidity over the past ten years in comparison to turbidity readings estimated for the 92 year median depth. This was conducted to examine the effects that the drought had on the turbidity readings over the past ten years, i.e. from 2000 – 2009. The 92 year average depth was considered using the current situation"s water levels, i.e. considering mouth linkage with the uMfolozi before 1952 and separation after 1952.

The wind speed used to determine the turbidity was the monthly average of the 95 percentile of the maximum for each day.

Note how the trend appears to be similar (higher in summer and lower in winter). However the turbidity within the lake has increased significantly.

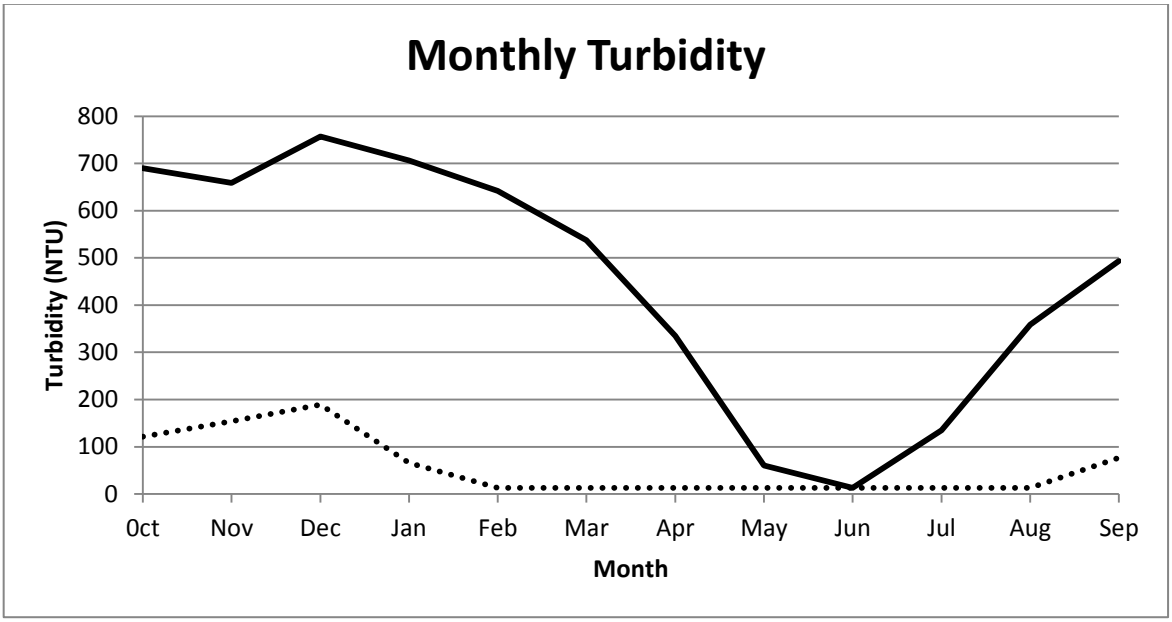

Figure 5.22: Effect the drought has had on turbidity levels within the lake. The solid black line represents the median of the monthly turbidity predictions from 2000 – 2009. The dotted black line represents monthly turbidity using the 92 year median depth.

Figure 5.22 shows that over the past ten years the monthly trend in turbidity has been the same, high during summer and low during winter. However the turbidity has significantly increased. This can be attributed to the effect the drought has had on reducing water levels.

The increase in turbidity over the past ten years would have significantly affected the biological functioning of the system. The higher turbidity during the winter months would result in lower zooplankton numbers (Carrasco et al, 2007) and hence less available food for the developing juvenile fish species within the lake.

Even though the turbidity levels have been higher over the past ten years the threshold proposed by Carrasco et al (2007) of 2.58 g/L (3538 NTU), according to the model, has not been exceeded. To examine whether this threshold proposed by Carrasco et al (2007) is exceeded, it would be advised to observe the 3 hourly turbidity values predicted by the model. However if the threshold is exceeded in the latter case, it would likely to only be exceeded for a few hours. Carrasco et al (2007) studied the effects of this high sediment load on the mysids for a period of 12 hrs., thus if the threshold is exceeded for only a few hours the associated effects would be significantly less than those observed by Carrasco et al (2007).

5.2.4 Daily Turbidity Trend

Figure 5.23 shows the typical daily trend in turbidity for the Southern Lake. The settling velocity was assumed as $9x10^{-5}$ m/s for the winter month and $4.5x10^{-5}$ m/s for the summer month. Note the effect of including deposition. This effect seems to reduce the turbidity peaks compared to cases that only include erosion. In comparison to cases that only included erosion, the effect of including the deposition also seemed to prolong the time the re-suspended sediment stays within the water column. However it can be seen that the sediment appears to deposit out of the water column relatively quickly.

Figure 5.23 shows a typical example of the daily trend in turbidity for (a) a typical summer month (February 2002) and (b) a typical winter month (July 2002).

The time interval used was three hours; this is in accordance with the time step established in table 5.1.

The concentration of sediment within the water column was calculated using equation (2-32).

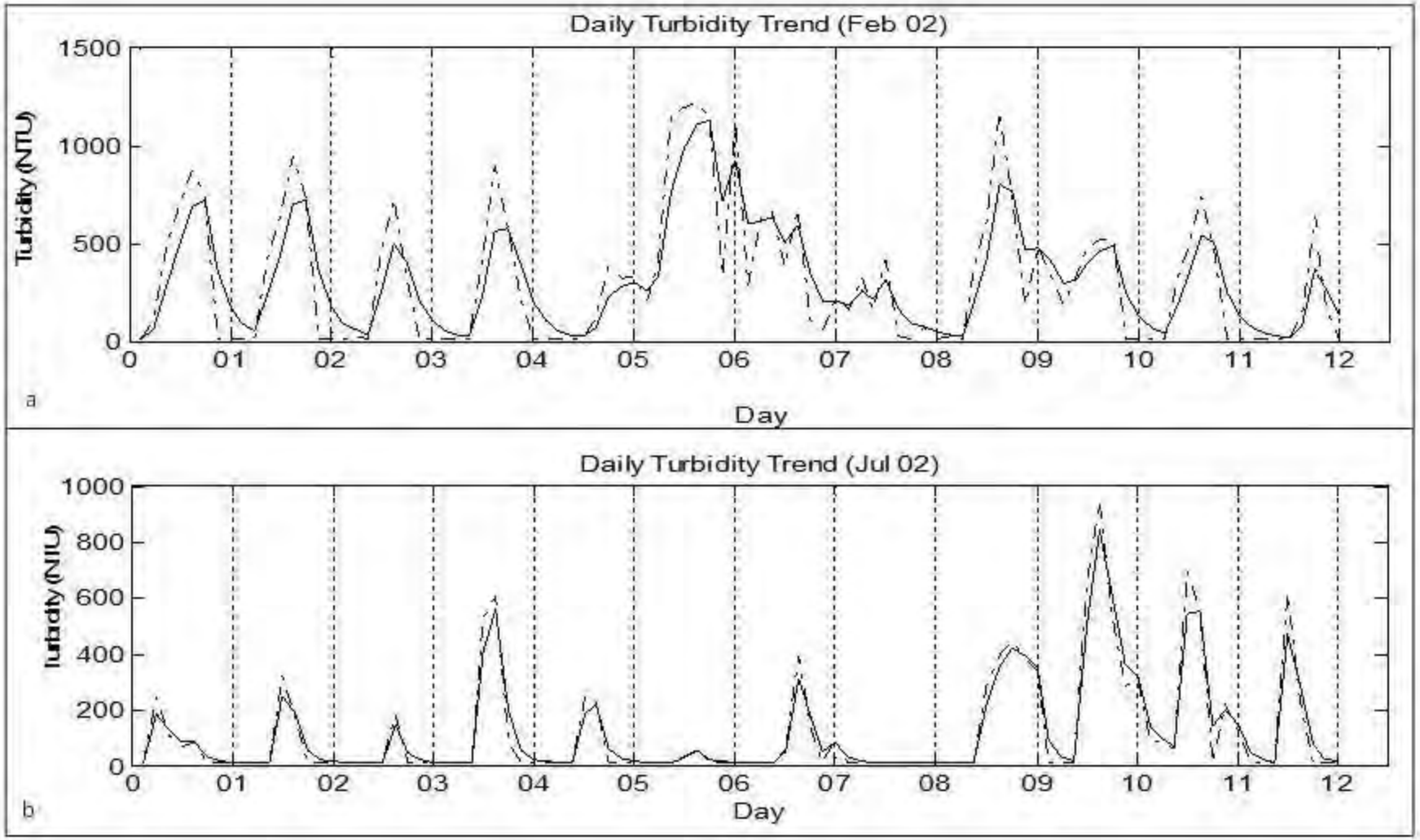

Figure 5.23: Daily Turbidity trend for (a) a typical summer month and (b) a typical winter month. The dashed line is turbidity considering the erosion only; the solid line is the turbidity in accordance with equation (2-32).

It is clear from figure 5.23 that the effect of including deposition decreases the turbidity peaks and prolongs the time which the sediment remains in suspension. This would then imply that the turbidity predicted in figures 5.17, 5.19 and 5.22 are possibly higher than what the actual turbidity readings would be if the deposition was incorporated. However without comparison to observed data this cannot be proven. The average value (for including deposition) might be similar to that of excluding deposition, because, even though the peaks are truncated, the troughs are higher. Therefore it is probable that the average value stays the same as if the deposition wasn"t included (as is the case for figures 5.17, 5.19 and 5.20). Determining the settling velocity is not as simple as using a set of predetermined equations derived by other research based on a different lake. The reason for this is that the settling velocity depends on the electrochemical, physical and biological characteristics (Bureau of Reclamation, 2006). The settling velocity used to produce figure 5.21(b) was $9x10^{-5}$ m/s. This settling velocity was a „crude" estimate suggested by Maine (2011), from observations of the behaviour of the Southern Lake sediment. This value was then halved in figure 5.21(b), since in summer the lake would generally be in a more turbulent state (due to the high wind speeds) thus resulting in a lower settling velocity.

While it is seen that there is potential error in determining the value of the settling velocity (as it was only an estimation), the associated deposition effect can be seen. However until an accurate estimation of the settling velocity is determined, it would be difficult to precisely state its effect, i.e. the prolonged effect of the sediment being entrained within the water column after the wind speed decreases.

The strong daily diurnal pattern in the turbidity predictions can be seen. This corresponds to the similar pattern observed in the wind speed.

5.2.5 EMD Results

Figure 5.24 shows the EMD of the wind speeds for the month of January 2000. The first graph is the wind signal obtained from SA weather. Each graph below the original signal represents a different intrinsic mode function (IMF). An IMF is obtained by subtracting each value in the original signal from the mean of the cubic spline envelope described in chapter 4.3.1. According to Huang et al (1996) an IMF is a function which satisfies two conditions, (1) the number of extrema and zero crossings must be equal, or at most differ by one, (2) the mean value defined by the envelope of the local maxima and local minima must be zero.

Each IMF shows the different component signals which the original signal is made up of. Each IMF also represents different trends, for example the first IMF appears to be wind gusts, while the seventh appears to be the weekly cycle and the last IMF represents the residual value. This residual value, or residue, represents a monotonic function from which no more IMF can be obtained (Huang et al, 1996).

The sum of IMF 3 – IMF 8 is represented by the red line on the original signal.

There is a clear diurnal pattern in the wind speed. The general trend is for the wind speed to increase during the day to its maximum around midday and then decrease in the evening. It is the observation of this pattern that led to the method of taking the 95th percentile of this maximum value as the wind speed causing sediment re-suspension. The large variation in the wind speed is also the reason why the average wind speed for the day can"t be used as the wind speed causing sediment re-suspension.

Taking the 95th percentile of the wind speed as the wind speed causing sediment re-suspension is in accordance with the biological responses to the turbidity within the day, i.e. phytoplankton production and algae growth occurs during times when the sun is shining (Perissinotto et al, 2010b). The average turbidity during the day (i.e. when the sun is shining) is important to the biologists since it limits the phytoplankton productivity (primary production requires photosynthesis) and algae growth due to the lack of available energy (from the sun) throughout the water column (Perissinotto et al, 2010b).

5.2.6 Spatial Model

Wave heights (figures 5.25 – 5.26) were calculated for the Southern Lake for two categories of wind speeds and water levels. Figure 5.25 shows the wave height contours for a 8m/s NE wind combined with two different water levels, that of 0 EMSL (a), corresponding to an average water depth of 1.14m, and -0.5 EMSL (b), corresponding to an average water depth of 0.79m (Hutchison, 1974). The half a metre drop in water level doesn't correspond to half a metre drop in the average lake depth (considering the Southern Lake). This is because the water level corresponds to the water level for the entire lake system (approximately 40km long according to figure 1.3). Each water level corresponds to a different water depth for each component of the lake system, and for the Southern Lake the depths are those mentioned previously. The comparison between the two different water depths was done to show the effect that the associated change had on the wave heights. Figure 5.26 shows the wave heights for a 8m/s SW wind considering water levels of 0 EMSL (a) and -0.5 EMSL (b). Note how even though there is a large change in water level (and hence bathymetry) the change in wave height is approximate 0.5m.

Figures 5.27 – 5.28 show the spatial distribution of turbidity within the Southern Lake for the different wind and water levels mentioned in the previous paragraph. Note that for half a metre drop in water level there is a significant change on turbidity.

Table 5.2: Percentage that the Lake is in depth limited conditions for the above wind and water level scenarios.

Wind Speed (m/s)	Wind Direction	Water Depth (m)	Percentage Depth Limited
8	NE	1.14	40%
8	NE	0.79	66%
8	SW	1.14	59%
8	SW	0.79	88%

From figures 5.25 and 5.26 it can be seen that the maximum significant wave height for each scenario appears to be very similar, i.e. for a water level of 0 EMSL (1.14m water depth) and a wind speed of 8m/s the maximum significant wave heights for both the NE wind and SW wind are 0.25m. It would be expected that if the wave height is large the turbidity would also be high; this would be the case if the water depth was uniform throughout the lake. However from figures 5.27 – 5.28 it can be seen that the wave heights causing the high turbidity values range from 0.05m – 0.15m. This implies that the contributing factors are the wave heights and the water depth acting in conjunction.

For both wind directions it can be seen that a drop of 0.5m in the average water level increases the turbidity throughout the lake significantly, even though there is a small change in wave height. This observation reveals the sensitivity of the model towards the change in water depth.

Table 5.2 shows the percentage of the lake that is in depth limited conditions. The depth limits were calculated using figure 5.16. It is interesting to note that for the SW wind more than 50% of the lake is in depth limited conditions for the two water level scenarios. In the case of the NE wind there is a greater change in percentage depth limited, but the amount of the lake in depth limited conditions is significantly less than for a SW wind. This can be explained as follows.

For ease of discussion figure 4.3 has been inserted on the following page, Winds blowing from the NE will initially blow over deep water (approximately 2m), initially the fetch is small and hence the depth below which the waves would be considered to be in depth limited conditions is small (refer to figure 5.16). Hence, initially the waves wouldn't be in depth limited conditions for a NE wind. However for winds blowing from the SW initially the water depths are shallow, and hence initially the waves are in depth limited conditions. By the time the wind has reached the deeper water (along the NE

edge of the lake) the fetch is long, hence the depth below which the waves are in depth limited conditions (refer to figure 5.16) is greater, allowing more of the waves travelling through the deeper water to be in depth limited conditions.

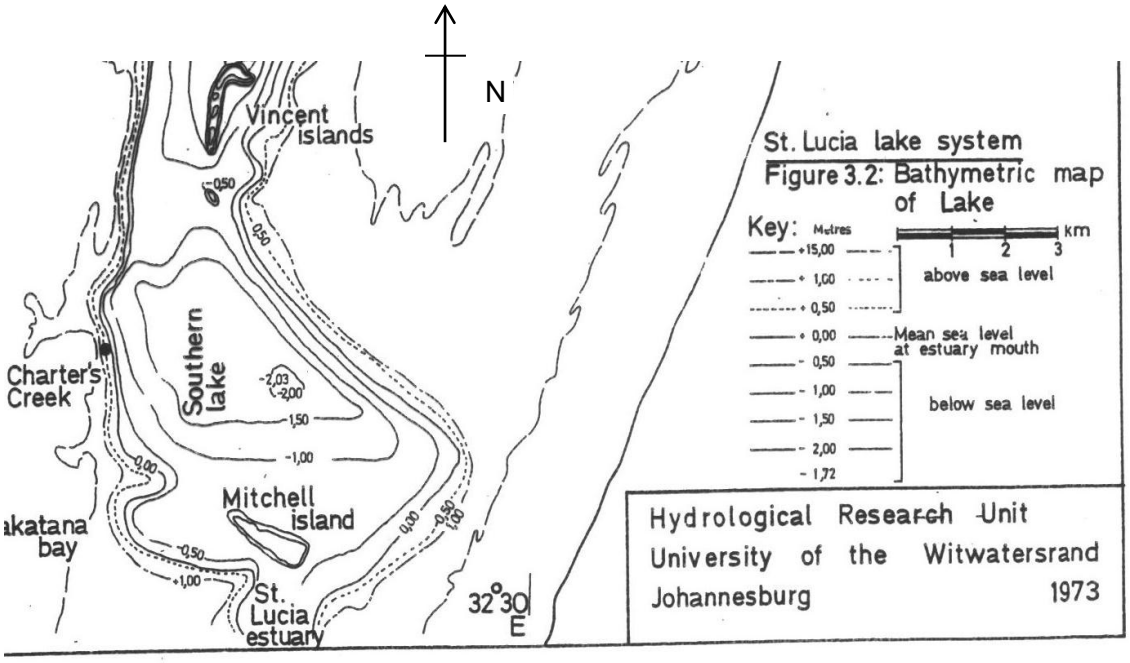

Figure 5.27: A copy of figure 4.3, the bathymetry of the Southern Lake, according to Hutchison (1974).

CHAPTER 6

SUMMARY AND CONCLUSIONS

Three questions were proposed by the research with the aim of characterising turbidity patterns within the Southern Lake of St. Lucia. The development of a mathematical model was achieved through the empirical relations of wave height, wind speed, fetch and water depth. This model was then calibrated using field observations and measurements. Once calibrated, the model was then used to show the typical trends in turbidity on a daily, monthly and monthly average over the past ten years. This chapter presents the summary of the results, conclusions and further recommendations.

6.1 Development of Mathematical Model

What are the physical processes by which wind-driven sediment re-suspension occurs within Lake St. Lucia, given it is a naturally shallow system with cohesive sediment, and how can they be integrated into a predictive model?

The mathematical model was developed through the combination of a number of modelling techniques for the different model parameters, such as wave height, shear stress and the erosion prediction. The wave heights and periods were calculated using the empirical relations derived by Young & Verhagen (1996). The shear stress exerted on the lake bed was determined by the wave boundary layer theory (Reeve et al, 2004). The concentration of re-suspended sediment was calculated by two methods, that suggested by the Partheniades (1962) [equation (2-26a)] and that suggested by Luettich et al (1990) [equation (2-27)].

The model was calibrated using the field measurements taken in the Southern Lake during the period from March 2011 to June 2011. From the calibration, the method of determining sediment re-suspension using equation (2-27) was chosen. This was chosen not only because it fitted the measured data better than the other method, but rather because of its inclusion of the settling velocity. The inclusion of the settling velocity is incorporated through the model parameter K. In order to determine the parameter K in equation (2-27), the erosion rate constant (M) is divided by the settling velocity. This is based on the fact that at the air-water interface (i.e. the free surface)

the net sediment flux is zero. Therefore the physics upon which equation (2-27) is based is more representative of the physical process of sediment re-suspension.

6.2 Turbidity Trends

The model was then used to predict the trends in turbidity for a number of different situations, discussed as follows:

The first situation that was considered, was the prediction of turbidity for the period from 2000 – 2009 on a monthly time step. This required linking the model with the current water balance model developed by Lawrie & Stretch (2008). What this showed was that over the past ten years the trend has been an increase in turbidity for the current situation (no combined mouth). This is what was expected since the system has been drought stricken for the past ten years. However what it also showed was that if the uMfolozi and St. Lucia system were combined (as they were before 1952) the turbidity would have been much lower than that experienced by the current situation and the trend would have been more stable, i.e. the general trend was not increasing but it would rather be some constant average value.

The model was then used to observe how current situations‟ monthly turbidity values (using the monthly average wind speeds) compared to the combined mouth scenario, using the 92 year median depth. This was done to gauge how the system normally behaves in response the changing wind pattern during the seasons. What this showed was that the monthly median turbidity for the current situation was much higher than the combined mouth scenario. It also showed that the response of the combined mouth scenario to change in wind speeds was much faster than the current situation. The reason for this is because the water level is more stable for the combined mouth unlike the current situation. Thus a change in average wind speed yields a fast response to the change in average turbidity under the combined system. These values were compared to values recorded by Cyrus & Blaber (1988). The observed trend was the same. This trend was high turbidity during summer and low during winter. The reason for the difference in readings was due to the location where Cyrus & Blaber (1988) recorded their readings. The location where they were recorded was near the estuary mouth which is 22Km south of the Lake, hence a large difference in readings is expected due to the different shaped basin, water depth and effect of the tidal currents.

Using the monthly average depths over the past ten years, the median monthly turbidity predictions (over the past ten years) were compared to the 92 year median depth monthly turbidity readings for the current situation. This was done to visualise the effects that the drought has had on the system. What it showed was that the monthly turbidity predictions over the past ten years have been much higher than what would have normally been experienced by the system. In most instances the turbidity has been double the normal value, refer to figure 5.22. Thus it can be concluded that the drought has had a severe effect on increasing the monthly average turbidity. However, according to the model, in no cases has the turbidity exceeded the threshold value suggested by Carrasco et al (2007) of 3538 NTU. This does not mean that there has not been a negative effect on the biological functioning of the system, since less light (and hence energy) would have reached the lower levels of the water column. The numbers of zooplankton would have been reduced according to Carrasco et al (2007) and hence there would have been less available food for juvenile fish.

The settling velocity was then incorporated and the daily turbidity pattern was predicted for a typical summer month (February 2002) and a typical winter month (July 2002). For the winter month the settling velocity was assumed to be 9.5×10^{-5} m/s. This was based on observations by Maine (2011) for sediment from the Southern Lake. This value was then halved for the summer month because it was assumed that the more turbulent conditions in summer would yield a lower settling velocity, as it is assumed that the higher turbulence would tend to break potential flocs. While it is seen as a gross approximation of settling velocity, as it is not based on any empirical relations, the decision was made to use it. The reason for this was because there was no daily turbidity data to compare the model predictions to, thus any predictions are simply viewed as predictions since it is not possible to state the accuracy of the values. It was seen more important to show the effect that including the deposition had on turbidity trends though out the day. This effect, of including deposition, was to reduce the peaks in turbidity due to erosion and prolong the time which the sediment stays in in the water column. This effect is what was expected, since including the deposition implies that the concentration of sediment within the water column at a given time would be due to the erosion and deposition flux. It was also clear from figure 5.23 that the daily trend in turbidity followed that of the wind speed, i.e. it increases to a maximum value around midday and then reduces to some lower value in the evening. The values of the turbidity during the winter day are very similar to the turbidity considering the erosion only, whereas during the summer day, the values differ significantly from considering

erosion only. This can be explained by the fact that the sediment stays in suspension longer in more turbulent condition.

When determining the monthly average turbidity predictions in chapters 5.2.1 – 5.2.3, the effect of deposition was not included. This was because the time step was seen as too large. When including the settling velocity for the daily turbidity trend a time step of three hours was used. This was in conjunction with the time limit established using equation (2-26a), i.e. it would take three hours for there to be equilibrium between erosion and deposition.

6.3 EMD Summary

The EMD (empirical mode decomposition) was successfully used to analyse the diurnal pattern in wind speed. The noise, or wind gusts, was separated from the original signal, leaving a trend line that showed the clear diurnal trend in wind speed. The trend showed an increase in wind speed, to a maximum around midday, and then a decrease in wind speed in the evening.

It is important for biologists to determine the relationship between re-suspended sediment and light availability and its effect on phytoplankton productivity. In light of this (Cloern, 1987), the 95th percentile of the maximum wind speed (once the noise was separated) was used as the characteristic wind speed for the day. This was because taking the average wind speed for the day (including wind speeds at night) would yield turbidity values which are not representative of the turbidity during the day. Excluding the night would be another method of determining the daily average turbidity; however this would probably yield a wind speed similar to the 75th percentile or higher.

6.4 Spatial Model Development

Can a model be used to predict the lake average turbidity value as well as the spatial distribution of turbidity within the lake?

The empirical method of determining wave heights and periods suggested by Young & Verhagen (1996) was then applied to a spatial model. The bathymetric map determined by Hutchison (1974) was used to determine the water depths relative to EMSL. A

simple rule was used to account for the effects of bottom friction on the wave heights and periods; if the actual water depth was less than the fetch averaged water depth, then the water depth to be used would be the actual water depth to estimate the wave characteristics.

This spatial model was then used to determine the turbidity for a SW and NE wind blowing at 8m/s and water levels of 0 EMSL and -0.5 EMSL (1.14m and 0.79m water depths respectively). What the model showed was that for 0.5m difference in water level there was only a small change in wave height, however the change in turbidity was significant. The results also showed that the high turbidity values occurred in the shallow water. This implies that considering the wave height as an indicator of high turbidity is short sighted and it is important to consider both the wave and water depth. The reason for this is that the effect of the wave on the lake bed (i.e. the shear stress) depends not only on the wave height but also the water depth.

Using the depth-fetch domain derived from the model (figure 5.16) the percentage of the lake that was in the depth limited condition was calculated. This showed that winds blowing from the SW resulted in a higher percentage depth limited conditions compared to the NE wind direction. This was due to the orientation of the lake and the location of the deep and shallow water.

The reduction of wave heights due to breaking and bottom friction were incorporated through a rule used in the model, mentioned previously. This indirectly incorporates the effects of wave breaking on the wave heights. However in order to improve the model it is advised to discard this rule and explore actual relations with wave heights and the effects of breaking. The rule was used by this model, since; research into the effects of bottom friction fell out of the scope of this research.

6.5 Biological Effect

What are the biological effects of the associated turbidity levels, for example is the threshold concentration, proposed by Carrasco et al (2007) of 2.58g/L, exceeded?

The threshold proposed by Carrasco et al (2007) of 3538 NTU appeared to not be exceeded. However from figures 5.17, 5.22 and 5.23 it is evident that turbidity levels exceed 500 NTU very regularly and even reaching as high as 1500 NTU (figure 5.17). These high levels of turbidity are certainly going to have an effect on the biological

functioning of the system. To put this into perspective Cyrus and Blaber (1988) suggested a scale to determine what level a system falls into regarding turbidity. The levels were as follows:

Less than10 NTU is a clear system. Between 10 and 50 NTU the system is classified as semi turbid. Between 51 and 80 NTU the system is predominately turbid. Greater than 80 NTU is a very turbid system. Thus over the past ten years the Southern Lake has by far exceeded the value of 80 NTU, which implies that either the scale needs to be re-evaluated or the system has been in a very bad condition over the last ten years.

The high turbidity values reduced the productivity of phytoplankton according to Perissinotto et al (2010b); this is in accordance with what is suggested by Cloern (1987), who states that turbidity limits the productivity of phytoplankton. The reduction in phytoplankton would have a negative effect throughout the food chain. The high turbidity levels would also have a negative effect on the juvenile organisms within the system. Initially the high turbidity would successfully mask the juvenile organisms as suggested by Perissinotto et al (2010a), however during the winter months, due to the high levels of turbidity; zooplankton numbers would reduce (Carrasco et al, 2007) thus resulting in less available food for the juvenile organisms to feed on.

6.6 Summation

The objectives of this study were achieved through the development and application of a mathematical model. The mathematical model represents the first attempt at modelling turbidity within the Southern Lake. This model was shown to be able to predict the turbidity within the Southern Lake as a result of wind either as a lake average value or as a spatial distribution. The model made use of empirical relations to predict the wave characteristics and wave boundary layer theory to determine the amount of sediment re-suspension as a result of the waves. Due to the low water levels it was shown that the turbidity levels over the past ten years have been much higher than if the system was combined with the uMfolozi. These high turbidity levels have had a negative effect on the biological functioning of the system.

6.7 Recommendations for Further Research

The major limitation of this research is that there has not been significant data collection of turbidity, wind speed and water depth data from the Southern Lake. In order to improve the model and validate the results, it would be suggested to set up one or more monitoring stations within the lake. These monitoring stations could then record turbidity, wind speed, direction, water depth and wave height at a number of locations within the lake.

It would also be recommended to measure the erosion rate parameters such as the critical shear stress, erosion rate constant and hence the model parameter K. These measurements could either be done insitu or in the laboratory. It could be beneficial to see the difference between the measurements observed in the field and those in the laboratory.

REFERENCES

Bailey, M.C. and Hamilton, D.P. 1996. Wind induced sediment resuspension: a lake-wide model, *Ecological Modeling*, vol 99, pp 217-228.

Breugem, W. A. and L. H. Holthuijsen. 2006. Generalised wave growth from Lake George, *J. Waterway, Port, Coastal, and Ocean Engineering*, ASCE (in press).

Burban, P.Y., Y.U. Xu, J. McNeil, and W. Lick. 1990. Settling Speeds of Flocs in Fresh Water and Seawater. *Journal of Geophysics Research,* vol. *95,* no. 10, pp. 18213-1 8200.

Bureau of Reclamation. 2006. Erosion and Sedimentation Manual in US Department of the Interior, Denver, Colorado, pp. 4-1-4-46.

CERC, 1977. Shore Protection Manual. U.S. Army Coastal Engineering Research Center. 3 Volumes.

Carrasco, N.K., Perissinotto, R. & Miranda, N.A.F. 2007. Effects of silt loading on the feeding and mortality of the mysid mesopodopsis africana in the St. Lucia estuary, South Africa, *Journal of experimental marine biology and ecology,* vol. 352, no. 1, pp. 152-164.

Carniello, L, D'Alpaos, A, Defina, A. 2011. Modelling wind waves and tidal flows in shallow micro tidal basins, *Estuarine, Coastal and Shelf science*, vol 92, pp 263-276.

Chao, X., Jia, Y., Shields Jr, F.D., Wang, S.S.Y. & Cooper, C.M. 2008. Three-dimensional numerical modeling of cohesive sediment transport and wind wave impact in a shallow oxbow lake, *Advances in Water Resources,* vol. 31, no. 7, pp. 1004-1014.

Chrystal, C.P. and Stretch, D.D. Sedimentation of the lake St Lucia and Mfolozi systems. In preparation.

Cloern, J.E. 1987. Turbidity as a control in phytoplankton biomass and productivity in estuaries. *Continental Shelf Research*, vol 7, nos 11/12, pp 1367 – 1381.

Cyrus D.P, Blaber S.J.M. 1988. The influence of turbidity on juvenile marine fishes in estuaries. Part 1: Field studies at Lake St Lucia on the southeastern coast of Africa. *Journal of Experimental Marine Biology and Ecology*, vol 109, pp53-70.

Cyrus D.P, Vivier L, Jerling H.L. 2010. Effect of hypersaline and low lake conditions on ecological functioning of St. Lucia estuarine sytem, South Africa: an overview 2002-2008. *Estuarine, Coastal Shelf Science*, vol 86, pp 535-542.

Davies-Colley, R.J and Smith, D.G., 2001. Turbidity, suspended sediment and water clarity: A Review, *Journal of the American Water Resources Association*, vol 37, No. 5, pp 1085-1101.

Day J.H, Millard A.H, Broekhuysen G.J. 1954. The ecology of South African estuaries part iv: the St. Lucia system. Department of Zoology, University of Cape Town, pp 129-141.

Grayson, R.B., Finlayson, B.L., Gippel, C.J., Hart, B.T. 1996. The potential for field measurements for the Computation of total phosphorous and suspended solids loads, *Journal of Environmental Management*, vol 45, pp 257-267.

Guang H, Yi-gang W, 2007. A new measure for direct measurement of the bed shear stress of wave boundary layer in wave flume, *Journal of Hydrogynamics*, vol 19, No. 4, pp 517-524.

Hamilton, D.P, Mitchell, S.F. 1996. An empirical model for sediment resuspension in shallow lakes. *Hydrobiologia*, vol 317, pp 209-220.

Hawley, N., Lesht, B.M. 1992. Sediment resuspension in lake St Clair. *American Society of Limnology and Oceanography*, vol 37, no 8, pp 1720 – 1737.

Holthuijsen, L.H. 2007. *Waves in Oceanic and in Coastal Waters*. Cambridge University Press, New York, USA.

Huang, N.E, Sheng, Z, Long, S.R, Wu, M.C, Shih, H.H, Zeng, Q, Yen, N.C, Tuang, C.C, Liu, H.H. 1996. Empirical mode decomposition and the Hilber spectrum for nonlinear and non-stationary time series analysis. *Preceedings: Mathematical and engineering sciences,* vol 454, no 1971, pp 903-995.

Hutchison, I.P.G., 1974. *St Lucia Lake and Estuary Hydrographic* Data. Report No. 3/74. Hydrological Research Unit, University of the Witwatersrand, Johannesburg, South Africa.

Hutchison, I.P.G., 1976. *Lake St. Lucia – Mathematical Modelling & Evaluation Of Amelioration Measures*. Report No. 1/76. Hydrological Research Unit, University of the Witwatersrand, Johannesburg,South Africa.

Ijima, T. & Tang, F. 1966. Numerical calculation of wind waves in shallow water, *Proc. 10th Conf. on Coastal Engineering (Japan)* ASCE, New York, pp. 38–49.

Jing, L. & Ridd, P.V. 1996. Wave-current bottom shear stresses and sediment resuspension in Cleveland Bay, Australia, *Coastal Engineering,* vol. 29, no. 1-2, pp. 169-186.

Jeffreys, H. 1925. On the formation of water waves by wind. *Proceedings of the Royal Society of London*, vol 107, no 742, pp189-206.

Kessarkar, P.M., Purnachandra Rao, V., Shynu, R., Ahmad, I.M., Mehra, P., Michael, G. & Sundar, D. 2009. Wind-driven estuarine turbidity maxima in Mandovi Estuary, central west coast of India, *Journal of Earth System Science*, vol. 118, no. 4, pp. 369-377.

Kinsman, B. 1965. *Wind Waves: Their Generation and Propagation on The Ocean Surface*. Prentice-Hall, Englewood Cliffs, USA.

Krone, R.B. 1962. Flume Studies of the Transport of Sediment in Estuarial Shoaling Processes. Technical Report, Hydraulic Engineering Laboratory, University of California, Berkeley California.

Lavelle J.W, Mofjeld H.O. 1987. Do critical shear stresses for incipient motion really exist? *Journal of Hydraulic Engineering Div ASCE*,vol 113, pp 370-385.

Lavelle J.W, Baker E.T. 1984. An in situ erosion rate for fine-grained marine sediment. *Journal of Geophysical research,* vol 89, pp 6543 – 6552.

Lawrie, R., Stretch, D. 2008. *Evaluation of the short-term link between the uMfolozi estuary and St. Lucia Lake*, Final report, Centre for research in Environmental, Coastal and Hydrological Engineering, Kwa-Zulu Natal, RSA.

Lawrie, R, Stretch, D. 2011. Anthropogenic impact on the water and salt budgets of the St Lucia estuarine lake in South Africa. *Estuarine, Coastal and Shelf Science*, vol 93, pp 58-67.

Liu Z. 2001. Sediment transport, Laboratoriet for Hydraulik og Havnebygning, Institut for Vand, Jord og Miljøteknik, Aalborg Universitet, .

Luettich, R.A., Harleman, D.R.F., Somlyody, L. 1990. Dynamic behavior of suspended sediment concentrations in a shallow lake perturbed by episodic wind events. *American Society of Limnology and Oceanography*, vol 35, no 5, pp. 1050-1067.

Lund G.B.A. 1976. The Proposed uMfolozi – St. Lucia Link Canal. Pietermaritzburg. N.P.A Building Services Department.

Maine C.M. 2011. Investigating the flocculation dynamics of cohesive sediments from the St. Lucia and uMfolozi estuaries. MSc Dissertation, School of Civil Engineering, Surveying and Construction, University of kwaZulu Natal, Durban, RSA.

Massel, S.R. 1996. *Ocean Surface Waves: Their Physics and Prediction*. World Scientific, USA.

Mehta A.J, Jain M. 2010. Wave-induced resuspension of fine sediment. In:ed Kim, Y, *Handbook of coastal and ocean engineering*, Ch. 27, pp775-806. World Scientific Publishing Co., Hackensack, USA.

Niclasen, B.A. & Simonsen, K. 2008. Note on wave parameters from moored wave buoys. *Applied Ocean Research*, vol 29, pp 231-238.

Partheniades, E. (1962). A Study of Erosion and Deposition of Cohesive Soils in Salt Water,Ph.D. Thesis, University of California, Berkeley.

Perissinotto, R, Pillay, D, Bate, G. 2010a. Microalgal biomass in the St. Lucia estuary during the 2004 to 2007 drought period. *Marine Ecological Progress Series*. vol 405, pp 147-167.

Perissinotto, R, Stretch, DD, Whitfield, AK, Adams, JB, Forbes, AT, Demetriades, NT. 2010b. *Temporarily Open/Closed Estuaries in South Africa.*Nova Publishers Inc, NY, USA.

Reeve, D., Chadwick, A. & Fleming, C. 2004. *Coastal Engineering - Processes, Theory and Design Practise,* Spoon Press, USA.

Sadar, M.J. 1998. Turbidity Science. *Technical Information Series* – Booklet no. 11.

Sadjadi, B. 2011. Personal Communication. Sales Director- Akamina Technologies. Canada.

Smith, P.M., Lin, C.S. 1984. A Laser Slope Wave Gauge and A Spar Buoy Wave Gauge: Tools For Validation Of Microwave Remote Sensors. Naval Ocean Research and Development Activity. USA.

Socolofsky, J. A, Jirka, G. H. 2004. *CVEN 489-501: Special topics in mixing and transport processes in the environment*. Texas A&M University, Texas, USA.

Standard Methods for the examination of water & wastewater, 21st Ed. 2005. 2540 D. Total suspended solids dried at 103-105°C. APHA, Washington, USA.

Tsai, J, Tsai, C. 2009. Wave measurements by pressure transducers using artificial neural networks. *Ocean Engineering*, vol 36, pp 1149-1157.

Tyler, J. E. 1968. The secchi disc. *Limnology and Oceanography*, vol 13, pp1-6.

Whitfield, A.K., Taylor, R.H., 2009. A review of the importance of freshwater inflow to the future conservation of Lake St Lucia. Aquatic Conservation: Marine & Freshwater Ecosystems 19 (7), 838-848.

Wright, J, Colling, A, Park, D. 1999. *Waves, Tides and Shallow-Water Processes*. Butterworth-Heinemann, Oxford, England.

Young, I. & Verhagen, L. 1996. The growth of fetch limited waves in water of finite depth. Part 1. Total energy and peak frequency, *Coastal Engineering,* vol. 29, no. 1-2, pp. 47-78.

YSI Incorporated. Environmental Monitoring Manual.

APPENDICES

Appendix A: Field observations.

Appendix B: TSS calculation.

Appendix C: Flow diagram of the mathematical model.

Appendix D: Monthly turbidity for the period 2000 – 2009.

Appendix E: Kestrel 4500 specifications.

APPENDIX A

TABULATED FIELD OBSERVATIONS AND MEASUREMENTS.

Table A-1: GPS marks and significant wave height measurements.

Date	Time	GPS	Wind Speed (m/s)	U_{10} (m/s)	Direction	Water Depth (m)	Hs (m)
22/3/11	10:29	6	1.2	1.52	S	0.45	
22/3/11	10:42	7	2.6	3.3	S	0.56	0.071
22/3/11	11.26	8	3.3	4.18	S	0.65	
22/3/11	11:57	9	3.6	4.56	S	0.47	0.11
22/3/11	12:24	10	3.3	4.18	S	0.55	0.084
24/3/11	9:37	na	3.3	4.18	S	0.9	
24/3/11	10:00	11	3.6	4.56	S	1.2	0.11
24/3/11	10:33	12	3.8	4.82	S	1.15	
24/3/11	11:00	13	6.1	7.73	S	1.25	
24/3/11	11:27	14	5.5	6.97	S	1.1	
24/3/11	12:00	15	5	6.34	S	1.2	
24/3/11	12:33	16	6.6	8.37	S	1.15	
24/3/11	12:52	17	7	8.87	S	1	
19/04/11	11:31	806	4.8	6.09	NE	0.65	0.11
19/04/11	14:21	807		0	NE	0.37	
19/04/11	14:50			0	NE		
19/04/11	15:00	808	5.8	7.35	NE	0.35	
19/04/11	15:10	808	5.8	7.35	NE	0.35	
19/04/11	15:20	809		0			
20/04/11	11:28	810	7.4	9.38	NE	0.35	0.13
20/04/11	12:05	811	7.5	9.51	NE	0.75	0.18
20/04/11	12:05	811	7.5	9.51	NE	0.75	
20/04/11	12:25	812	7	8.87	NE	0.95	0.24
20/04/11	12:43	813	7.4	9.38	NE	0.75	0.20
20/04/11	13:00	814	7.1	9.00	NE	0.75	0.22
20/04/11	13:28	815	7.7	9.76	NE	0.85	0.31
20/04/11	13:45	816	8.1	10.27	NE	0.8	0.20
20/04/11	14:00	817	7.7	9.76	NE	0.9	0.25
20/04/11	14:21	818	9.2	11.66	NE	0.85	0.32

APPENDIX B

LABORATORY RESULTS FOR THE TSS CALCULATION.

Table B-1: Summary of TSS and Turbidity results.

Sample ID	Filter weight (g)	Filter + Sed (g)	TSS (g/L)	Turbidity (NTU)
1B	0.16099	0.17542	0.1443	6.7
7B	0.15424	0.16522	0.1098	5.3
8A	0.15874	0.17021	0.1147	4.1
7A	0.1552	0.16605	0.1085	3.7
10A	0.15946	0.16953	0.1007	4.8
4A	0.15565	0.16897	0.1332	6.3
2B	0.15844	0.17151	0.1307	6.7
2A	0.15965	0.1724	0.1275	8.4
1A	0.15936	0.17365	0.1429	8.5
7E	0.15864	0.17031	0.1167	20
8F	0.16025	0.17279	0.1254	37
7C	0.16118	0.18443	0.2325	13.5
3C	0.14826	0.15824	0.0998	13
8C	0.14765	0.16061	0.1296	34
10F	0.16051	0.17179	0.1128	11.3
3A	0.14781	0.16083	0.1302	44.7
9B	0.14712	0.15825	0.1113	45
5B	0.15893	0.17121	0.1228	26
6B	0.15545	0.17256	0.1711	37.4
9A	0.14842	0.15937	0.1095	28
4C	0.15982	0.17605	0.1623	54.9
10E	0.15561	0.19905	0.4344	402.45
6E	0.15503	0.19059	0.3556	446.1
9F	0.15631	0.19781	0.415	446.1
6D	0.15575	0.21891	0.6316	578
1F	0.15625	0.19398	0.3773	316.4
1E	0.15736	0.23514	0.7778	620
8E	0.15695	0.2129	0.5595	580
8D	0.15674	0.22775	0.7101	880
2D	0.15379	0.21297	0.5918	590
1C	0.15352	0.1679	0.1438	33.2
5C	0.14765	0.16044	0.1279	39.8
4B	0.15586	0.17372	0.1786	95.1
8A	0.1479	0.17378	0.2588	228.7
4G	0.15763	0.18774	0.3011	291.7
5A	0.15678	0.20083	0.4405	568.8
7D	0.15725	0.20422	0.4697	566.9
2B	0.15571	0.17565	0.1994	138.1
4A	0.14715	0.16726	0.2011	144.4
7C	0.15757	0.18288	0.2531	233.2
3F	0.15575	0.17908	0.2333	252.4
5F	0.15548	0.18758	0.321	325
8F	0.15639	0.20777	0.5138	662
7A	0.16141	0.22537	0.6396	938.6
4F	0.1604	0.24202	0.8162	1078.1
10A	0.155	0.22918	0.7418	1007.2
9E			0	12.7

The TSS was calculated as follows:

$$TSS = 10x(W_{(f+s)}-W_{(f)}). \quad \text{(B-1)}$$

Where: $W_{(f+s)}$ is the combined dry weight (g) of the sediment and the filter and $W_{(f)}$ (g) is the dry weight of the filter.

APPENDIX C

FLOW CHART FOR MODELLING THE SEDIMENT RE-SUSPENSION.

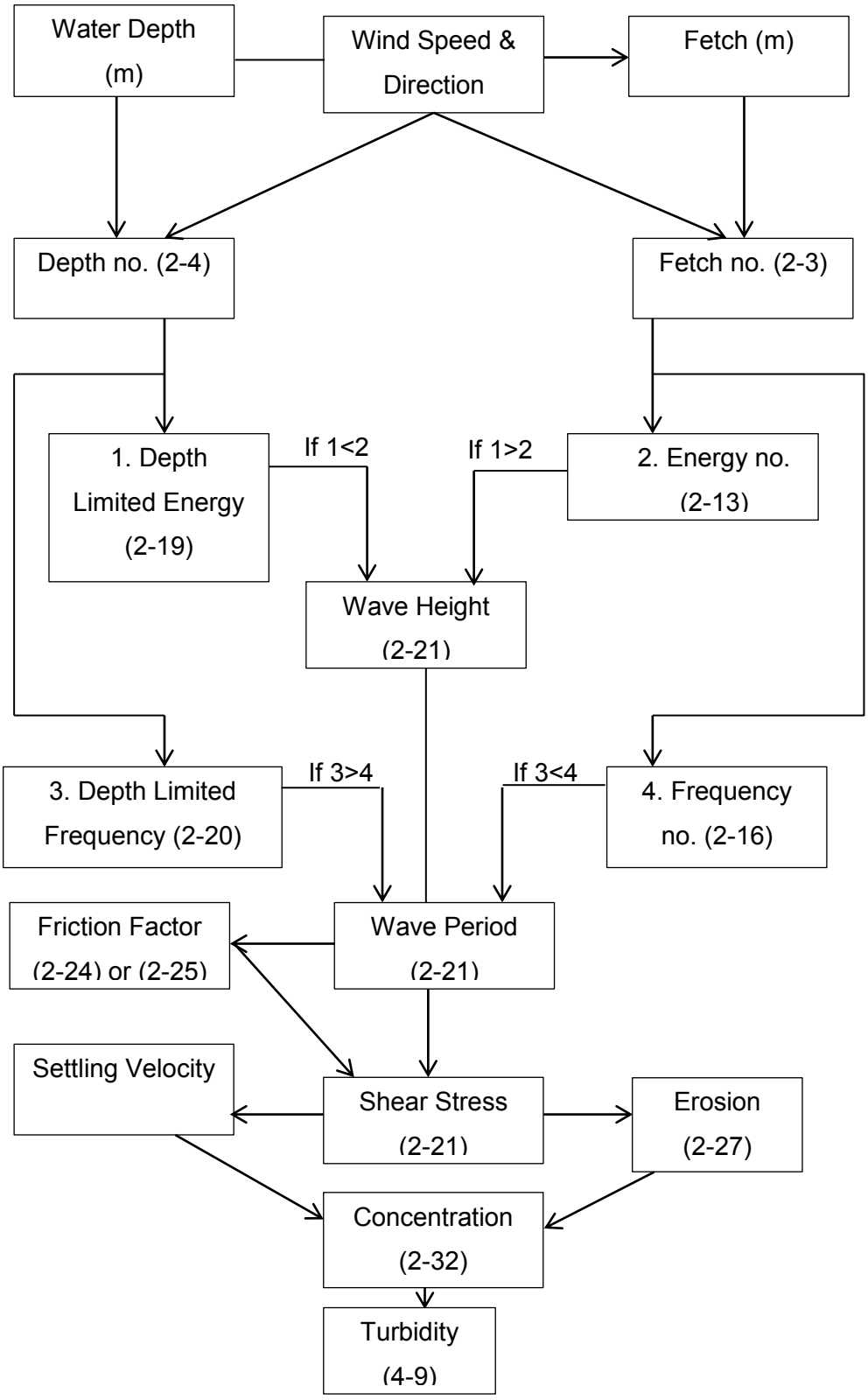

Figure C-1: Flow chart showing model procedure.

APPENDIX D

MONTHLY TURBIDITY VALUES FOR THE PERIOD FROM 2000 – 2009

Table D-1: Monthly Turbidity for the month of January (2000 – 2009).

Date	Wind Speed (m/s)	Water Depth (m)	Fetch (m)	Wave Height (m)	Period (s)	Shear (Pa)	Cer (g/L)	Turbidity (NTU)
Jan-00	7.67	1.14	3249.85	0.18	1.82	0.28	0.20	223.67
Jan-01	8.12	0.97	3130.62	0.19	1.81	0.34	0.38	402.64
Jan-02	8.67	0.67	2744.31	0.17	1.69	0.43	0.67	703.85
Jan-03	7.56	0.25	1938.05	0.09	1.18	0.52	0.93	968.88
Jan-04	8.82	0.25	1938.05	0.10	1.23	0.59	1.12	1172.52
Jan-05	8.01	0.41	2211.16	0.13	1.42	0.48	0.80	836.28
Jan-06	8.09	0.41	2211.16	0.13	1.43	0.48	0.81	849.44
Jan-07	7.76	0.41	2211.16	0.12	1.41	0.46	0.76	795.02
Jan-08	8.53	0.41	2211.16	0.13	1.45	0.51	0.88	918.76
Jan-09	8.22	0.41	2211.16	0.13	1.44	0.49	0.83	870.82

Table D-2: Monthly Turbidity for the month of February (2000 – 2009).

Date	Wind Speed (m/s)	Water Depth (m)	Fetch (m)	Wave Height (m)	Period (s)	Shear (Pa)	Cer (g/L)	Turbidity (NTU)
Feb-00	6.49	1.14	3249.85	0.16	1.71	0.22	0.03	45.67
Feb-01	6.06	0.97	3130.62	0.14	1.62	0.23	0.06	79.45
Feb-02	8.14	0.56	2454.06	0.15	1.57	0.43	0.67	703.98
Feb-03	8.03	0.41	2211.16	0.13	1.43	0.48	0.80	840.09
Feb-04	7.06	0.25	1938.05	0.09	1.16	0.49	0.84	883.82
Feb-05	7.49	0.41	2211.16	0.12	1.40	0.45	0.72	751.57
Feb-06	7.73	0.41	2211.16	0.12	1.41	0.46	0.75	789.93
Feb-07	7.86	0.41	2211.16	0.12	1.42	0.47	0.77	811.74
Feb-08	8.22	0.41	2211.16	0.13	1.44	0.49	0.83	870.60
Feb-09	6.90	0.25	1938.05	0.09	1.16	0.48	0.82	855.58

Table D-3: Monthly Turbidity for the month of March (2000 – 2009).

Date	Wind Speed (m/s)	Water Depth (m)	Fetch (m)	Wave Height (m)	Period (s)	Shear (Pa)	C_{er} (g/L)	Turbidity (NTU)
Mar-00	6.97	1.14	3249.85	0.17	1.76	0.24	0.10	119.12
Mar-01	4.80	0.97	3130.62	0.11	1.48	0.16	0.00	12.70
Mar-02	8.58	0.56	2454.06	0.15	1.60	0.46	0.74	773.41
Mar-03	8.02	0.41	2211.16	0.13	1.43	0.48	0.80	838.08
Mar-04	6.58	0.41	2211.16	0.11	1.34	0.40	0.56	594.71
Mar-05	6.04	0.41	2211.16	0.10	1.31	0.37	0.47	498.63
Mar-06	7.73	0.41	2211.16	0.12	1.41	0.46	0.75	790.26
Mar-07	8.38	0.41	2211.16	0.13	1.44	0.50	0.86	896.21
Mar-08	7.14	0.41	2211.16	0.12	1.38	0.43	0.66	691.96
Mar-09	6.49	0.25	1938.05	0.08	1.14	0.46	0.75	784.03

Table D-4: Monthly Turbidity for the month of April (2000 – 2009).

Date	Wind Speed (m/s)	Water Depth (m)	Fetch (m)	Wave Height (m)	Period (s)	Shear (Pa)	C_{er} (g/L)	Turbidity (NTU)
Apr-00	5.59	1.14	3249.85	0.14	1.61	0.17	0.00	12.70
Apr-01	5.82	0.79	3006.66	0.13	1.54	0.26	0.15	165.28
Apr-02	8.14	0.56	2454.06	0.15	1.57	0.44	0.67	705.12
Apr-03	7.35	0.41	2211.16	0.12	1.39	0.44	0.69	727.07
Apr-04	6.68	0.56	2454.06	0.12	1.47	0.36	0.44	464.85
Apr-05	6.83	0.41	2211.16	0.11	1.36	0.41	0.61	638.45
Apr-06	7.24	0.41	2211.16	0.12	1.38	0.44	0.67	708.43
Apr-07	6.21	0.41	2211.16	0.10	1.32	0.38	0.50	530.31
Apr-08	6.39	0.41	2211.16	0.11	1.33	0.39	0.53	561.90
Apr-09	6.56	0.13	1372.73	0.06	0.88	0.52	0.93	973.31

Table D-5: Monthly Turbidity for the month of May (2000 – 2009).

Date	Wind Speed (m/s)	Water Depth (m)	Fetch (m)	Wave Height (m)	Period (s)	Shear (Pa)	C_{er} (g/L)	Turbidity (NTU)
May-00	4.34	1.14	3249.85	0.11	1.45	0.11	0.00	12.70
May-01	5.76	0.79	3006.66	0.13	1.53	0.26	0.14	154.53
May-02	6.61	0.56	2454.06	0.12	1.47	0.35	0.43	452.20
Mar-04	6.58	0.41	2211.16	0.11	1.34	0.40	0.56	594.71
May-03	6.20	0.41	2211.16	0.10	1.32	0.38	0.50	528.39
May-04	6.10	0.56	2454.06	0.12	1.43	0.32	0.34	363.73
May-05	6.82	0.41	2211.16	0.11	1.36	0.41	0.61	637.98
May-06	5.86	0.56	2454.06	0.11	1.41	0.31	0.30	320.97
May-07	5.98	0.56	2454.06	0.11	1.42	0.32	0.32	342.92
May-08	6.12	0.41	2211.16	0.10	1.31	0.37	0.49	514.46
May-09	5.98	0.13	1372.73	0.05	0.86	0.49	0.83	867.40

Table D-6: Monthly Turbidity for the month of June (2000 – 2009).

Date	Wind Speed (m/s)	Water Depth (m)	Fetch (m)	Wave Height (m)	Period (s)	Shear (Pa)	C_{er} (g/L)	Turbidity (NTU)
Jun-00	3.76	1.14	3249.85	0.09	1.36	0.08	0.00	12.70
Jun-01	4.16	0.79	3006.66	0.10	1.35	0.16	0.00	12.70
Jun-02	6.85	0.56	2454.06	0.13	1.48	0.37	0.47	493.16
Jun-03	-	0.41	2211.16	-	-	-	-	-
Jun-04	5.95	0.56	2454.06	0.11	1.41	0.32	0.31	337.27
Jun-05	5.83	0.41	2211.16	0.10	1.29	0.36	0.43	460.65
Jun-06	5.42	0.56	2454.06	0.10	1.37	0.28	0.22	240.90
Jun-07	5.81	0.56	2454.06	0.11	1.40	0.31	0.29	311.73
Jun-08	5.37	0.41	2211.16	0.09	1.26	0.33	0.35	374.26
Jun-09	5.31	0.13	1372.73	0.05	0.84	0.45	0.70	738.37

Table D-7: Monthly Turbidity for the month of July (2000 – 2009).

Date	Wind Speed (m/s)	Water Depth (m)	Fetch (m)	Wave Height (m)	Period (s)	Shear (Pa)	C_{er} (g/L)	Turbidity (NTU)
Jul-00	5.39	0.97	3130.62	0.13	1.55	0.20	0.00	12.70
Jul-01	4.53	0.79	3006.66	0.10	1.40	0.18	0.00	12.70
Jul-02	6.53	0.56	2454.06	0.12	1.46	0.35	0.41	439.11
Jul-03	6.41	0.41	2211.16	0.11	1.33	0.39	0.54	565.96
Jul-04	5.49	0.67	2744.31	0.11	1.44	0.26	0.16	178.01
Jul-05	6.17	0.41	2211.16	0.10	1.32	0.38	0.49	522.79
Jul-06	7.36	0.56	2454.06	0.14	1.52	0.39	0.55	579.54
Jul-07	6.16	0.67	2744.31	0.13	1.51	0.30	0.27	296.29
Jul-08	6.04	0.41	2211.16	0.10	1.31	0.37	0.47	499.61
Jul-09	6.64	0.13	1372.73	0.06	0.89	0.53	0.95	989.32

Table D-8: Monthly Turbidity for the month of August (2000 – 2009).

Date	Wind Speed (m/s)	Water Depth (m)	Fetch (m)	Wave Height (m)	Period (s)	Shear (Pa)	C_{er} (g/L)	Turbidity (NTU)
Aug-00	6.92	0.97	3130.62	0.16	1.70	0.28	0.20	218.75
Aug-01	6.03	0.79	3006.66	0.13	1.56	0.27	0.18	200.94
Aug-02	6.85	0.56	2454.06	0.13	1.48	0.37	0.47	493.16
Aug-03	9.36	0.41	2211.16	0.14	1.49	0.55	1.00	1048.27
Aug-04	6.89	0.67	2744.31	0.14	1.57	0.34	0.40	421.20
Aug-05	7.90	0.41	2211.16	0.12	1.42	0.47	0.78	818.36
Aug-06	7.37	0.56	2454.06	0.14	1.52	0.39	0.55	580.88
Aug-07	7.88	0.56	2454.06	0.14	1.55	0.42	0.63	662.36
Aug-08	7.78	0.41	2211.16	0.12	1.41	0.47	0.76	798.22
Aug-09	7.78	0.59	2454.06	0.14	1.57	0.41	0.58	613.69

Table D-9: Monthly Turbidity for the month of September (2000 – 2009).

Date	Wind Speed (m/s)	Water Depth (m)	Fetch (m)	Wave Height (m)	Period (s)	Shear (Pa)	Cer (g/L)	Turbidity (NTU)
Sep-00	8.18	0.97	3130.62	0.19	1.81	0.34	0.39	412.86
Sep-01	9.19	0.79	3006.66	0.19	1.81	0.43	0.67	700.90
Sep-02	7.85	0.41	2211.16	0.12	1.42	0.47	0.78	816.04
Sep-03	8.99	0.41	2211.16	0.14	1.47	0.53	0.95	991.58
Sep-04	8.66	0.67	2744.31	0.17	1.69	0.43	0.67	702.69
Sep-05	8.45	0.41	2211.16	0.13	1.45	0.50	0.87	907.46
Sep-06	8.14	0.56	2454.06	0.15	1.57	0.44	0.67	704.65
Sep-07	7.81	0.56	2454.06	0.14	1.55	0.42	0.62	651.52
Sep-08	8.69	0.41	2211.16	0.13	1.46	0.51	0.90	944.13
Sep-09	8.28	0.59	2454.06	0.15	1.60	0.43	0.66	694.41
Sep-10	9.42	0.58	2454.06	0.17	1.66	0.49	0.84	880.48

Table D-10: Monthly Turbidity for the month of October (2000 – 2009).

Date	Wind Speed (m/s)	Water Depth (m)	Fetch (m)	Wave Height (m)	Period (s)	Shear (Pa)	Cer (g/L)	Turbidity (NTU)
Oct-00	7.39	0.97	3130.62	0.17	1.75	0.30	0.27	291.37
Oct-01	8.31	0.79	3006.66	0.18	1.75	0.39	0.54	569.75
Oct-02	9.67	0.41	2211.16	0.15	1.50	0.56	1.05	1094.17
Oct-03	8.61	0.25	1938.05	0.10	1.22	0.58	1.09	1139.65
Oct-04	9.21	0.56	2454.06	0.16	1.63	0.49	0.83	869.72
Oct-05	9.26	0.41	2211.16	0.14	1.49	0.54	0.99	1032.67
Oct-06	8.72	0.56	2454.06	0.16	1.60	0.46	0.76	795.31
Oct-07	8.54	0.56	2454.06	0.15	1.59	0.46	0.73	766.72
Oct-08	8.48	0.41	2211.16	0.13	1.45	0.50	0.87	912.16
Oct-09	8.74	0.59	2454.06	0.16	1.62	0.46	0.73	765.34

Table D-11: Monthly Turbidity for the month of November (2000 – 2009).

Date	Wind Speed (m/s)	Water Depth (m)	Fetch (m)	Wave Height (m)	Period (s)	Shear (Pa)	Cer (g/L)	Turbidity (NTU)
Nov-00	7.53	0.97	3130.62	0.17	1.76	0.31	0.29	314.03
Nov-01	8.16	0.67	2744.31	0.16	1.66	0.41	0.59	625.45
Nov-02	9.65	0.41	2211.16	0.15	1.50	0.56	1.04	1090.83
Nov-03	8.94	0.25	1938.05	0.11	1.24	0.59	1.14	1192.37
Nov-04	9.09	0.56	2454.06	0.16	1.63	0.48	0.81	850.83
Nov-05	9.12	0.41	2211.16	0.14	1.48	0.54	0.97	1011.64
Nov-06	8.58	0.56	2454.06	0.15	1.60	0.46	0.74	773.32
Nov-07	8.45	0.56	2454.06	0.15	1.59	0.45	0.72	752.47
Nov-08	8.50	0.41	2211.16	0.13	1.45	0.50	0.87	914.29
Nov-09	8.51	0.59	2454.06	0.16	1.61	0.44	0.70	731.04

Table D-12: Monthly Turbidity for the month of December (2000 – 2009).

Date	Wind Speed (m/s)	Water Depth (m)	Fetch (m)	Wave Height (m)	Period (s)	Shear (Pa)	Cer (g/L)	Turbidity (NTU)
Dec-00	7.83	0.97	3130.62	0.18	1.78	0.32	0.34	359.90
Dec-01	8.29	0.67	2744.31	0.16	1.67	0.42	0.61	645.38
Dec-02	8.52	0.41	2211.16	0.13	1.45	0.51	0.88	918.64
Dec-03	10.05	0.25	1938.05	0.12	1.27	0.65	1.30	1360.77
Dec-04	9.16	0.56	2454.06	0.16	1.63	0.49	0.82	861.30
Dec-05	8.88	0.41	2211.16	0.14	1.47	0.52	0.93	973.72
Dec-06	7.96	0.41	2211.16	0.13	1.42	0.48	0.79	828.27
Dec-07	8.35	0.41	2211.16	0.13	1.44	0.50	0.85	891.13
Dec-08	8.46	0.41	2211.16	0.13	1.45	0.50	0.87	909.05
Dec-09	9.17	0.59	2454.06	0.17	1.65	0.48	0.79	831.26

APPENDIX E

KESTREL 4500 SPECIFICATIONS

Kestrel®
Pocket Weather® Meters

Certificate of Conformity

This instrument was produced under rigorous factory production control and documented standard procedures. It was individually visually inspected, leak tested and function tested for display, backlight, button and software performance. The accuracy of each of its primary measurements was individually calibrated and/or tested against standards traceable to the National Institute of Standards and Technology ("NIST") or calibrated intermediary standards. This instrument is certified to have performed at the time of manufacture in compliance with the following specifications as they apply to this meter's specific model, measurements and features.

Methods Used in Calibration and Testing

Wind Speed:

The Kestrel Pocket Weather Meter impeller installed in this unit was individually tested in a subsonic wind tunnel operating at approximately 300 fpm (1.5 m/s) and 1200 fpm (6.1 m/s) monitored by a Gill Instruments Model 1350 ultrasonic time-of-flight anemometer. The Standard's maximum combined uncertainty is ±1.04% within the airspeed range 706.6 to 3923.9 fpm (3.59 to 19.93 m/s), and ±1.66% within the airspeed range 166.6 to 706.6 fpm (0.85 to 3.59 m/s).

Temperature:

Temperature response is verified in comparison with a Eutechnics 4600 Precision Thermometer or a standard Kestrel 4000 Pocket Weather Tracker calibrated weekly against the Eutechnics 4600. The Eutechnics 4600 is calibrated annually and is traceable to NIST with a maximum relative expanded uncertainty of ±0.020°C.

Direction / Heading

The sensitivity of the magnetic directional sensor is verified at the component level by applying a magnetic field to the sensor and measuring the signal output at 4 points, as well as after assembly by orienting the unit to the cardinal directions and measuring the magnetic field output. In both cases the compass output must be accurate to within +/- 5 degrees.

Relative Humidity:

Relative humity receives a two-point calibration in humidity and temperature controlled chambers at 75.3% RH and 32.8% RH at 25° C. The calibration tanks are monitored with an Edgetech Model 2002 DewPrime II Standard Chilled Mirror Hygrometer. Following calibration, performance is further verified at an RH of approximately 43.2% against the Edgetech Hygrometer. The Edgetech Hygrometer is calibrated annually and is traceable to NIST with a maximum relative expanded uncertainty of +/- 0.5 %RH.

Barometric Pressure:

Pressure response is verified against a Mensor Series 6000 Digital Barometer or a standard Kestrel 4000 Pocket Weather Tracker calibrated weekly against the Mensor Barometer. The Mensor Barometer is calibrated annually and is traceable to NIST with a maximum relative expanded uncertainty of +/- 0.2 hPa.

Approved By:

Michael Naughton, Engineering Manager

The enclosed Kestrel Pocket Weather Meter was manufactured by Nielsen-Kellerman Co. at its facilities located at 21 Creek Circle, Boothwyn, PA 19061 USA.